Séminaire du cours de Pascale Senellart
Collège de France - 06 janvier 2026

Centres NV du diamant
Du matériau aux capteurs quantiques

Jean-François Roch
jean-francois.roch@ens-paris-saclay.fr

Laboratoire LUMIN
ENS Paris-Saclay, Université Paris-Saclay,
CentraleSupelec & CNRS

What is a quantum sensor?

C. L. Degen, F. Reinhard, and P. Cappellaro, Rev. Mod. Phys. **89**, 035002 (2017)

1. Probe: controllable quantum system with quantized energy levels
   Neutral atoms, electronic/nuclear spins, superconducting qubits

2. Information on physical quantity: encoded in energy levels
   Readout e.g. through measurements of Bohr frequencies

3. Sensitivity: use of quantum coherence
   Measurement of phase shift in temporal superposition states

single qubit or incoherent ensemble of qubits

4. Quantum entanglement: improve the measurement sensitivity, beyond what is possible classically.

more than one qubit

Many concepts are well known, resulting from decades of developments in high-resolution spectroscopy: atomic physics, magnetic resonance

Hanle effect (Claude Cohen-Tannoudji CDF 2003-2004)

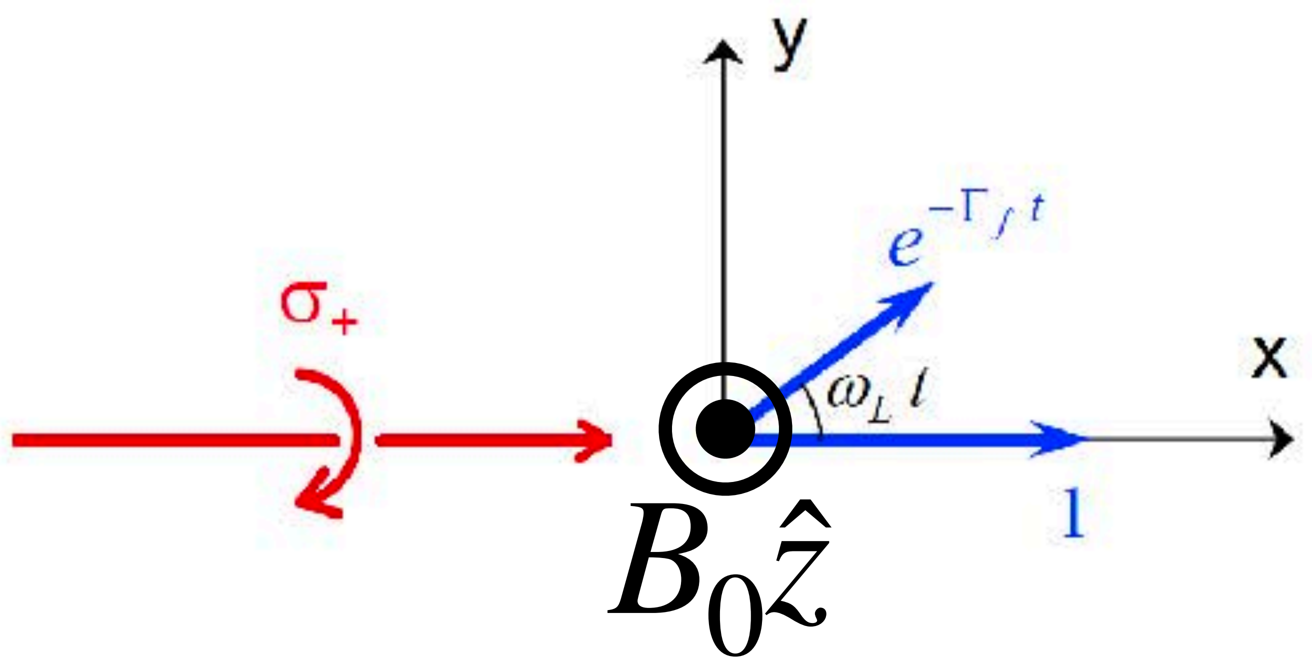

Dans le plan xy perpendiculaire au champ B_0, compétition entre
- le pompage optique qui tend à orienter les spins le long de x.
- la précession de Larmor qui les fait tourner à la fréquence ω_L dans le plan xy.

Etat fondamental de l'atome de Rb
$\Gamma_f \approx 1\,\mathrm{s}^{-1}$ et $\omega_L \approx 1\,\mathrm{MHz}\cdot\mathrm{Gauss}^{-1}$
$\rightarrow$ largeur de la résonance $\delta\omega_L \approx \Gamma_f$
soit $\delta B_0 \approx 10^{-6}\,\mathrm{Gauss}$

transition $J = 0 \rightarrow J = 1$ excitation vers $|J = 1, M = 1\rangle_x$

fluorescence σ_+ diffusée selon y : $S(t) \propto (1 + \sin\omega_L t)^2 e^{-\Gamma t}$

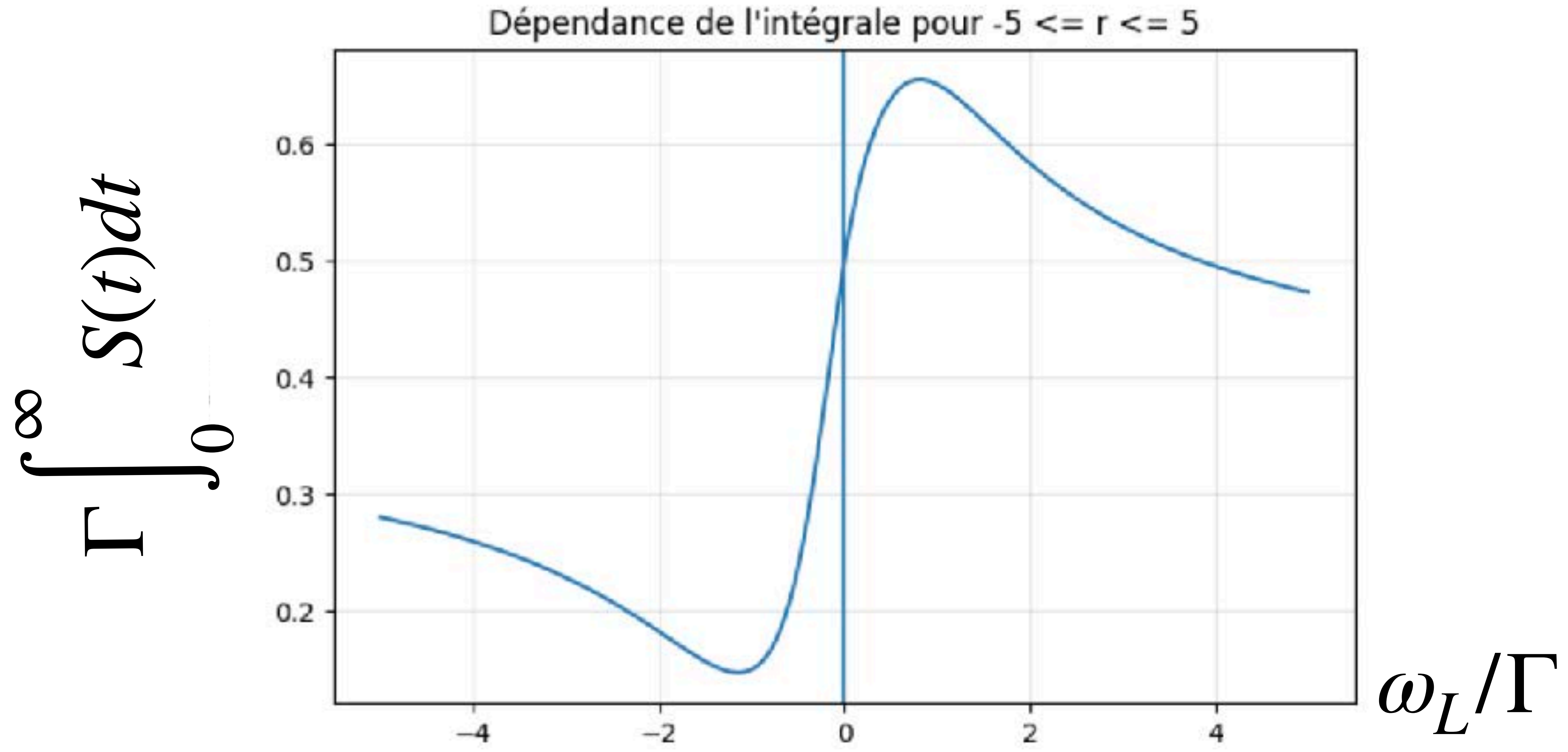

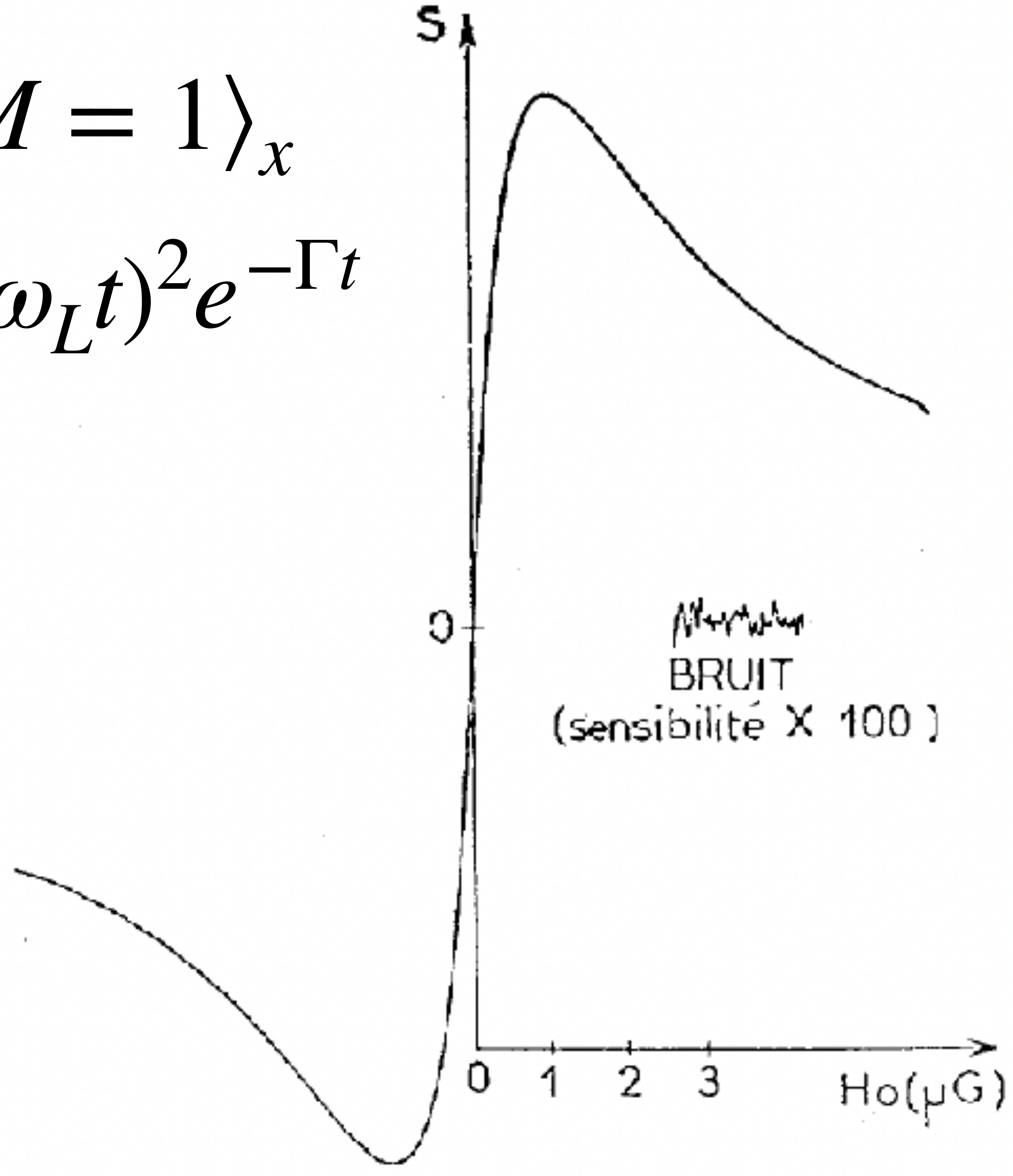

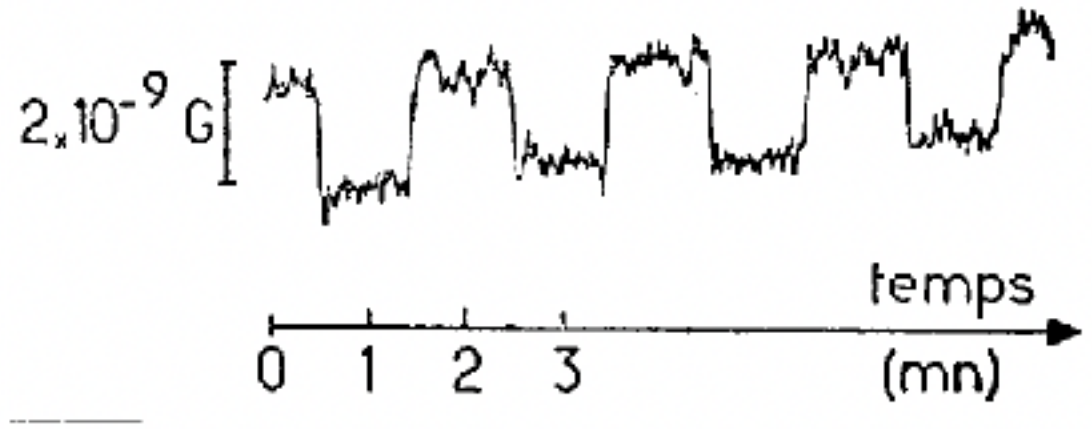

200 fT !

J. Dupont-Roc, S. Haroche et C. Cohen-Tannoudji, Phys. Lett. **28A**, 638 (1969)

Atomic magnetometry

Volume 28A, number 9 PHYSICS LETTERS 10 February 1969

p even and the same width as the Hanle curve (strictly independent of the r. f. power). We make a selective amplification of the modulation ω (p = 1) and a phase sensitive detection with a time constant of 3 sec. By this way, we have got, for optimal pumping beam intensity, a signal to noise ratio of 2.5×10^3 with a width of 5 μG.

For detection of very weak magnetic fields, we fix H_0 at the zero value, corresponding to the maximum slope of the dispersion shaped resonance. We can test the sensitivity of the apparatus by sending on sweeping coils square pulses of current corresponding to a given variation, δH_0, of H_0. Fig. 1 shows the signal obtained for $\delta H_0 = 2.1 \times 10^{-9}$ gauss. This sensitivity can be still improved for repetitive signals by using noise averaging multichannel techniques. Fig. 2 shows 3×10^{-10} gauss amplitude pulses.

Such a high sensitivity, the highest to our knowledge, seems promising for several applications: measurement of the very weak interstellar fields, biomagnetism [7], measurement of the static magnetization of very dilute magnetic samples, . . .

The authors are grateful to M. A. Bouchiat and J. Brossel for their constant interest during the course of this work.

References

1. W. Hanle. Z. Phys. 30 (1924) 93.
2. J. C. Lehmann and C. Cohen-Tannoudji, Comptes Rend. 258 (1964) 4463.
3. M. A. Bouchiat and J. Brossel, Phys. Rev. 147 (1966) 41.
4. E. B. Alexandrov, A. M. Bonch-Bruevich and B. A. Khodovoi, Opt. Spectry. 23 (1967) 151.
5. T. Ito, K. Kondo and T. Hashi, Jap. J. Appl. Phys. 7 (1968) 565.
6. N. Polonsky and C. Cohen-Tannoudji. Comptes Rend. 260 (1965) 5231.
   For excited states see:
   C. J. Favre and E. Geneux, Phys. Letters 8 (1964) 190.
   E. B. Alexandrov et al., Zh. Eksp. i Teor. Fiz. 45 (1963) 503.
7. A. Kolin, Physics Today, November 1968, p. 39.

Today's sensitivity of atomic magnetometers $\approx \mathrm{fT}/\sqrt{\mathrm{Hz}}$

MAG4Health

magnetoencephalography

Could similar methods be implemented using solid-state quantum systems?

Point defects in crystals (Nevill Mott)

Perfect crystal

Translational symmetry.

The electron moves in the average field of other electrons and nuclei

→ Bloch states delocalized on the whole crystal

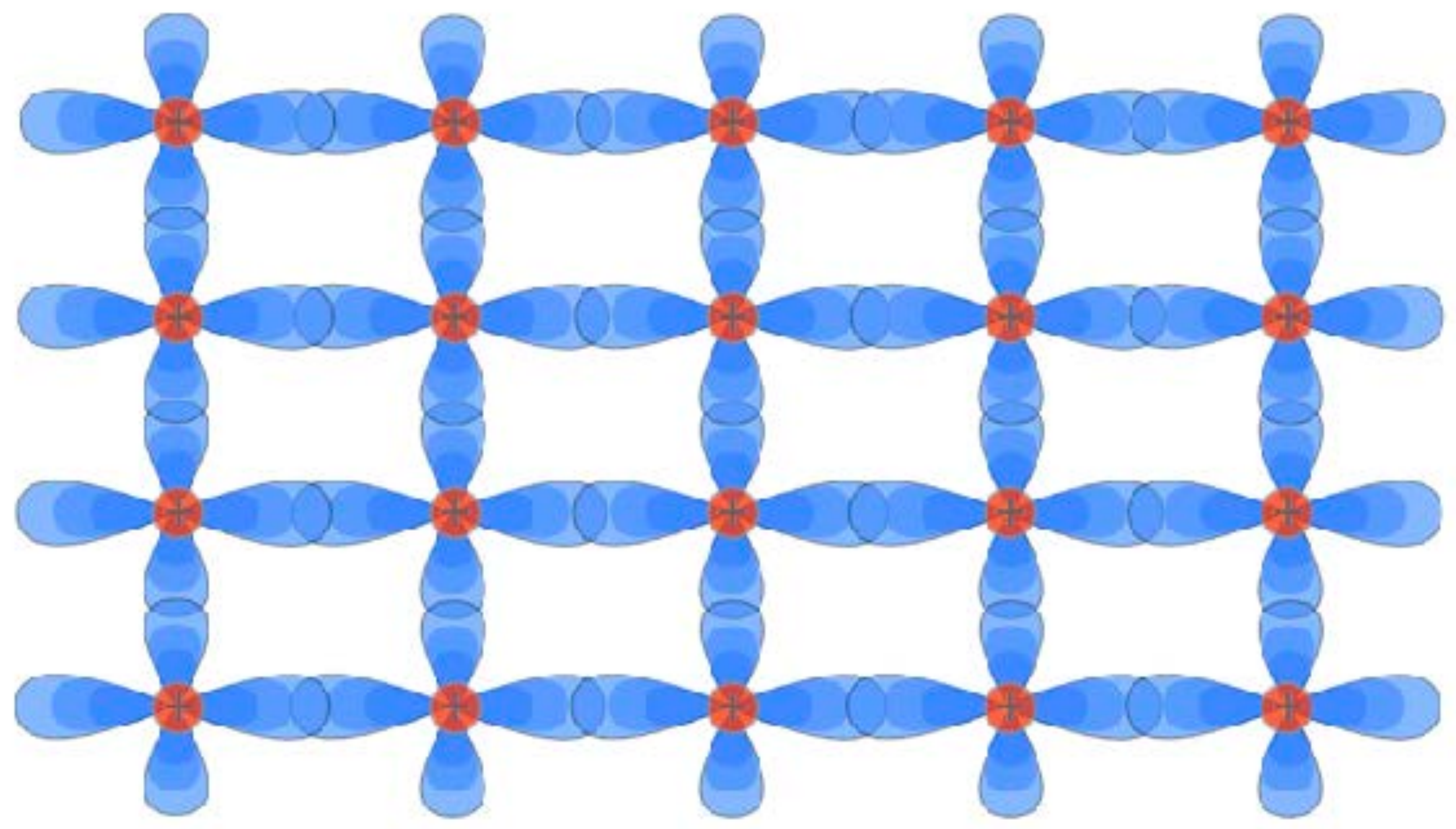

Localized vacancy

Symmetry reduced to reflections and rotations.

Unpaired electrons → dangling bonds

→ state localized on the vacancy, discrete energy levels

Electronic spin, coupling to nuclear spins

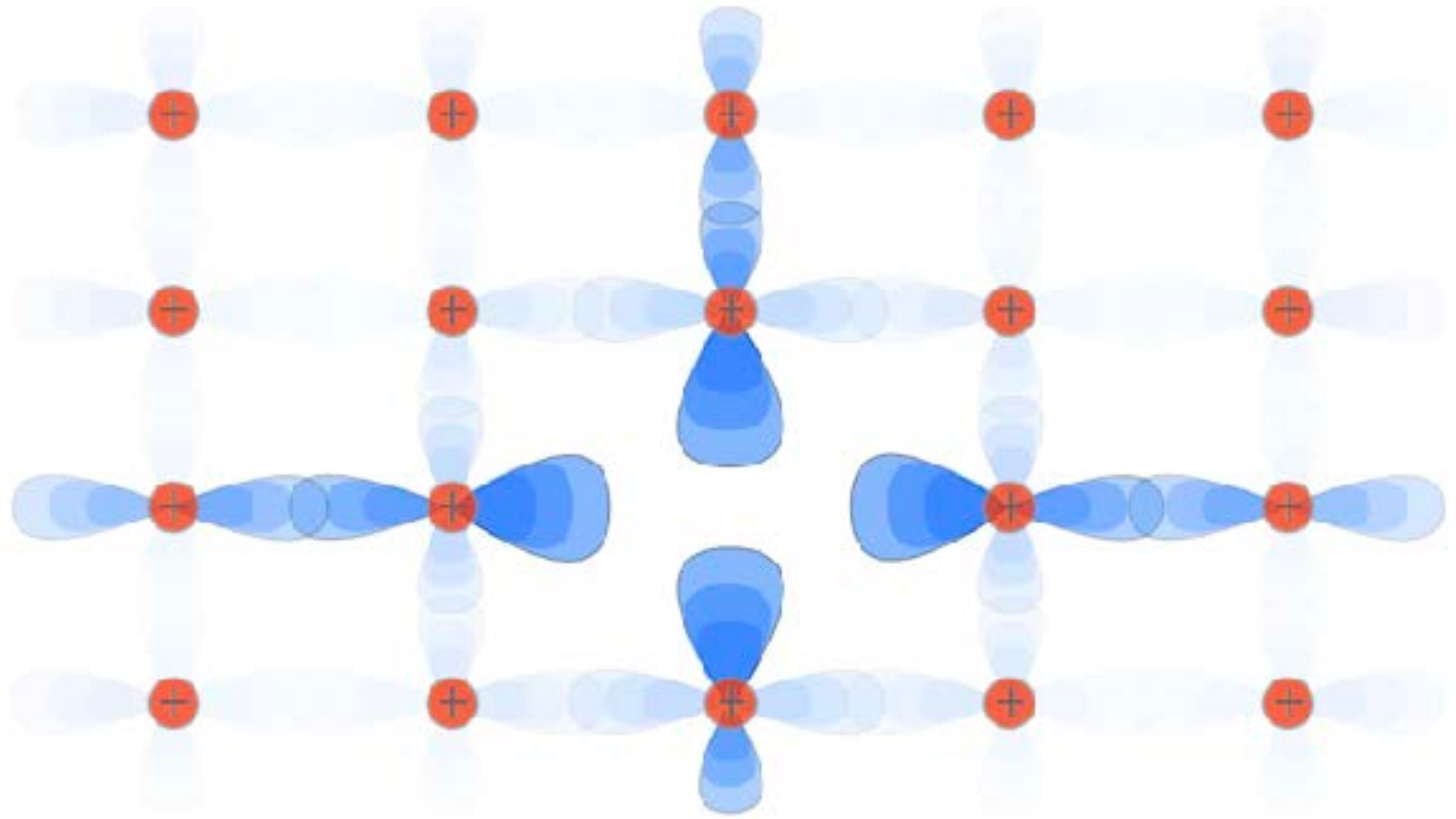

A point defect is an artificial molecule in the solid state

Example: The Nitrogen-Vacancy (NV) center in diamond

Jörg Wrachtrup (1997)

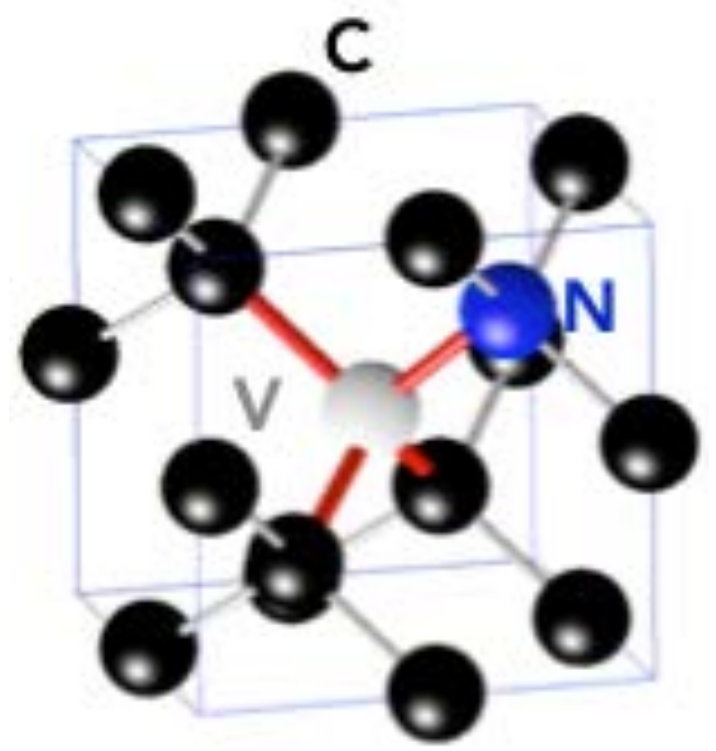

NV center in diamond: a solid-state atomic-like system

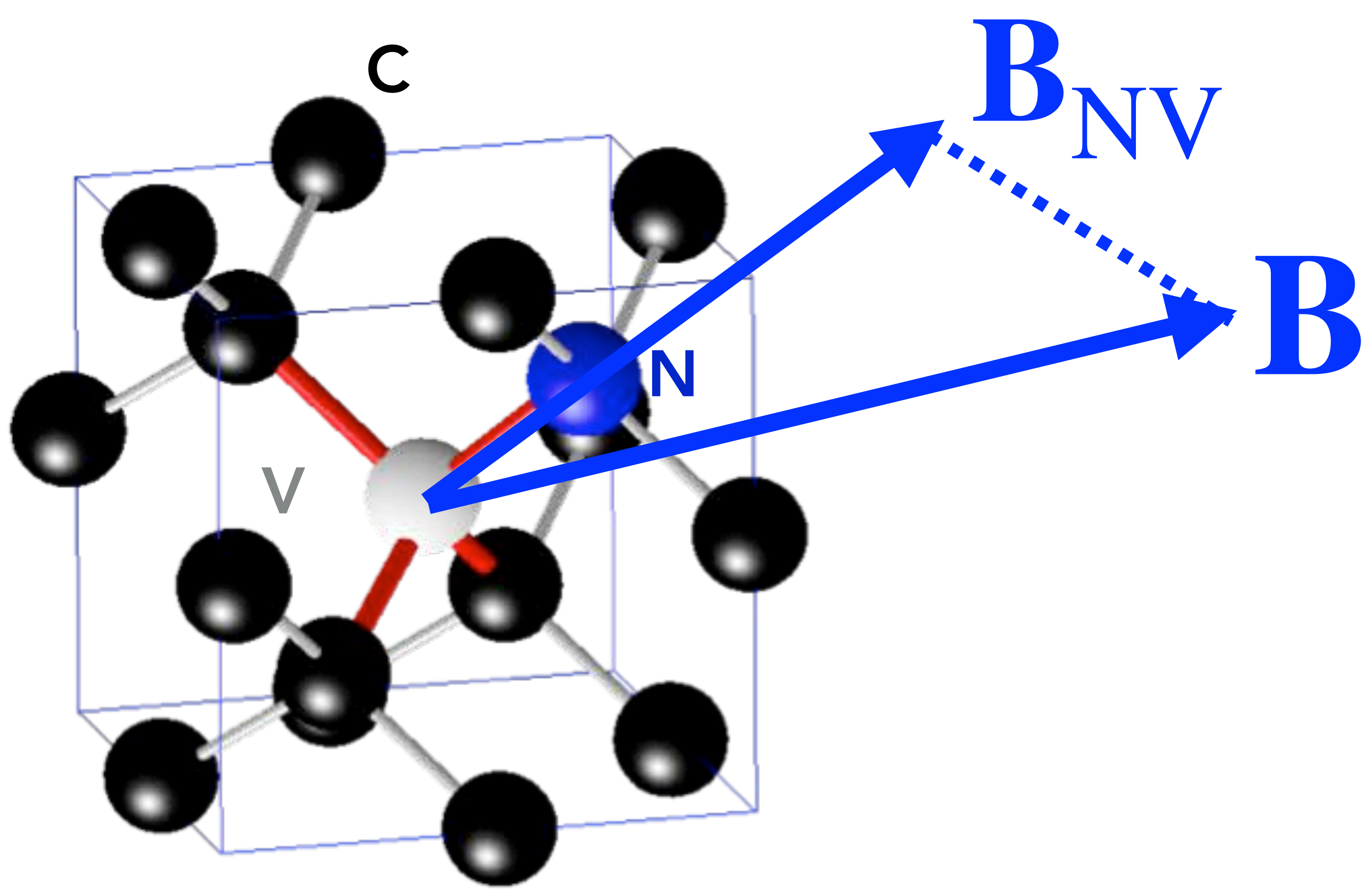

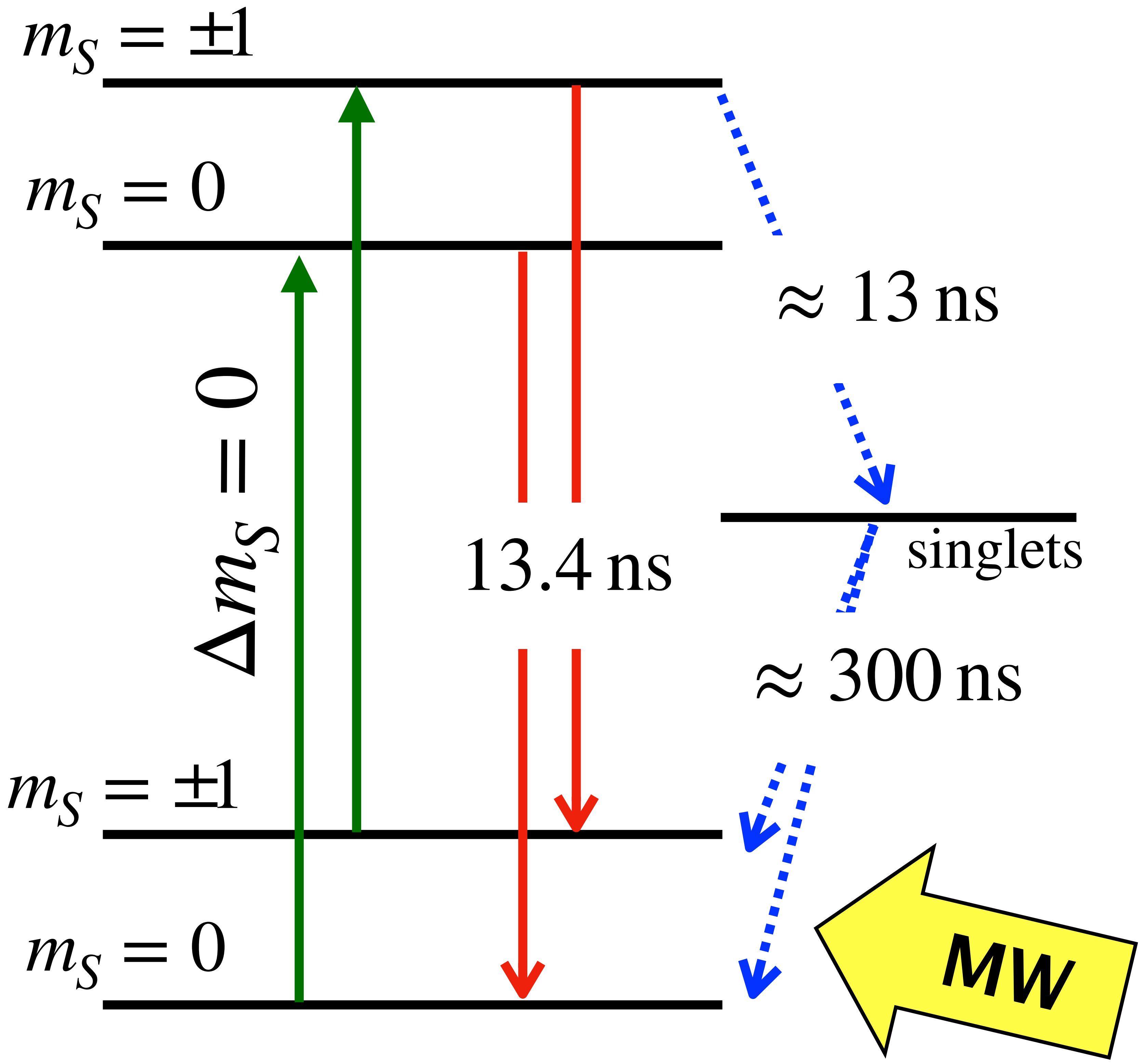

Atomic-like energy levels within the 5 eV diamond bandgap

Electronic ground state is a spin triplet $S = 1$

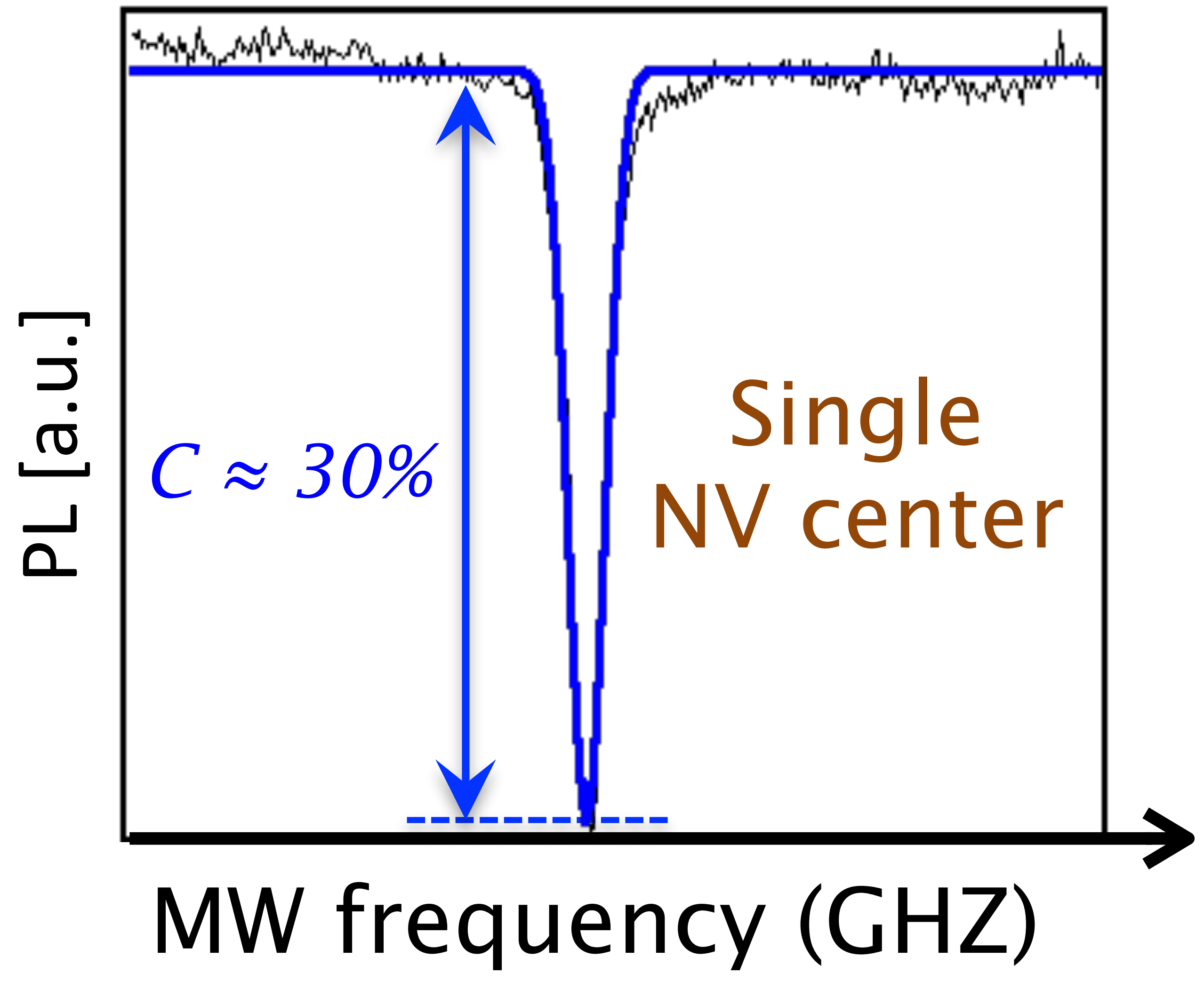

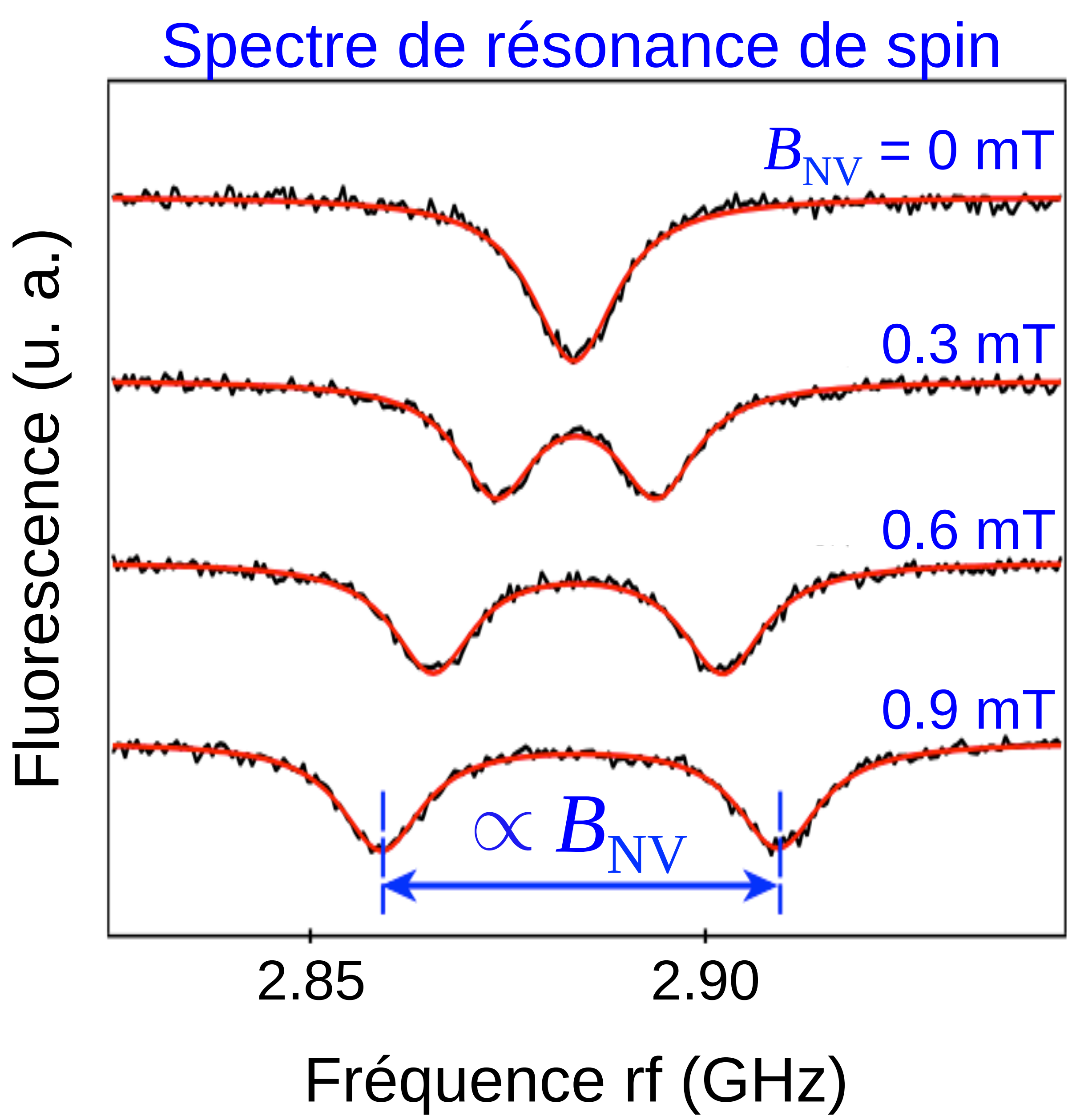

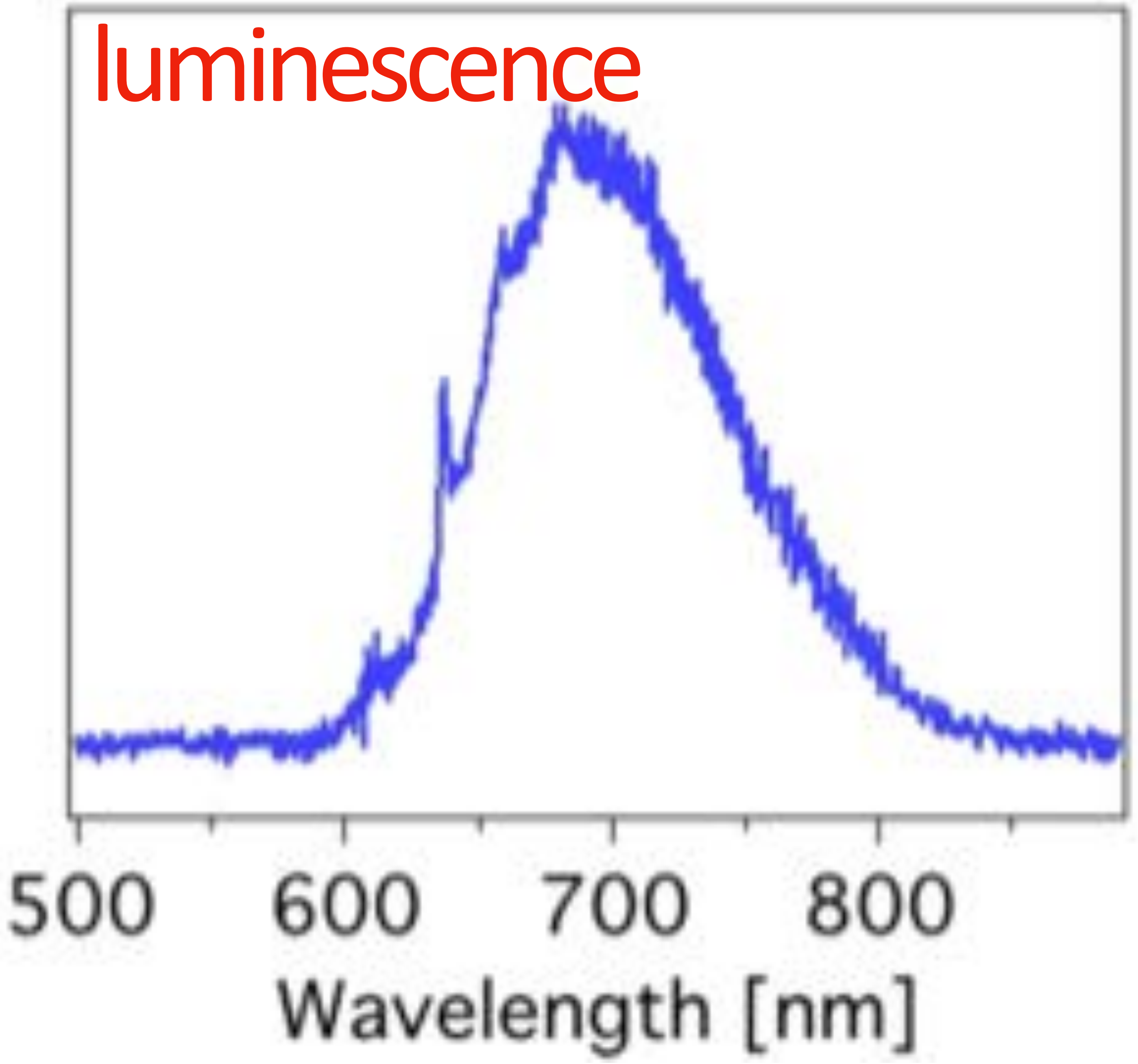

NV center : magnetometer
of atomic size with sensitivity
to static magnetic field of 10^{-6} T
→ myriad of applications!

Review: L. Rondin et al.,
Rep. Prog. Phys. **77**, 056503 (2014)

Widefield magnetic imaging using NV centers also called "Quantum diamond magnetometry"

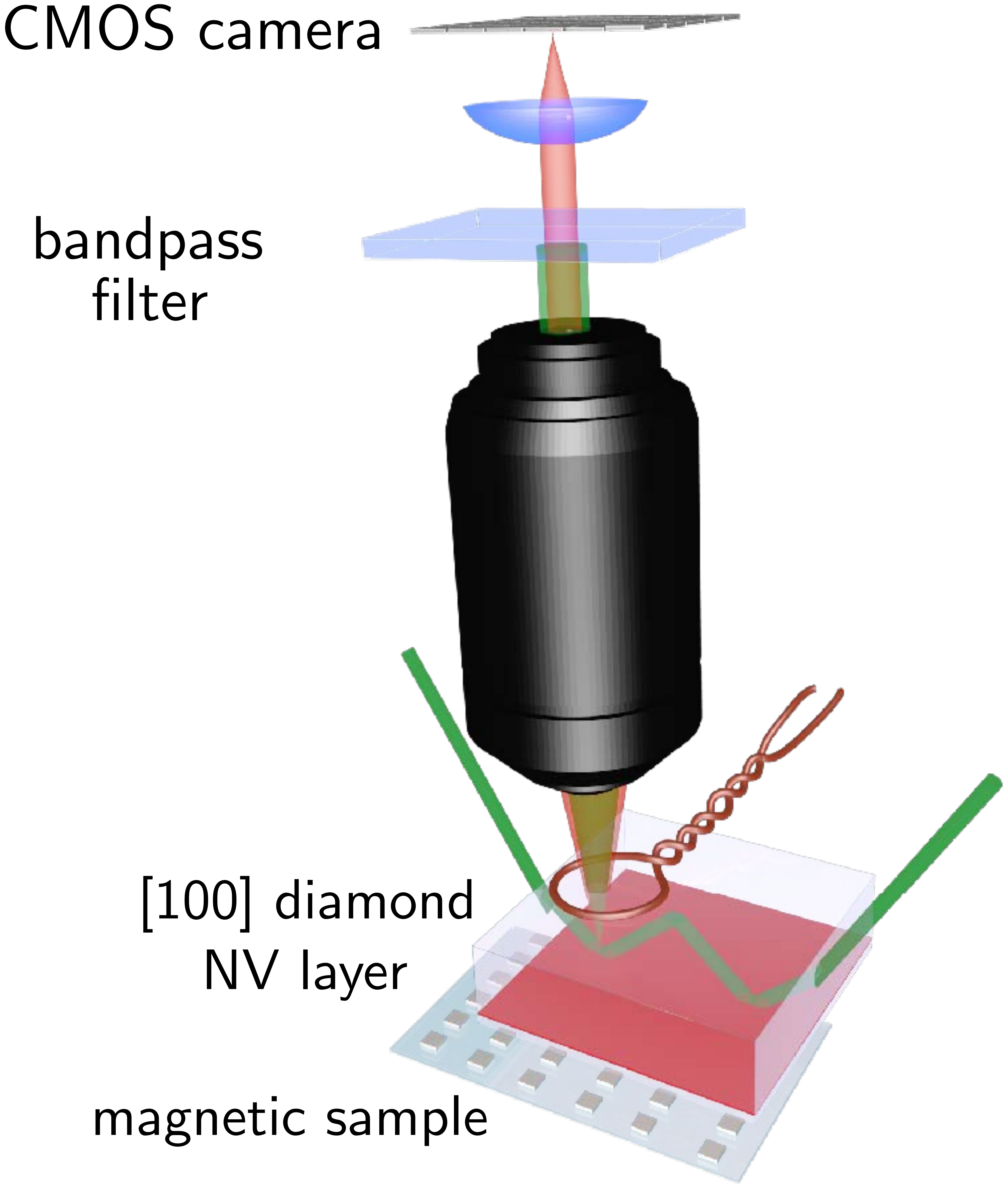

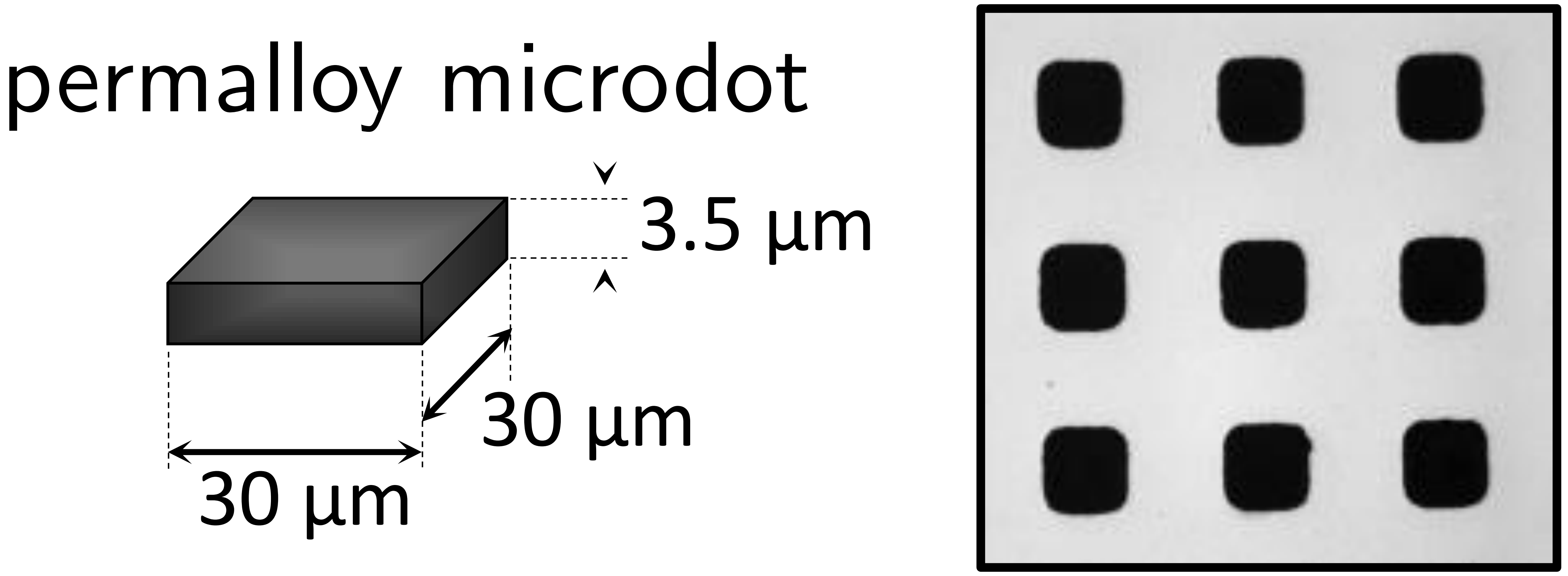

THALES Th. Debuisschert

Optically-based magnetic field mapping

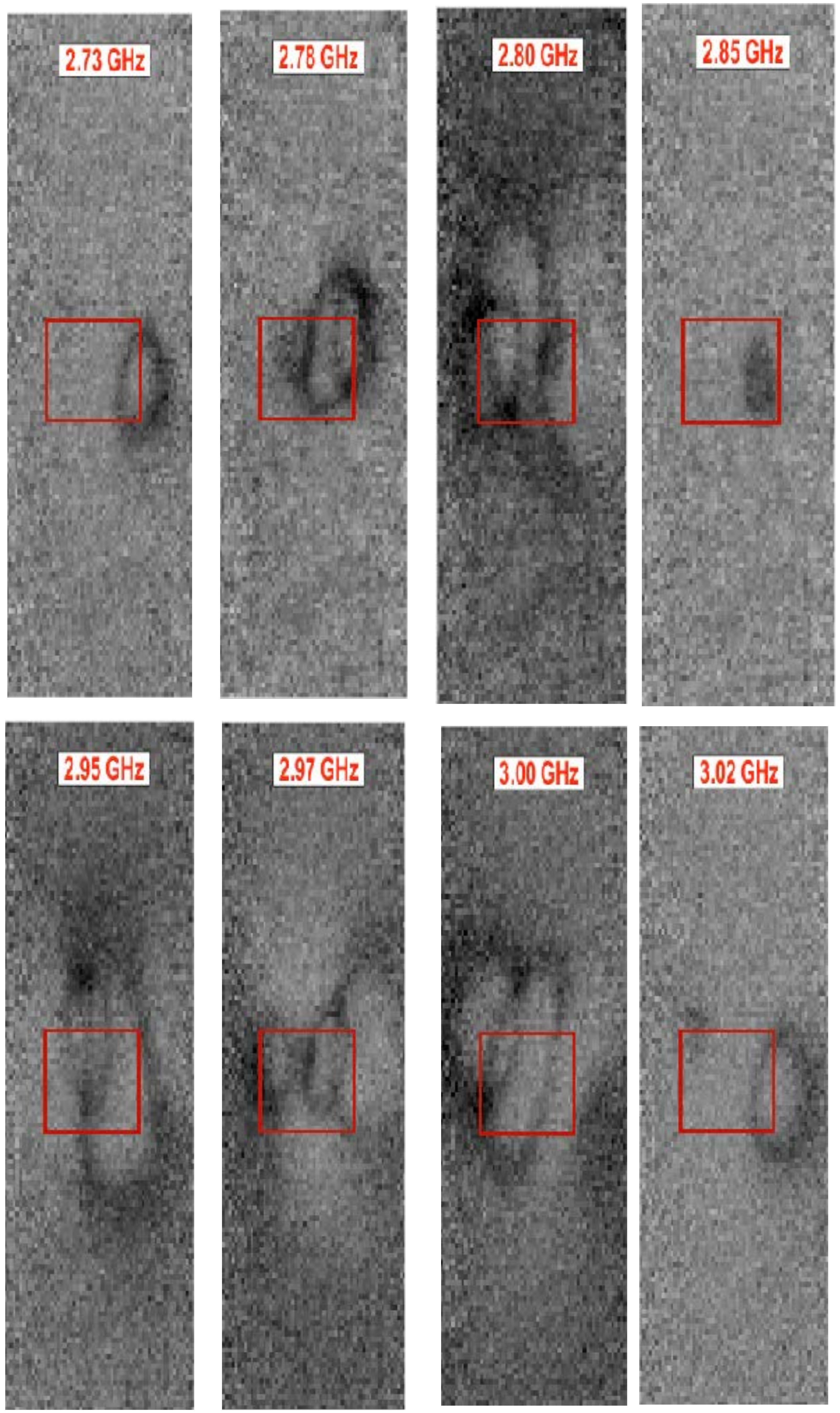

square = micromagnet

each pixel records a snapshot of ESR spectra
with the four NV orientations in the (110) crystal

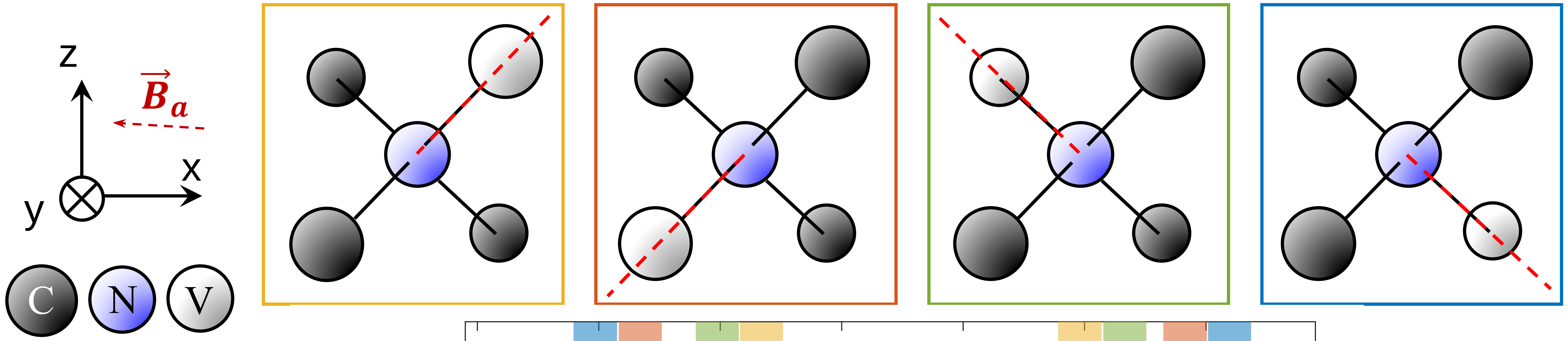

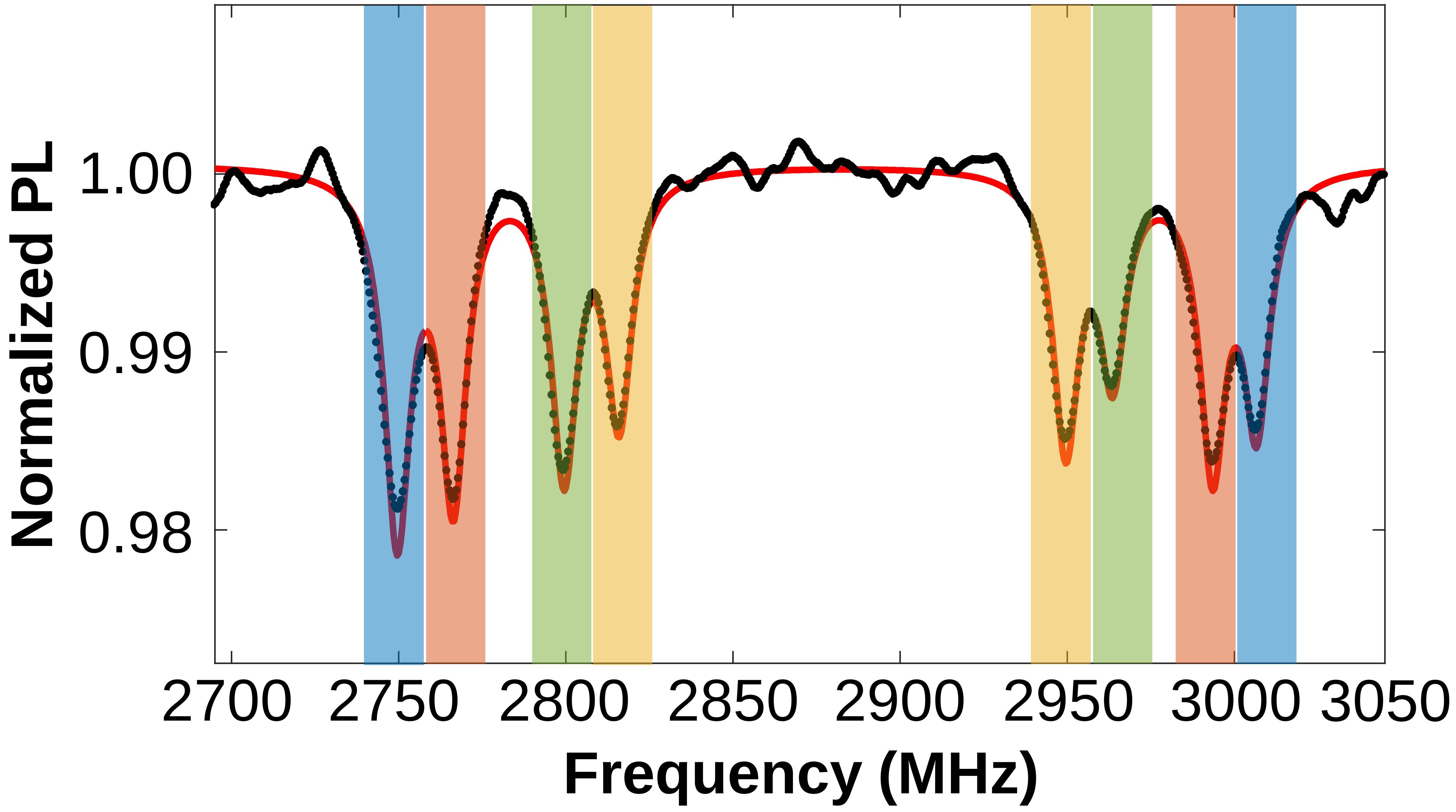

4 correlated measurements $\rightarrow$ (B_x, B_y, B_z)

M. Chipaux et al. Eur. Phys. J. D 69, 166 (2015)

Microscale measurement of magnetization

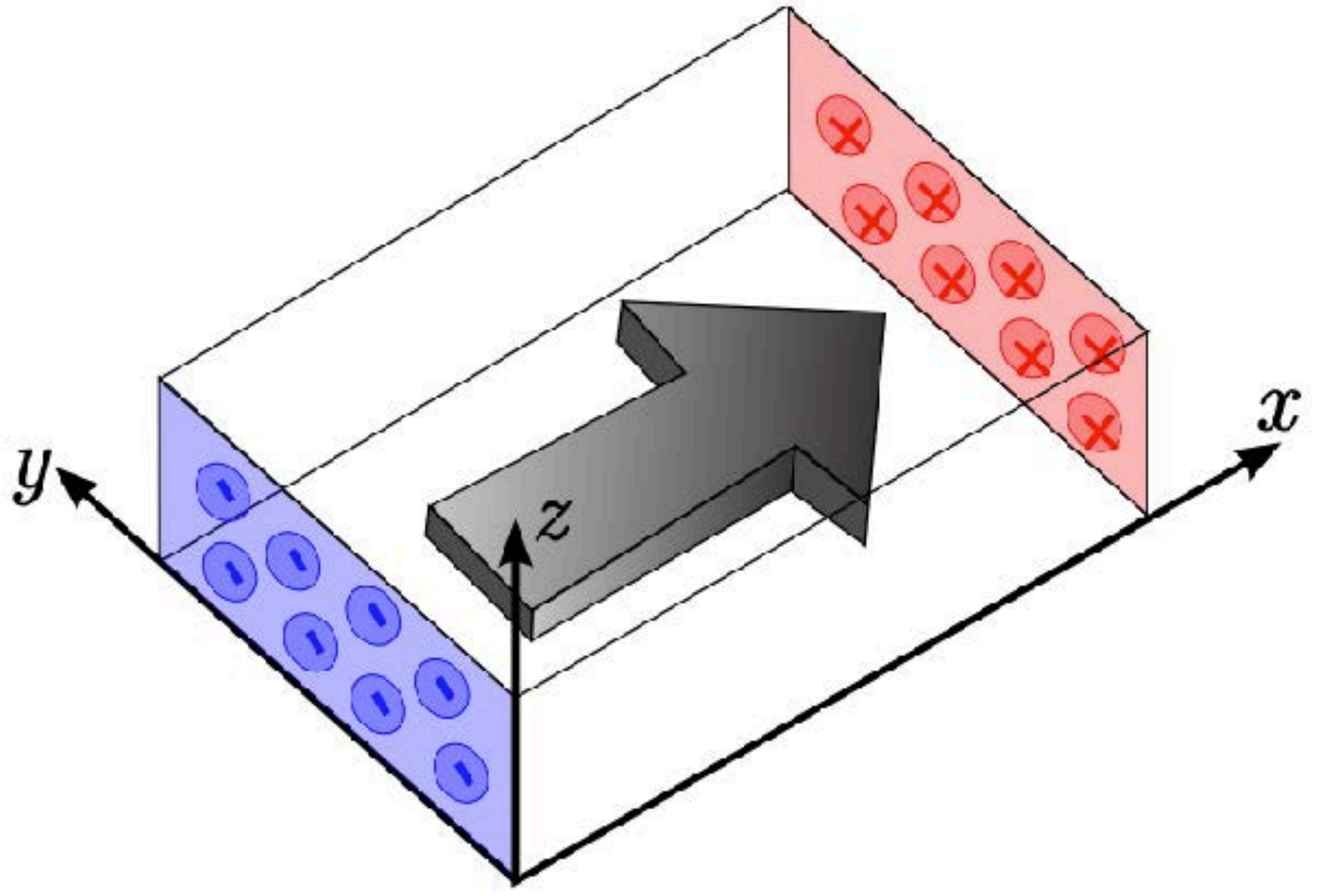

In each permalloy micromagnet, the magnetization M is induced by the applied magnetic field B_a

$10^4\,\mathrm{NVs}/\mu\mathrm{m}^{-2}$

$B_a = 6.3\,\mathrm{mT}$

distance NV-sample : $d = 19.5\,\mu\mathrm{m}$

$M = (8 \pm 2) \times 10^{-4}\,\mathrm{A/m}$

equivalent to $10^{-7}\,\mathrm{emu} \approx 10^{13}\,\mu_\mathrm{B}$

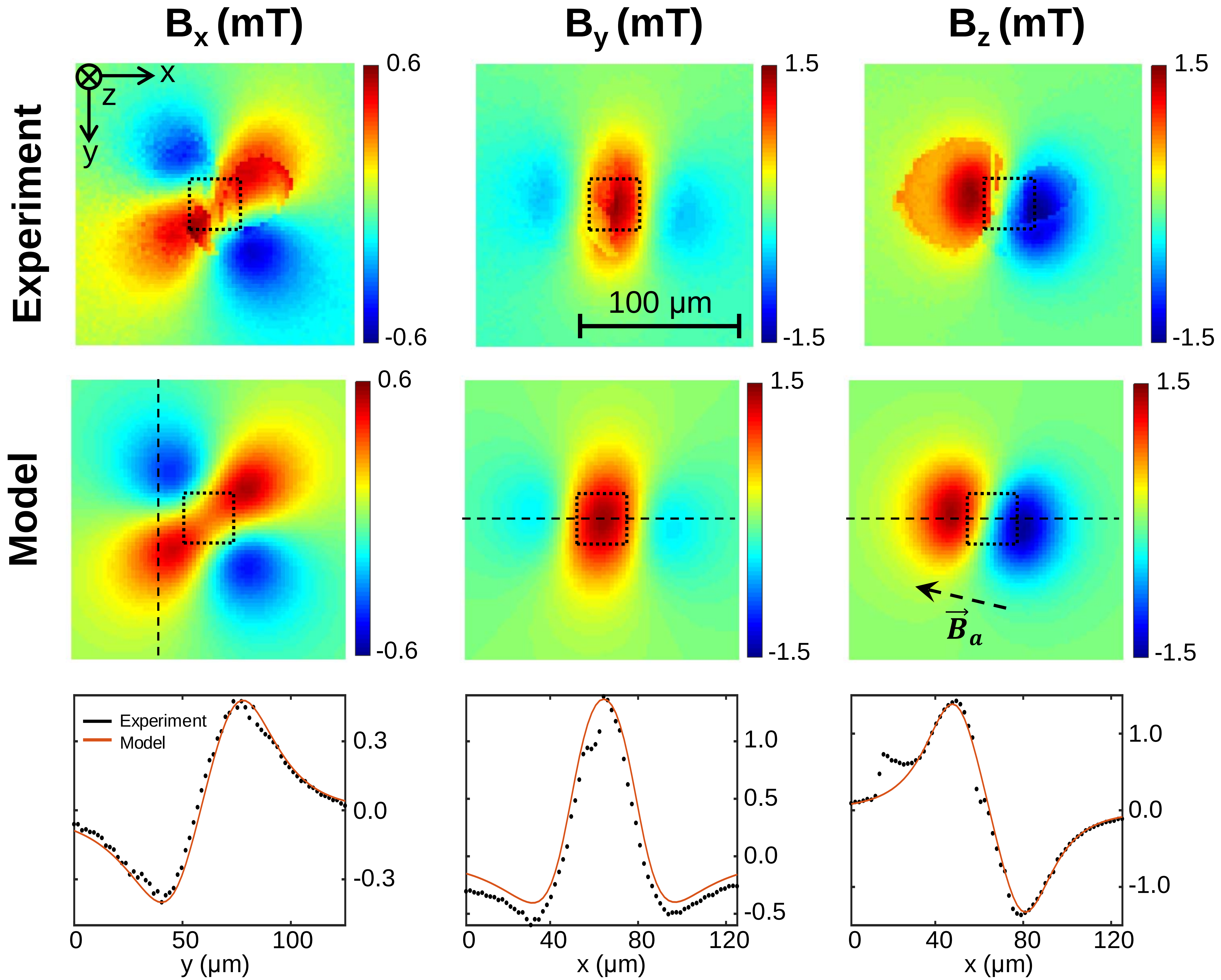

Signal for $d \approx 20\,\mu\mathrm{m}$ ≡ sensitivity of commercial SQUID

L. Toraille et al., Nano Letters **18**, 7635 (2018)

What can we measure with NV centers?

$$\mathscr{H}_{\rm NV} = DS_z^2 + g\mu_{\rm B}\mathbf{B}\cdot\mathbf{S} + \mathbf{S}\cdot\overline{\overline{\mathscr{A}}}\cdot\mathbf{I}$$

optical pumping
532 nm

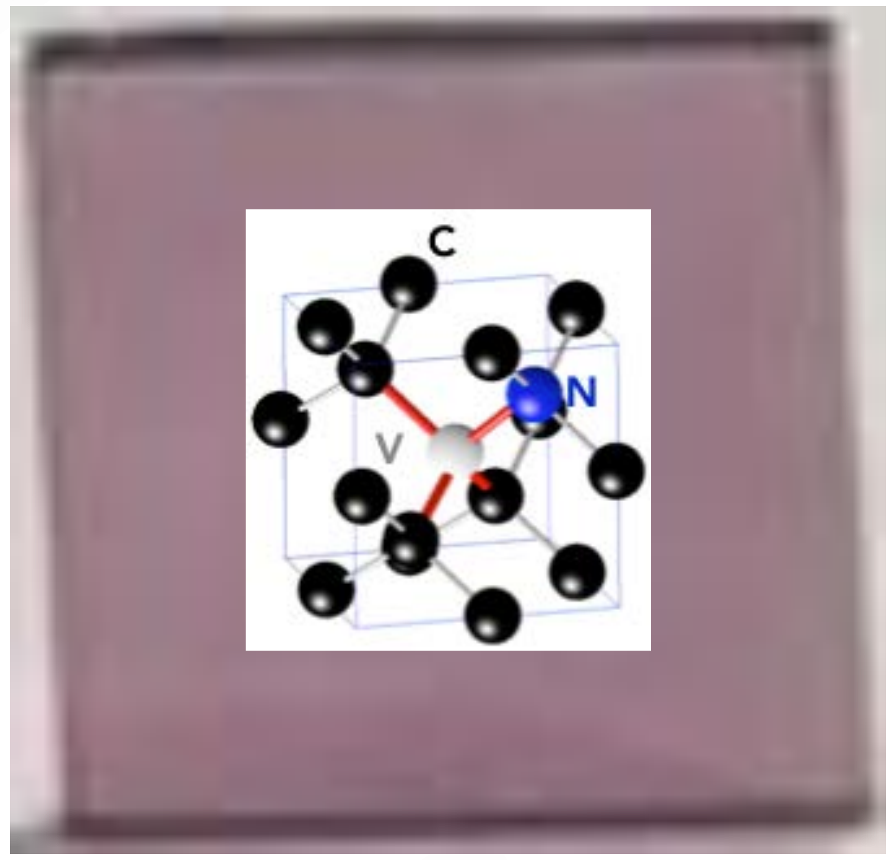

microwave
2.87 GHz

luminescence

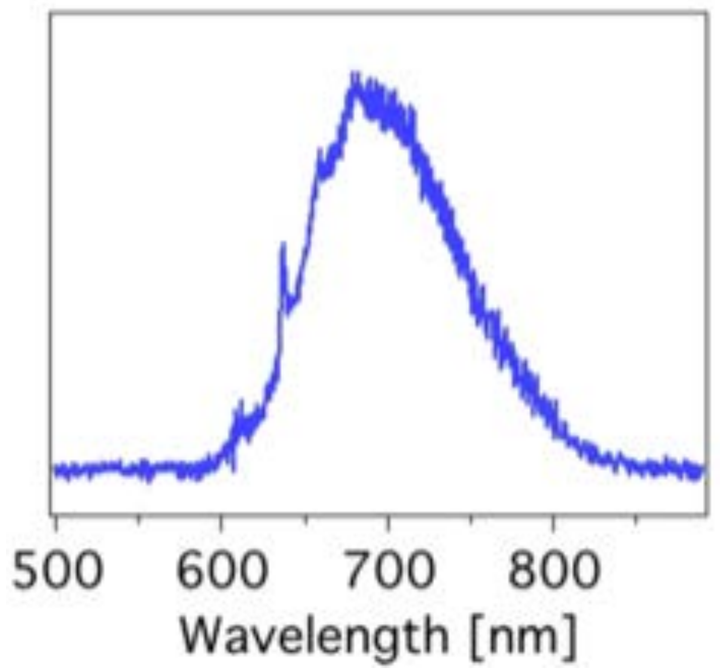

B Magnetic field

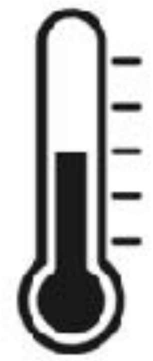

T Temperature

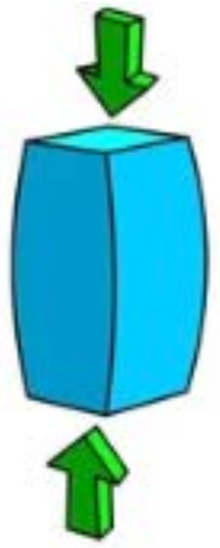

$\overline{\overline{\sigma}}$ Stress tensor

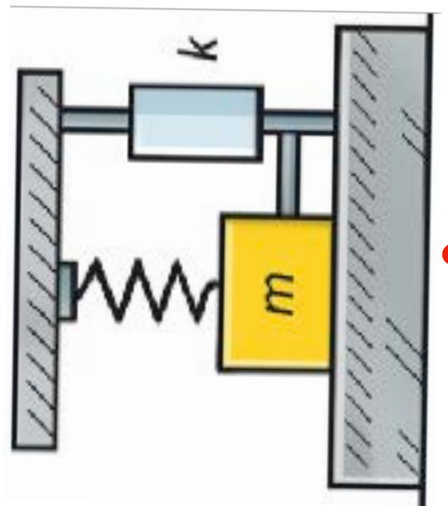

a Acceleration

ESR
NMR
Nearby spins

NV center sensing modalities

Temperature

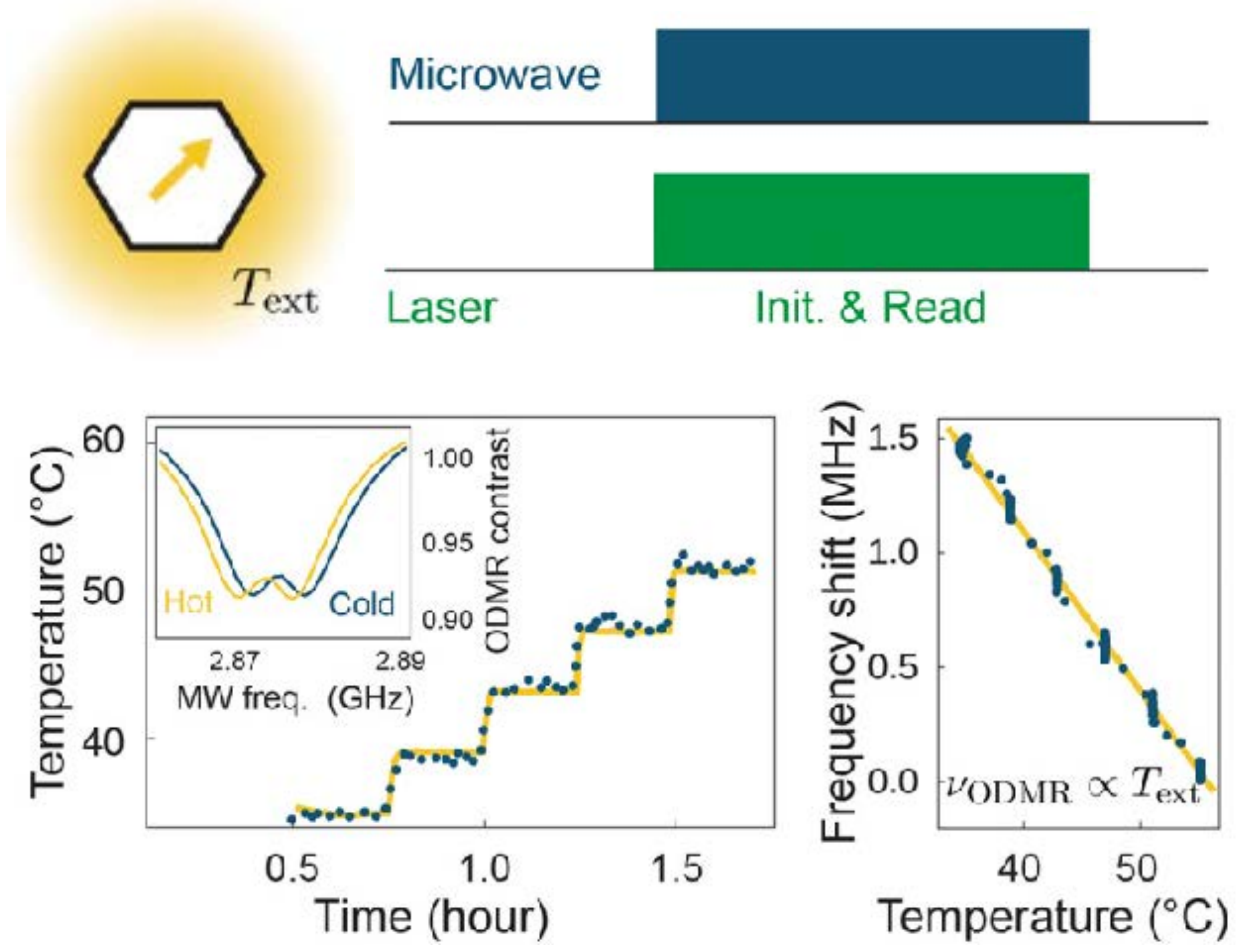

Electronic spins

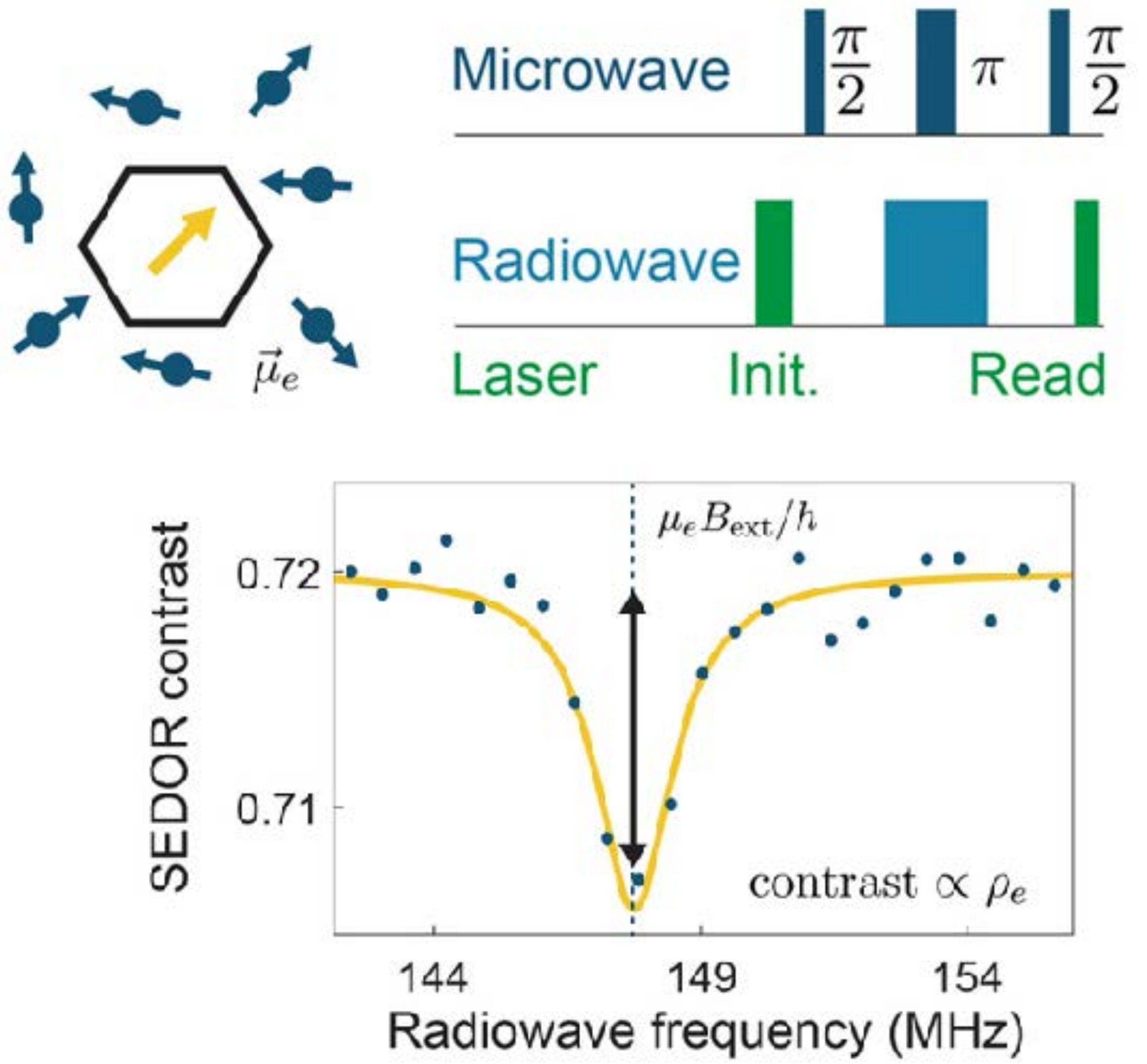

Nuclear spins

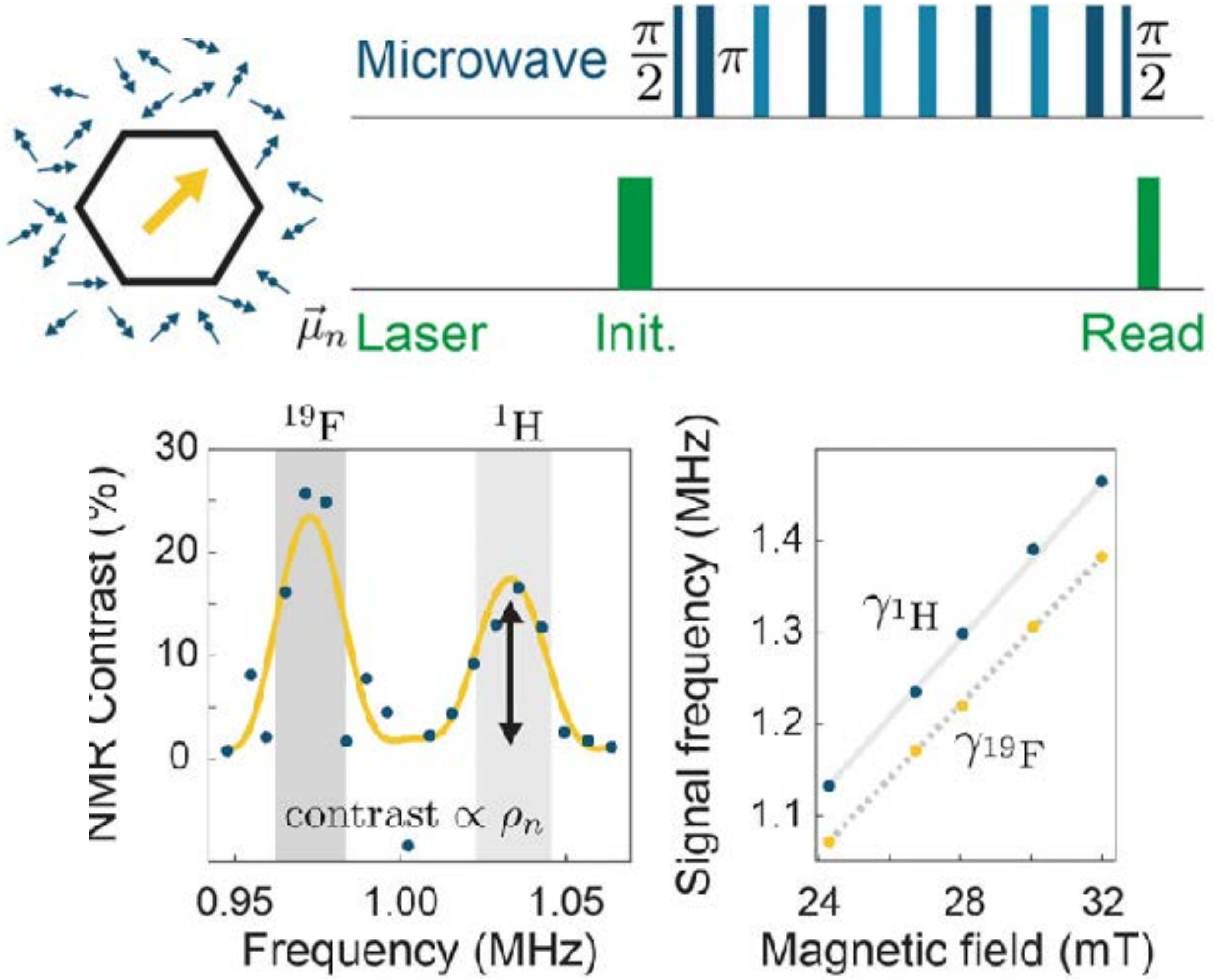

and a few more!

superconductivity high pressure

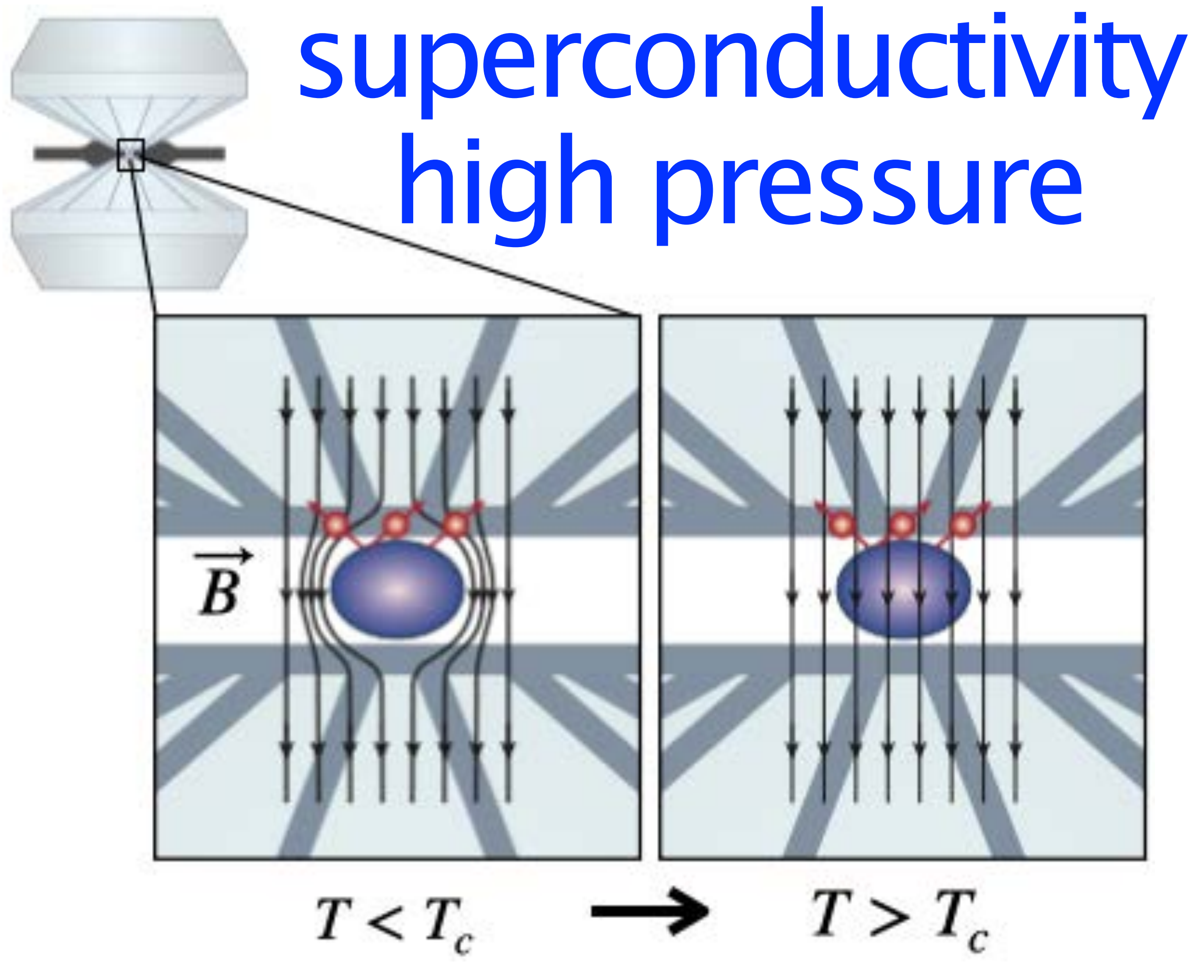

detection of ions, ROS using spin relaxometry

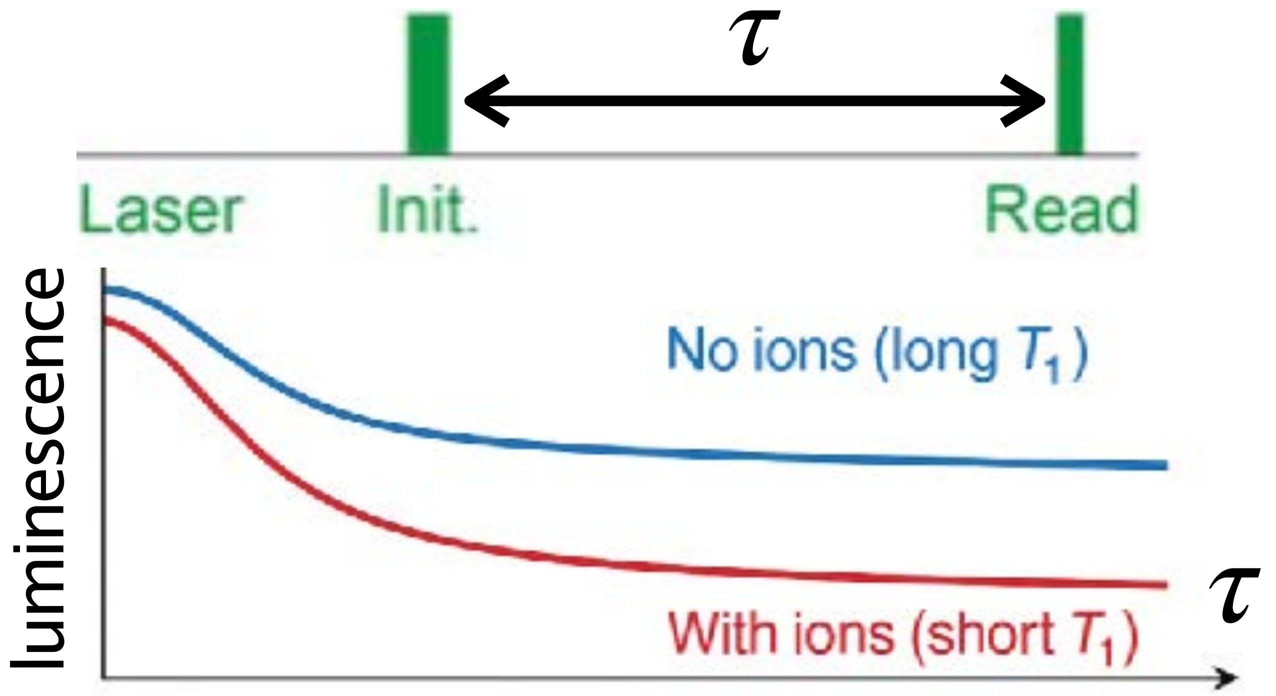

charge state conversion voltage sensing

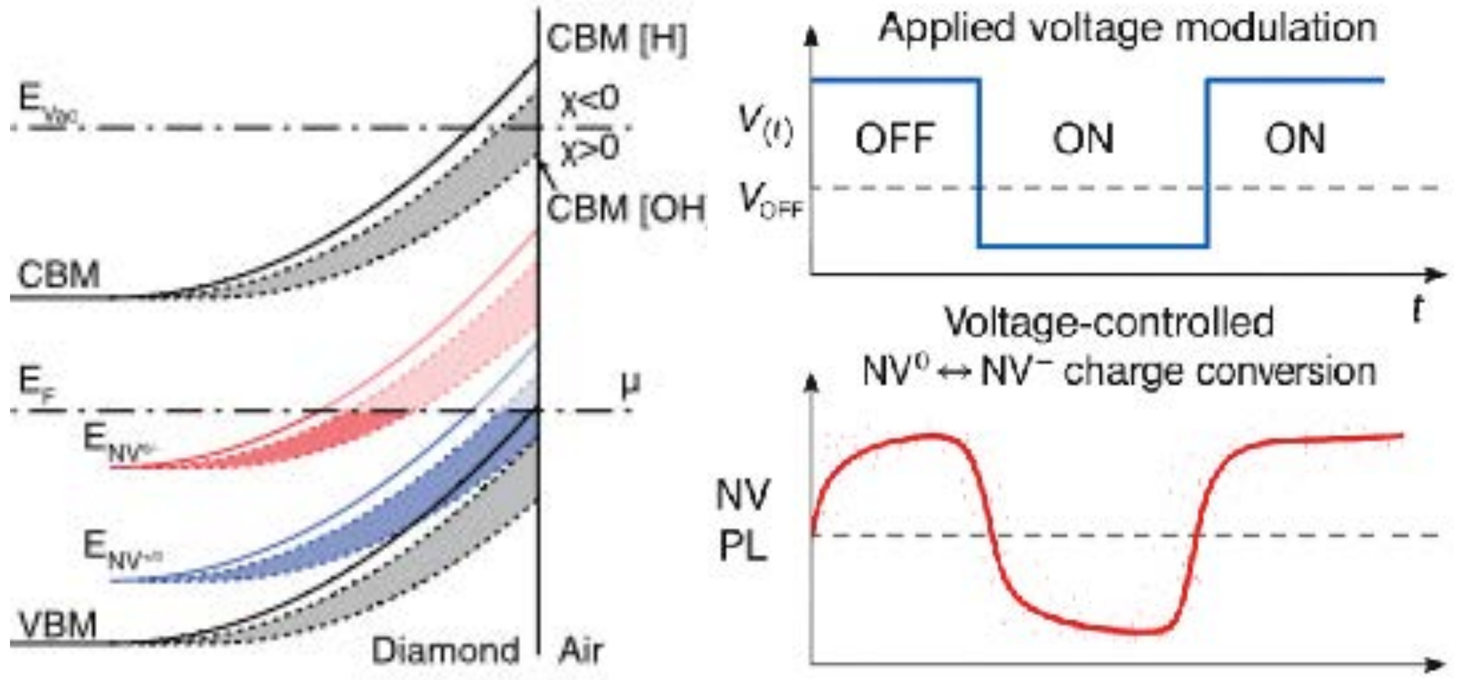

Optically accessible spin centers: More and more systems!

Diamond

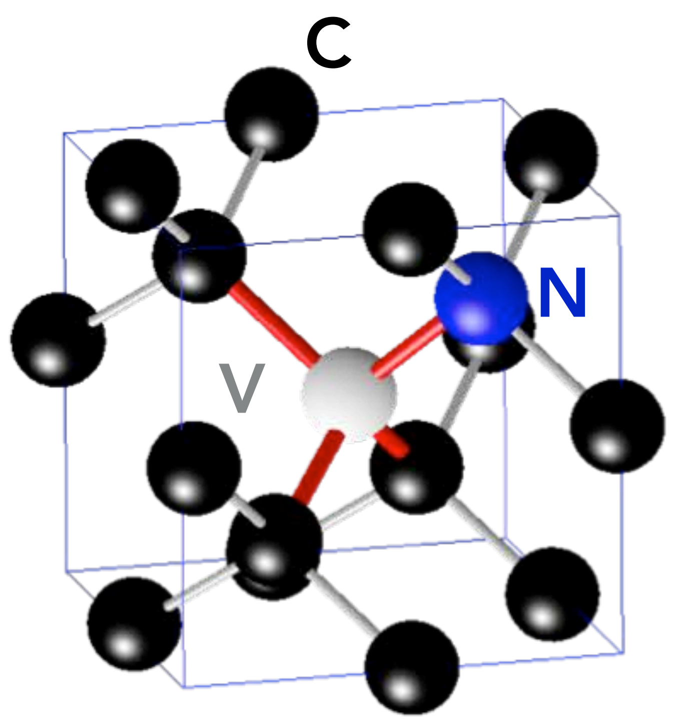

nitrogen vacancy NV center

Wrachtrup et al., Science (1997)

Silicon carbide

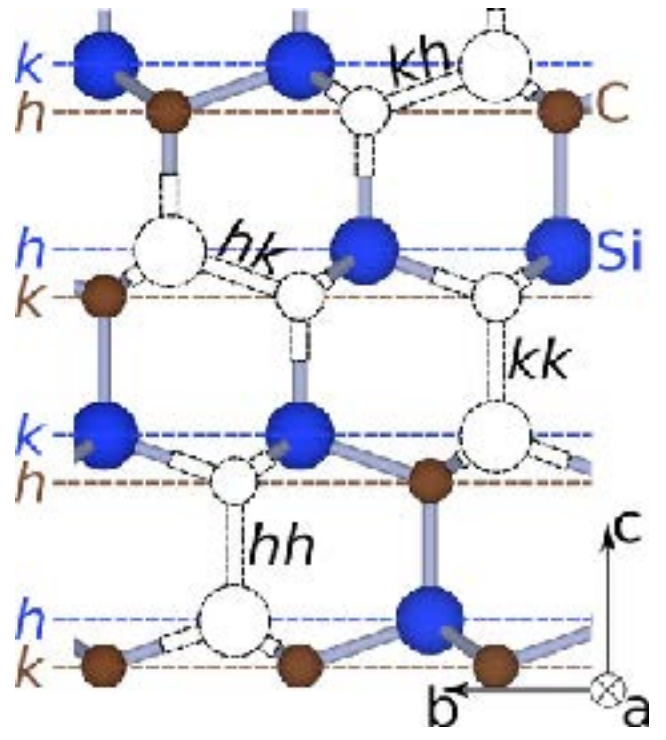

$V_{Si}V_C$ in 4H-SiC

Li et al., Nat. Sci. Rev. (2022)

2D: hexagonal boron nitride

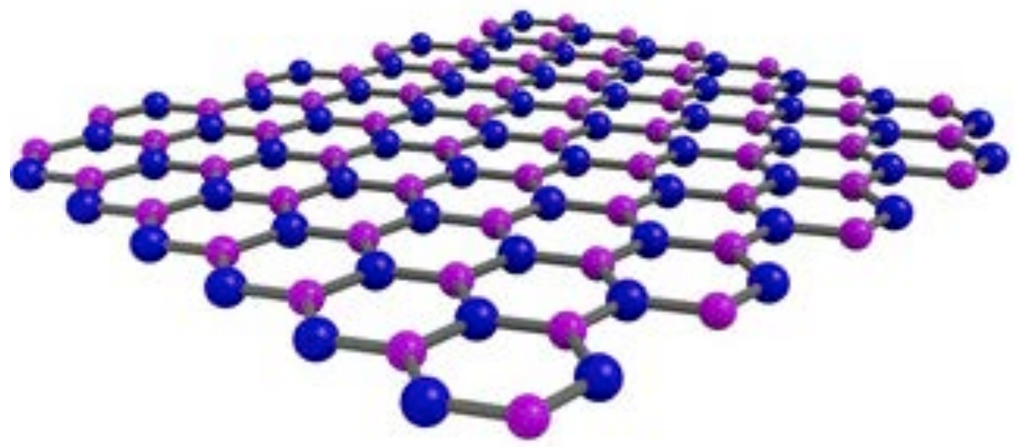

C-related defect (?)

Stern et al., Nat. Mat. (2024)

Gallium Nitride (and AlN, silicon)

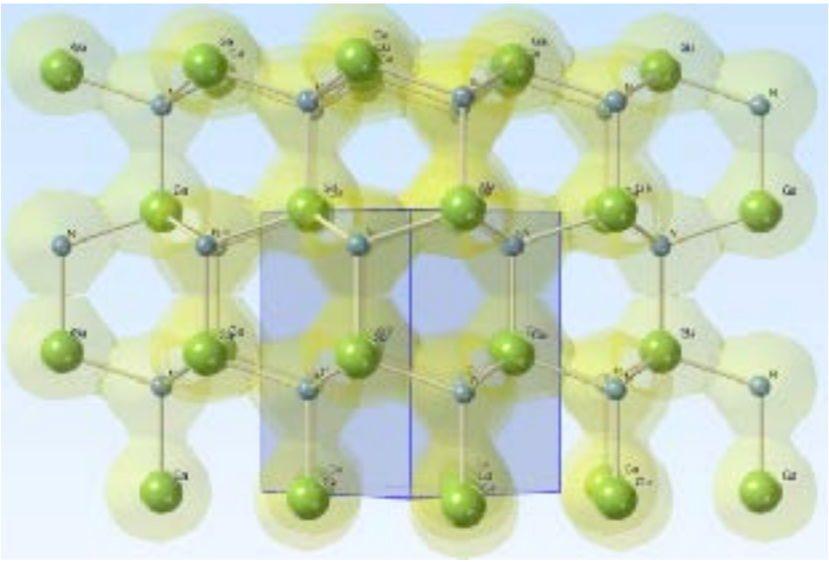

Two different species (?)

Luo et al., Nat. Mat. (2024)

Molecular systems

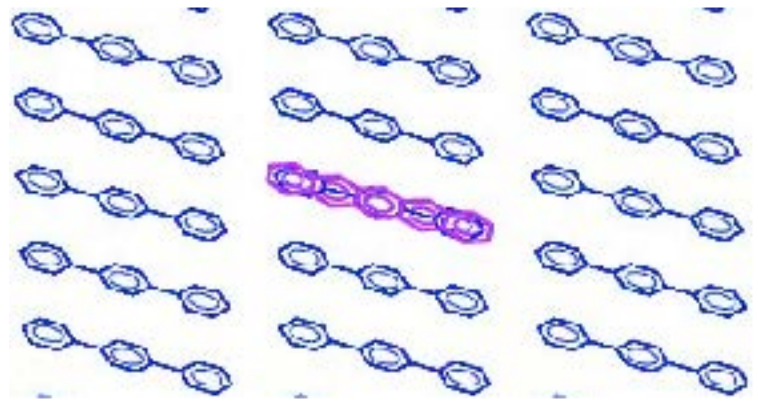

pentacene in para-terphenyl

Mena et al., Phys. Rev. Lett. (2024)

EYFP protein

Feder et al., Nature (2025)

Sensitivity of ODMR-based sensors

Shotnoise limit: $\eta \propto \frac{1}{\gamma} \times \frac{1}{C} \times \frac{1}{\sqrt{N \times T'}}$

γ : gyrometric ratio

C : readout fidelity (ODMR contrast)

N : number of spins (NV centers)

T' : interrogation time (spin dephasing time T_2^*)

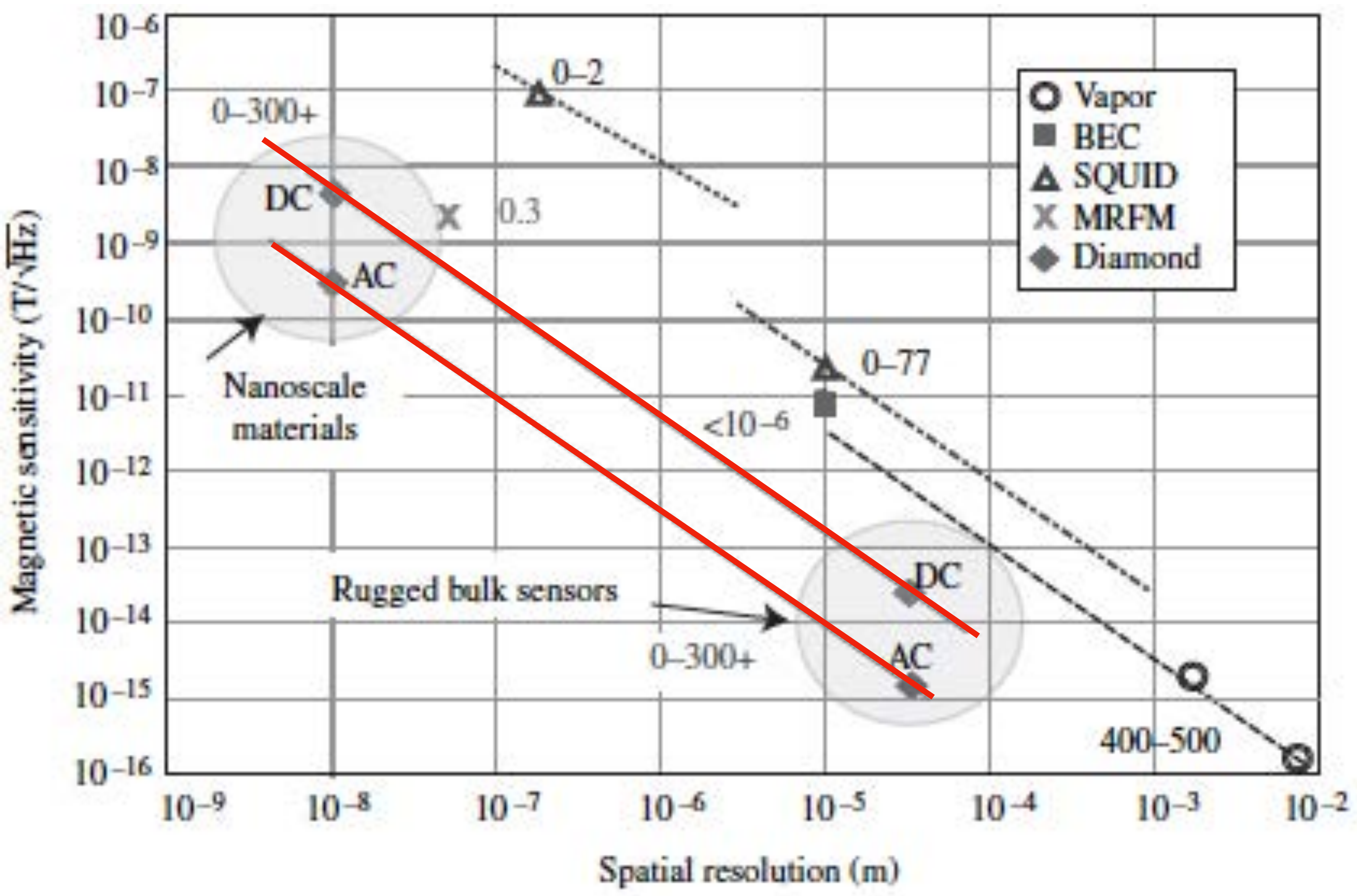

Budker & Kimball, Optical Magnetometry (Cambridge University Press, 2013)

Improvement strategies:

1) "Quantum–grade" diamond optimizing T_2^*
2) Improving light extraction ($n_{\mathrm{diamond}} = 2.4$)
   – Nanostructure fabrication
   – Micro and nanoscale optical lenses
3) Electrical detection of the NV resonance

“Quantum-grade” diamond: Spin dephasing time T_2^*

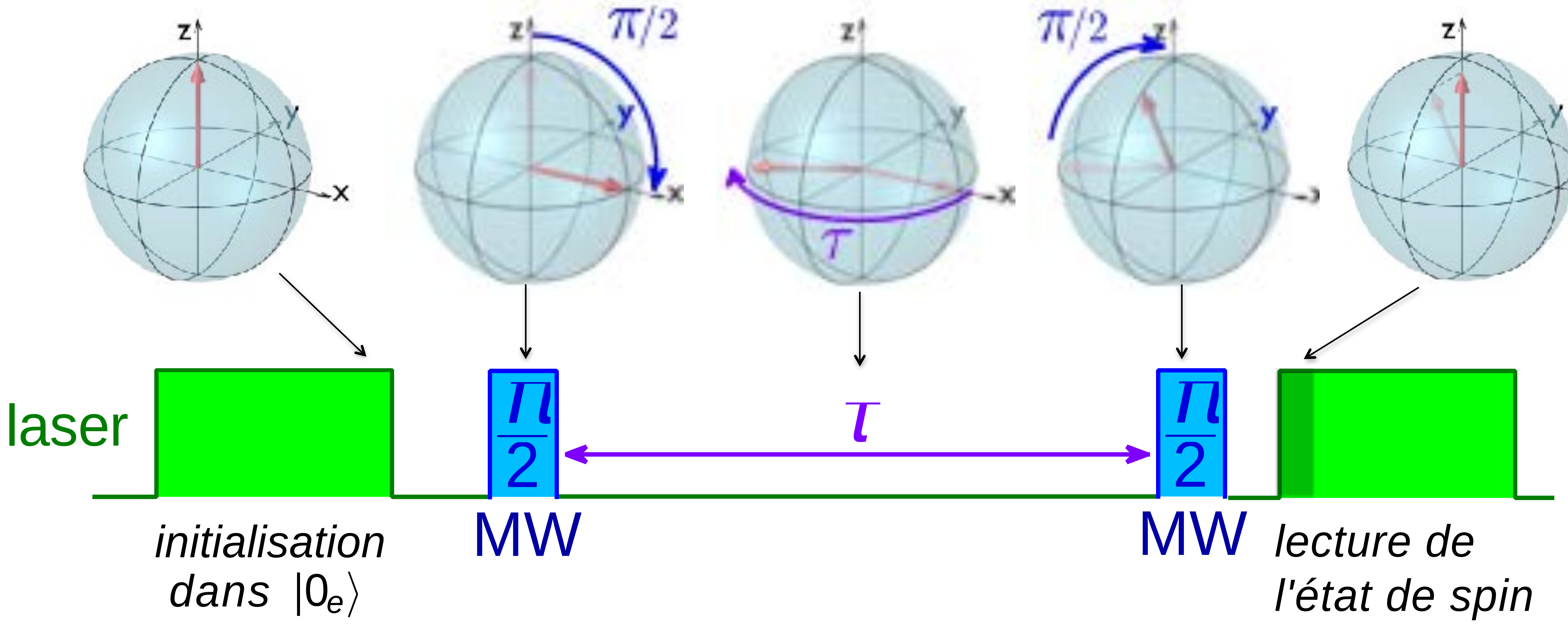

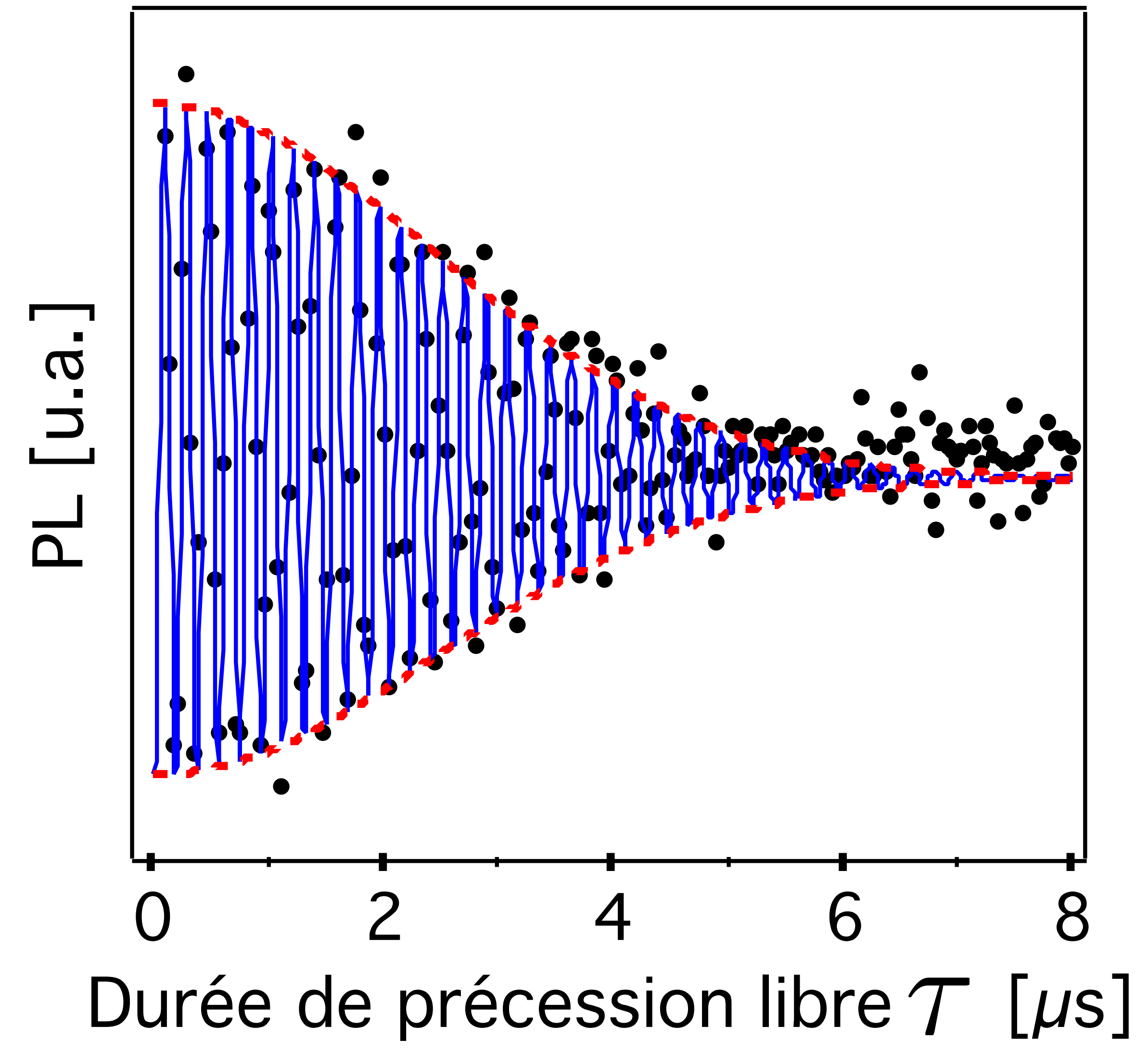

HPHT	CVD	^{12}C enriched

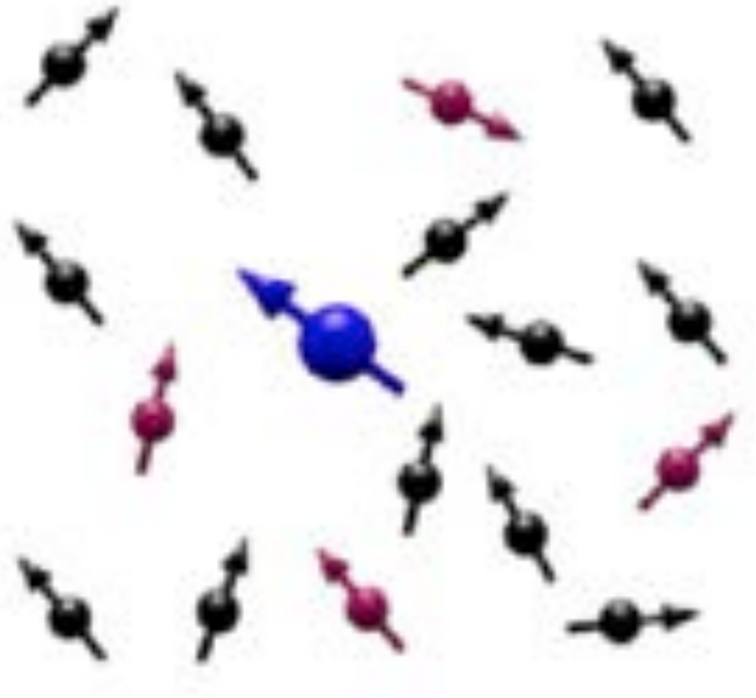

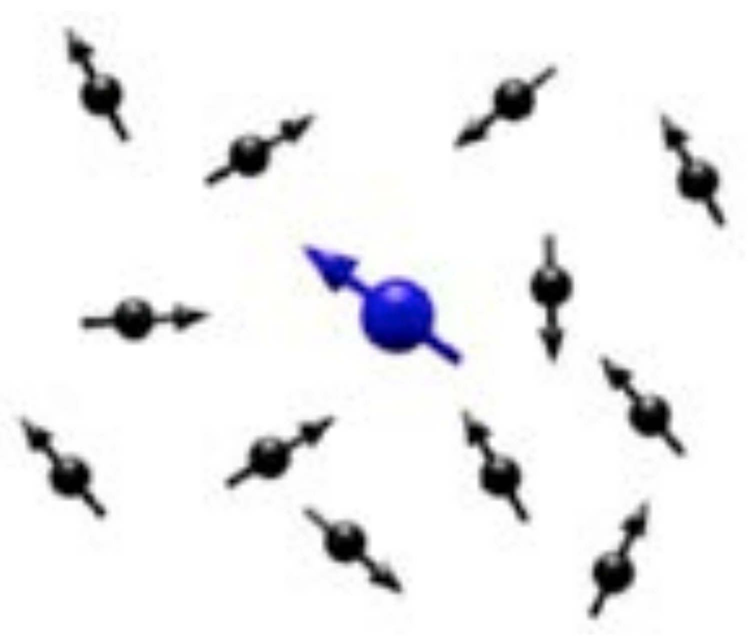

nitrogen electronic spins
$[N] \approx 100$ ppm

^{13}C nuclear spins
$[^{13}C] \approx 1.1\ \%$

$[^{13}C] \approx 0.1\ \%$

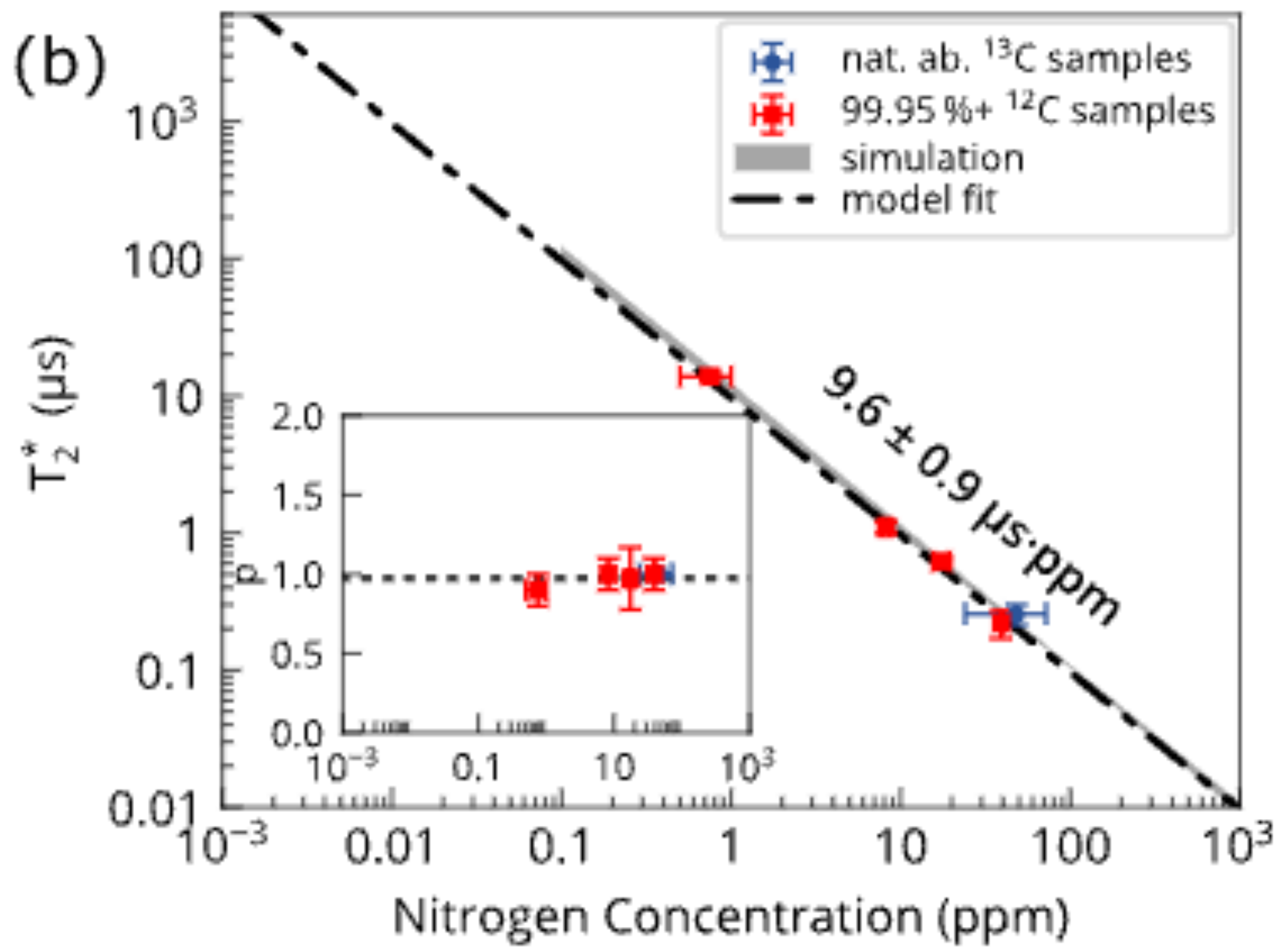

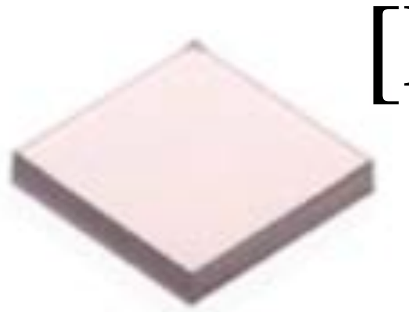

$[NV] \approx 3$ ppm $T_2^* \approx 3\ \mu s$

HIQUTE DIAMOND

Low-dimensional nanostructures

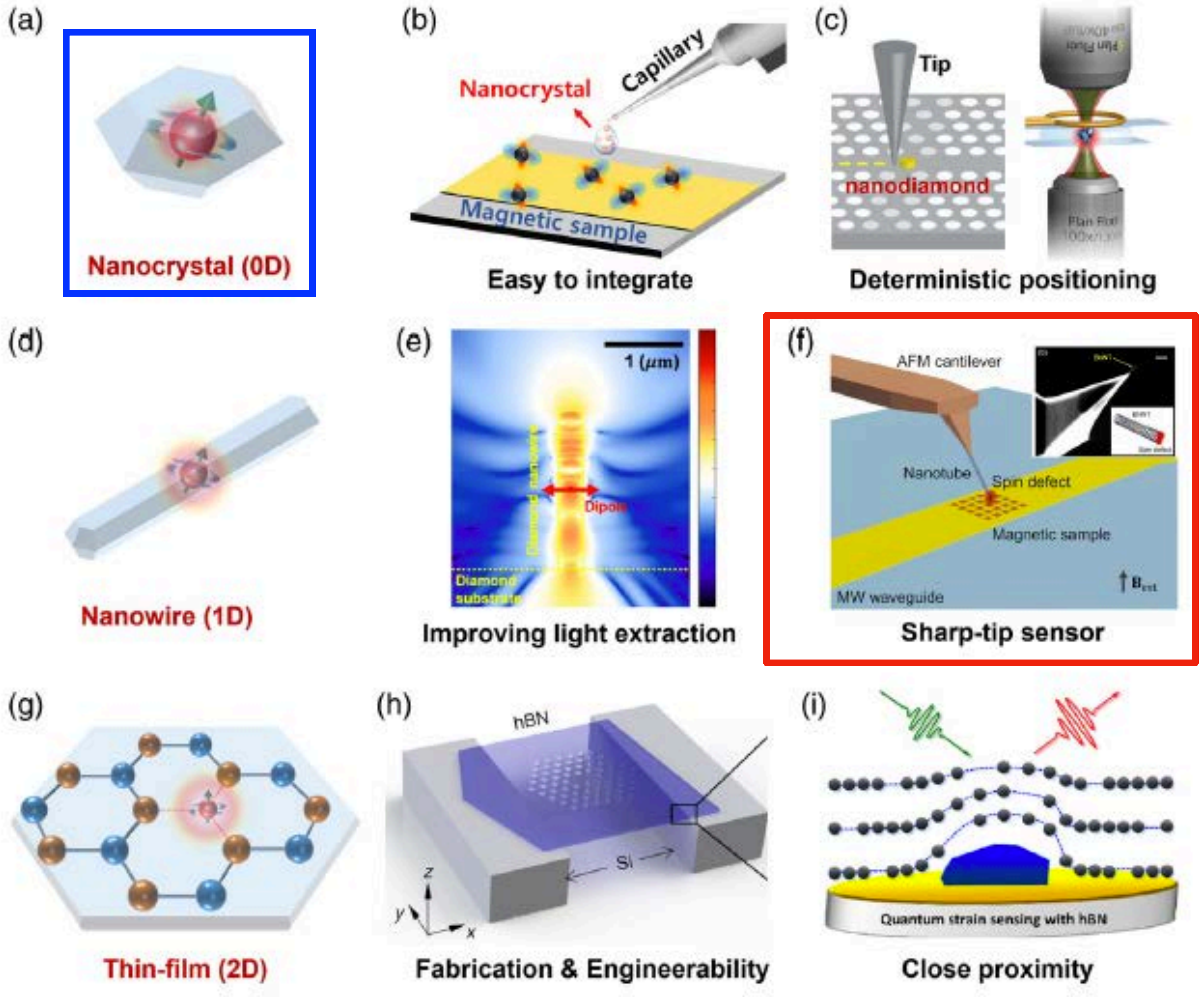

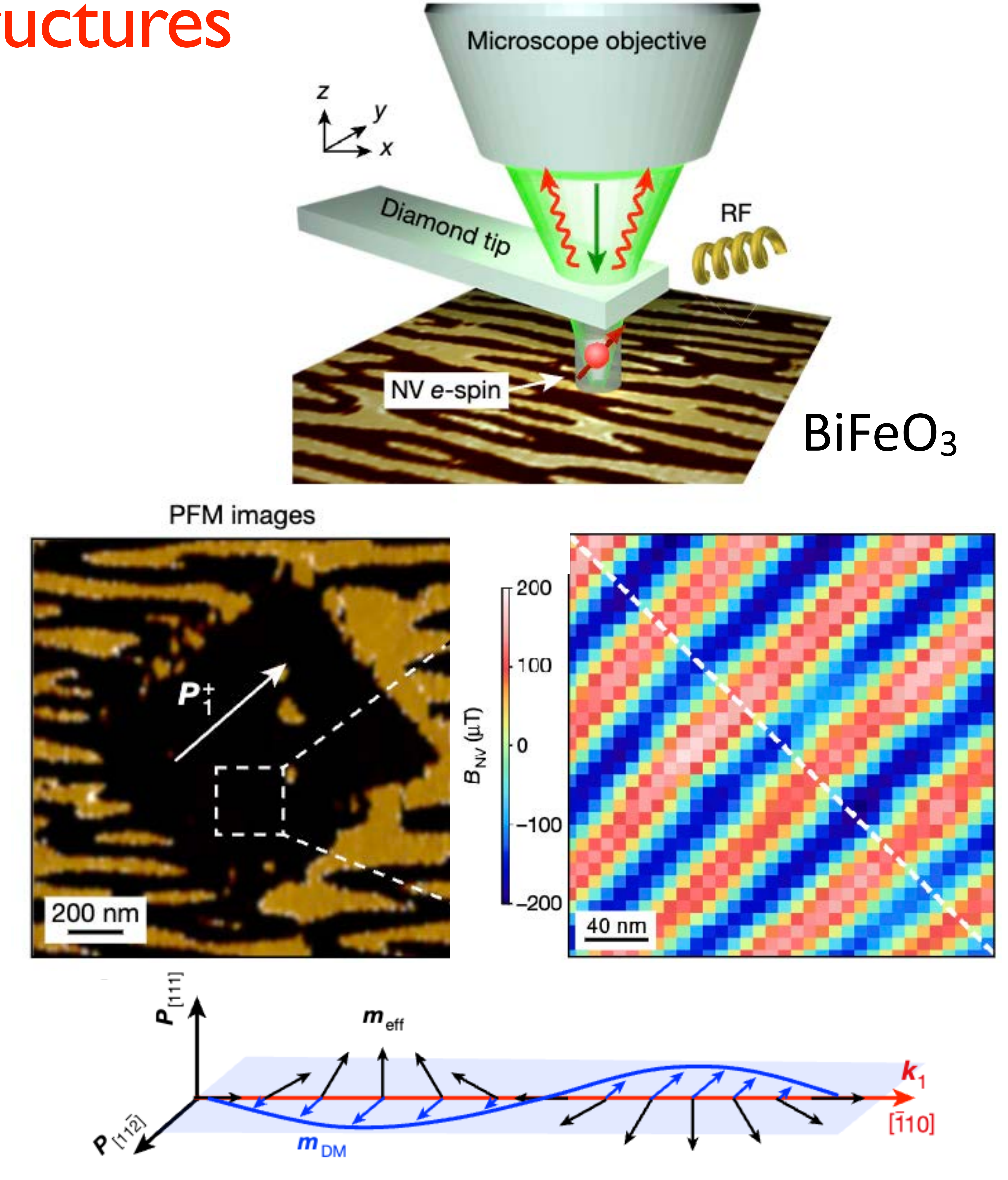

Kim et al., *Advanced Photonics* **7**, 064002 (2025)

Vincent Jacques (L2C, Montpellier)
see e.g. Nature ***549****, 242 (2017)*

Thermal mapping with NV-doped nanodiamonds

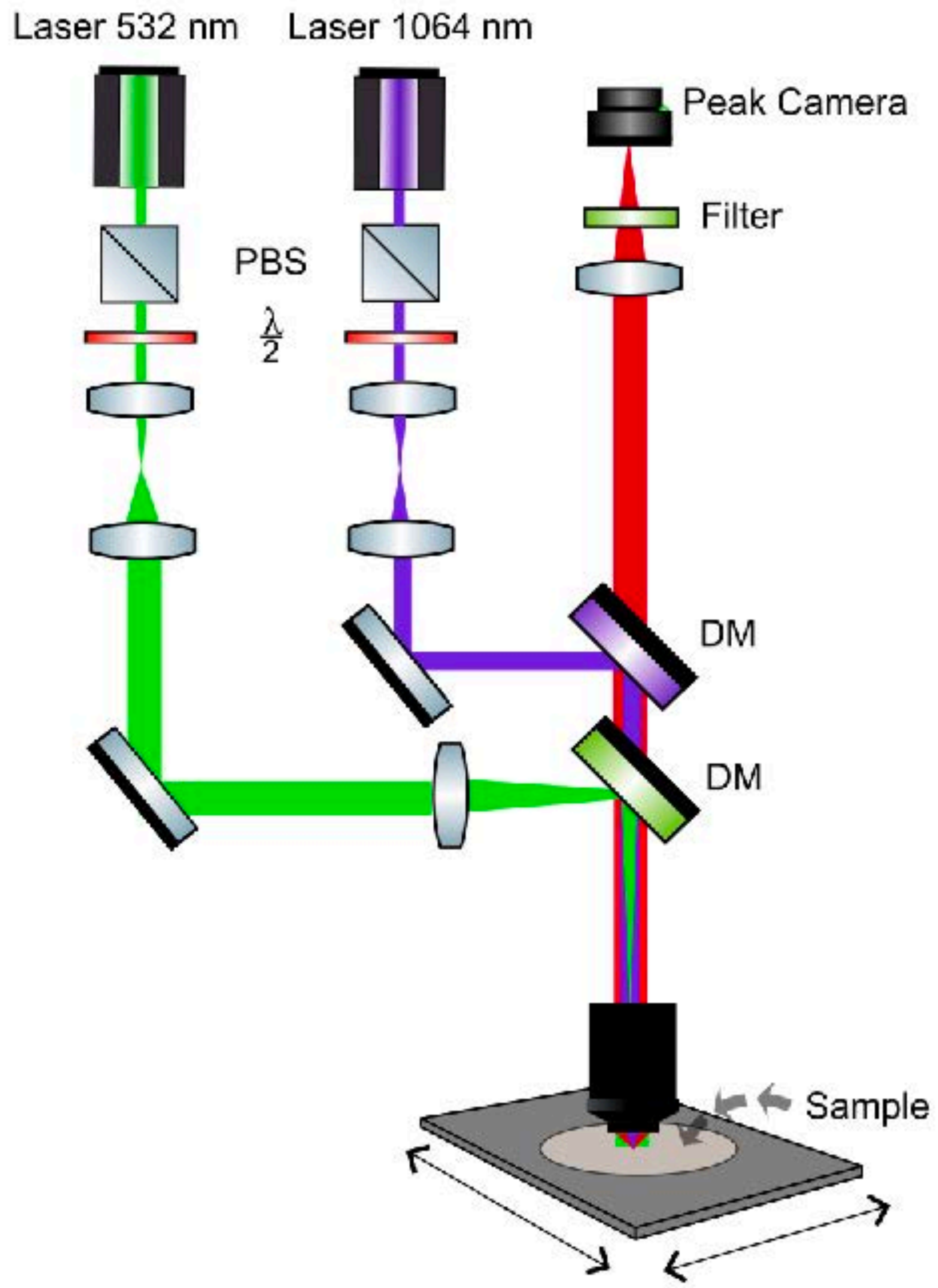

Electrospray

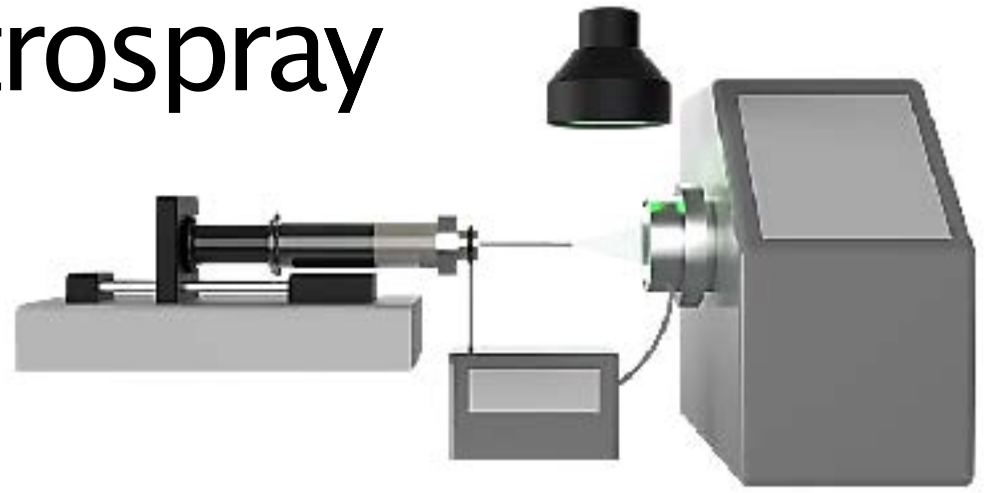

Huan-Chen Chang
(Academia Sinica, Taiwan)

Homogeneous resin

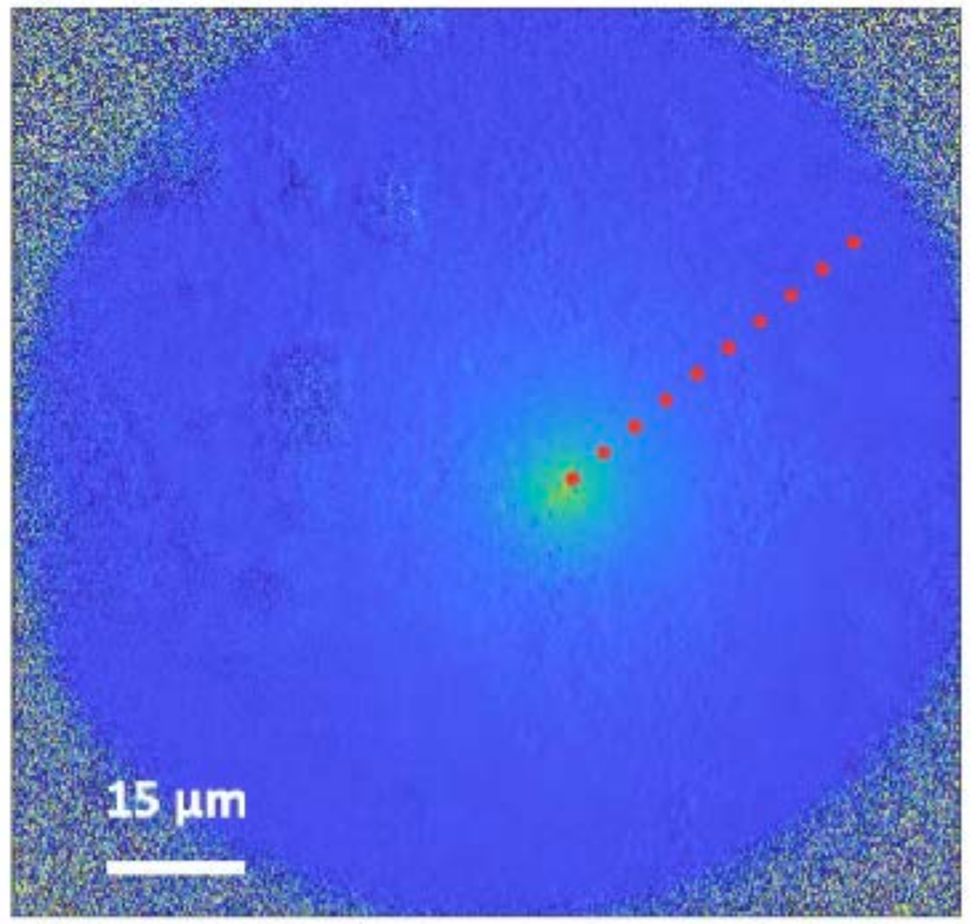

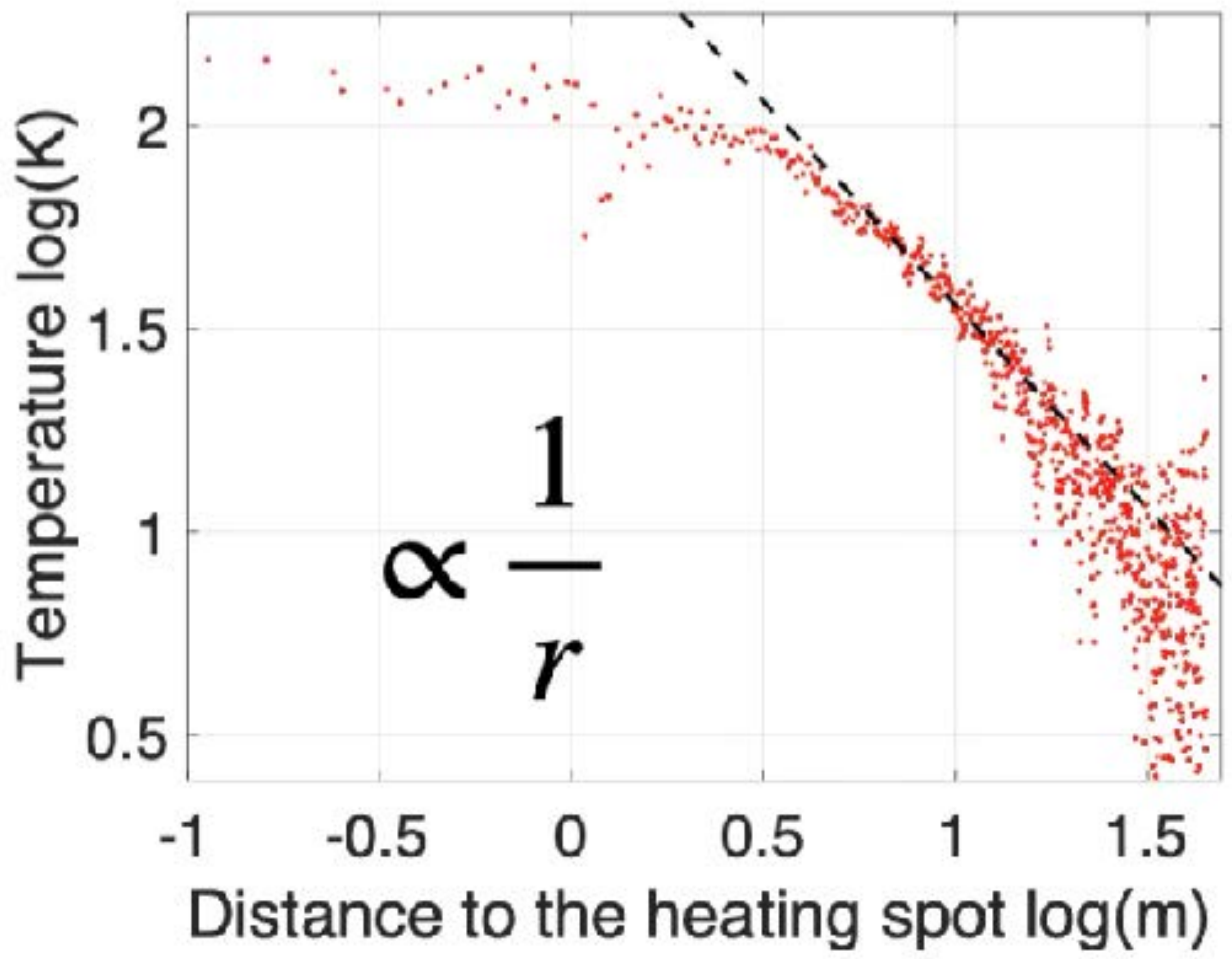

Heterogeneous carbon foam

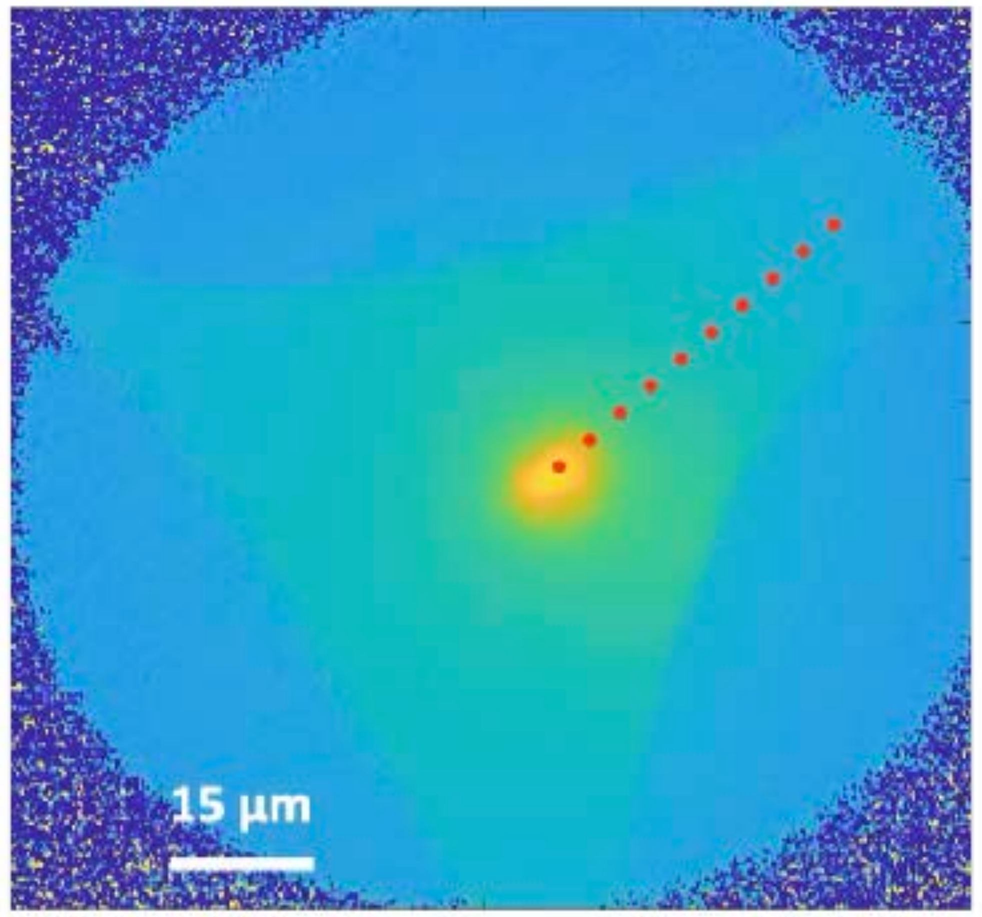

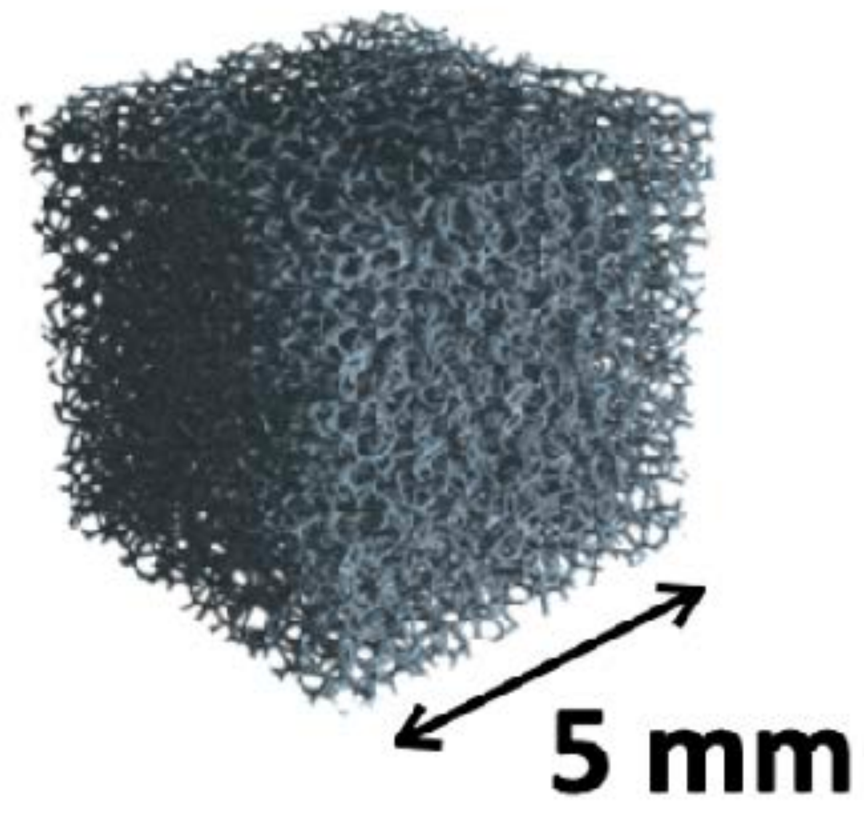

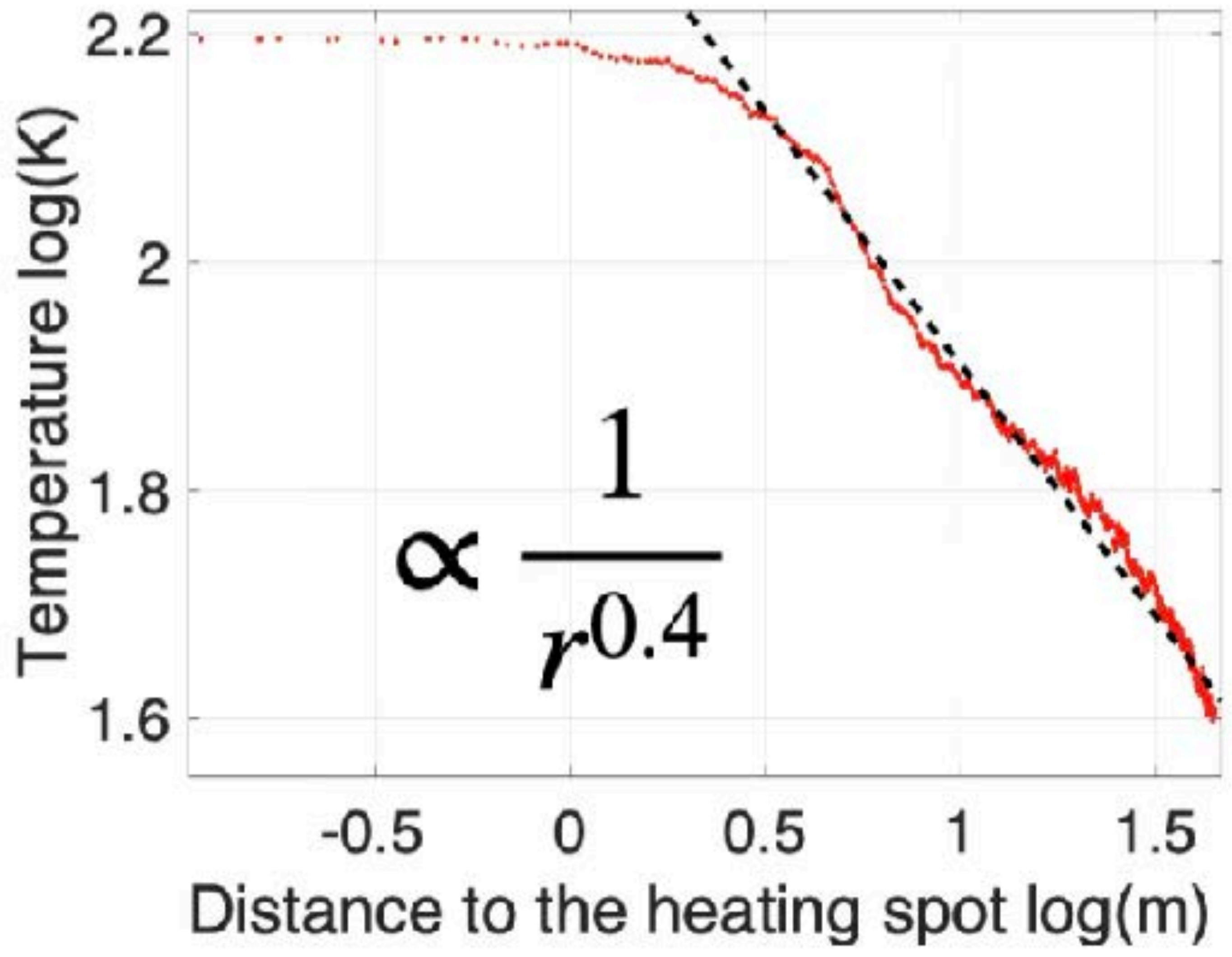

Developed with Denis Rochais & Loïc Toraille (CEA-DAM)
Léonie Evanno, Melissa Techer et al., in preparation

Improvement of collection efficiency using optics with high NA

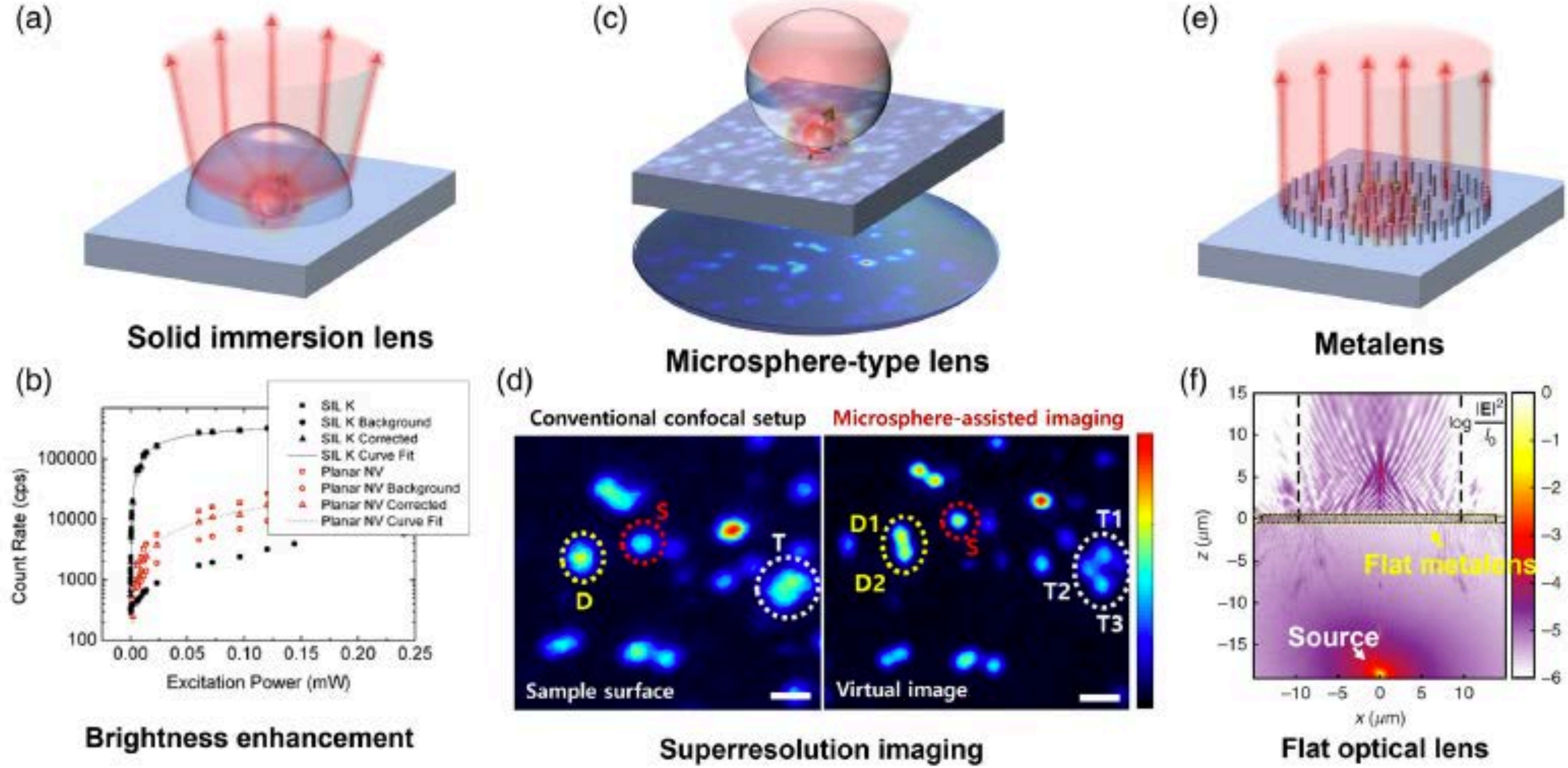

Kim et al., *Advanced Photonics* ***7***, *064002 (2025)*

How to make engineered nanostructure devices from diamond?

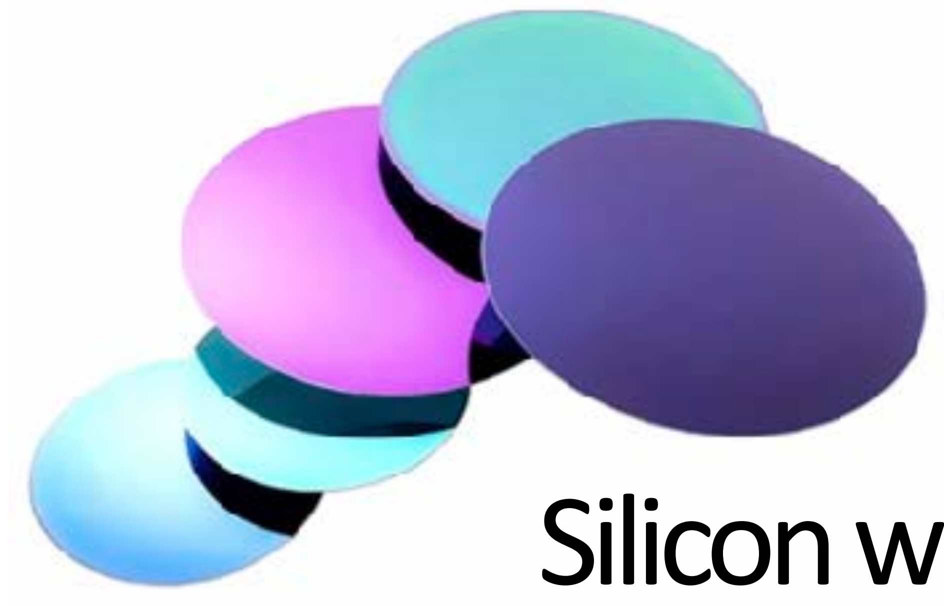

Silicon wafer with thin film
for photonic waveguide

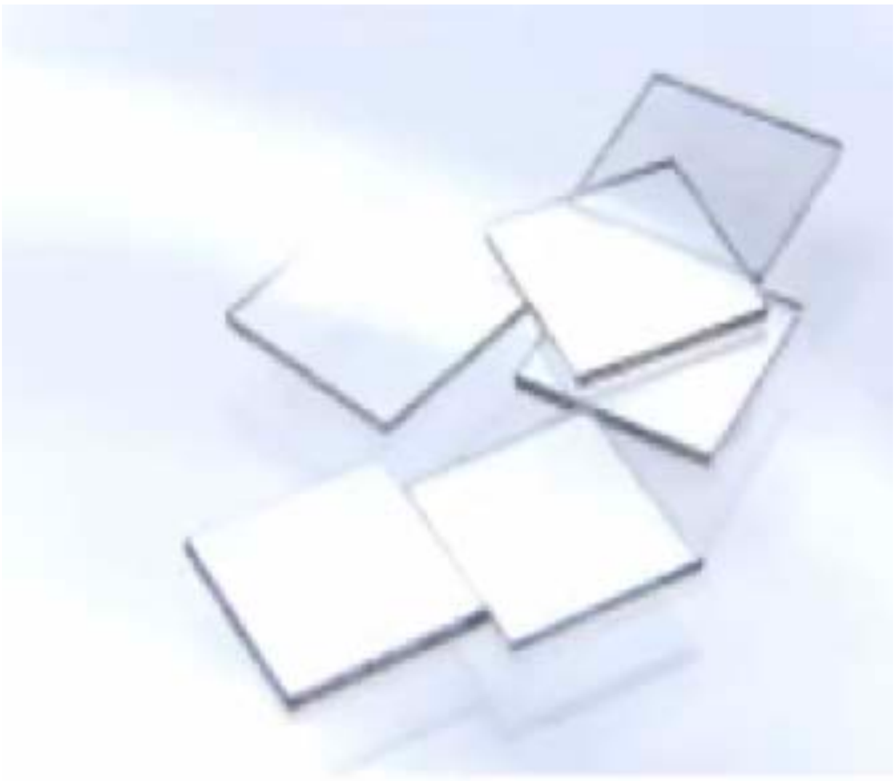

Bulk diamond single-crystal chips
to suspended membranes
for nanostructuring

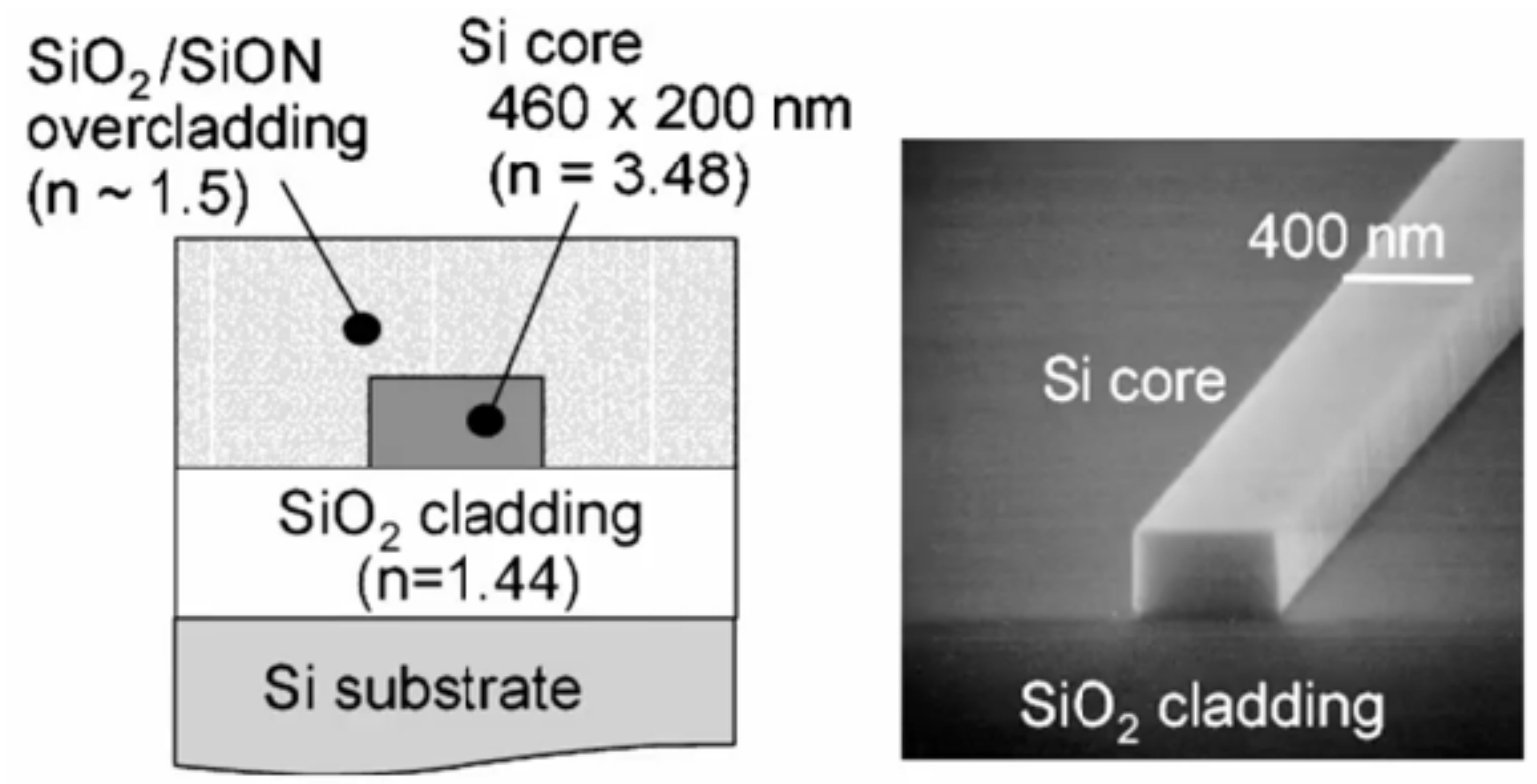

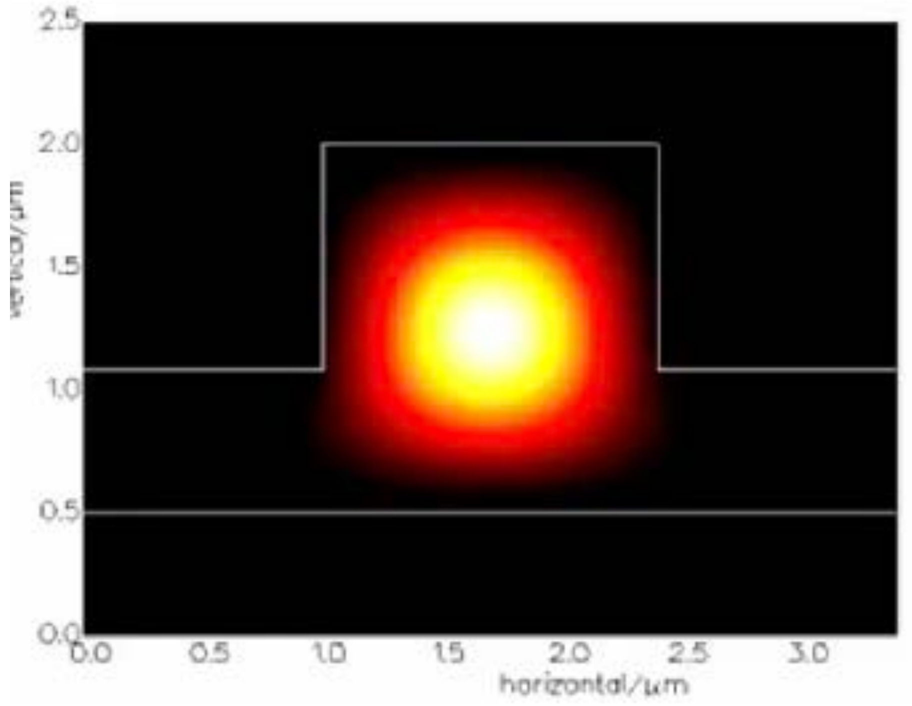

silicon photonic wire waveguide

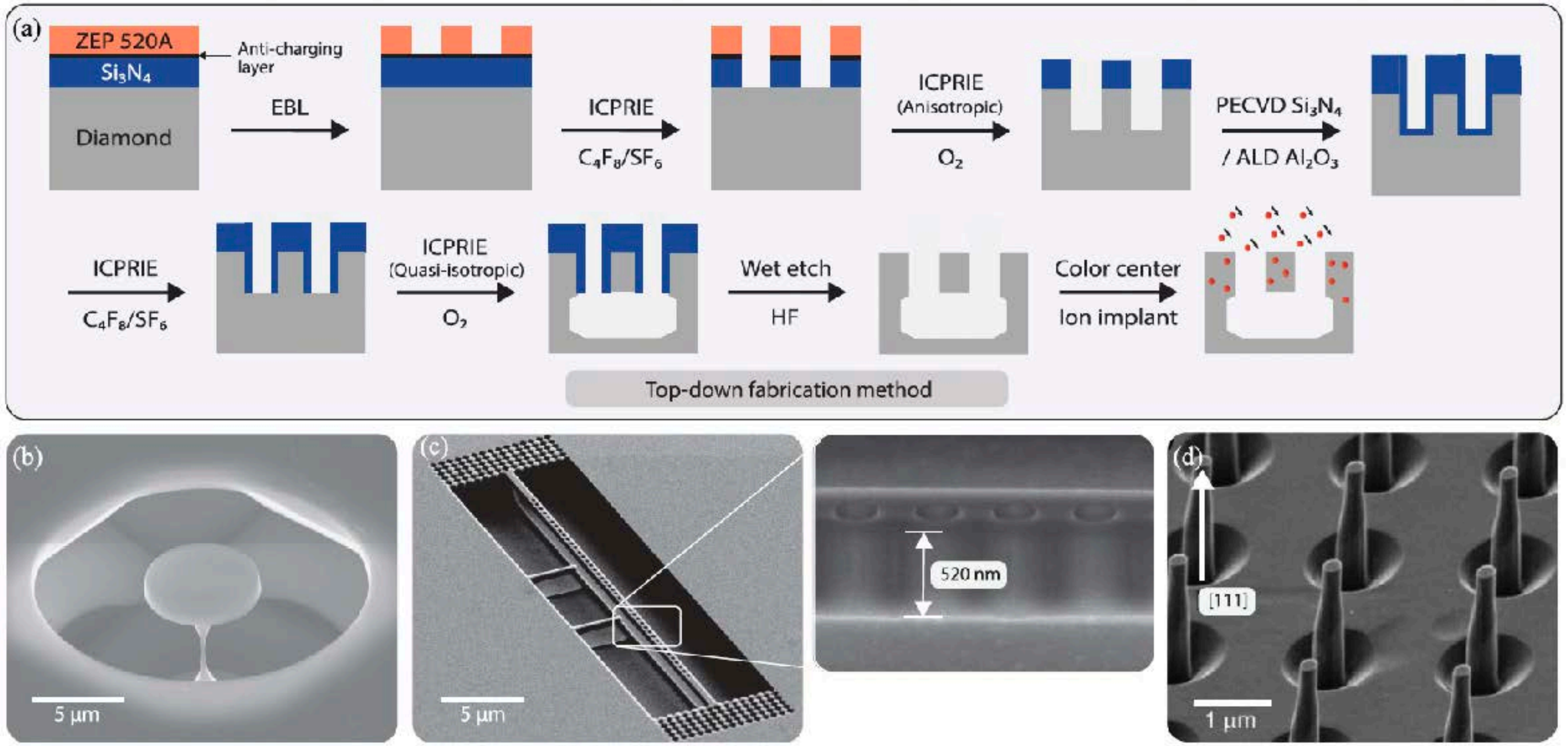

M. Loncar (Harvard), D. Englund (MIT), P. Barclay (Calgary), …

Diamond micropillars

Fabrication using ICP
on a single-crystal diamond wafer
X. Checoury (C2N)
Project SINFONIA (PEPR Quantique)
& EquipEx+ e-Diamant

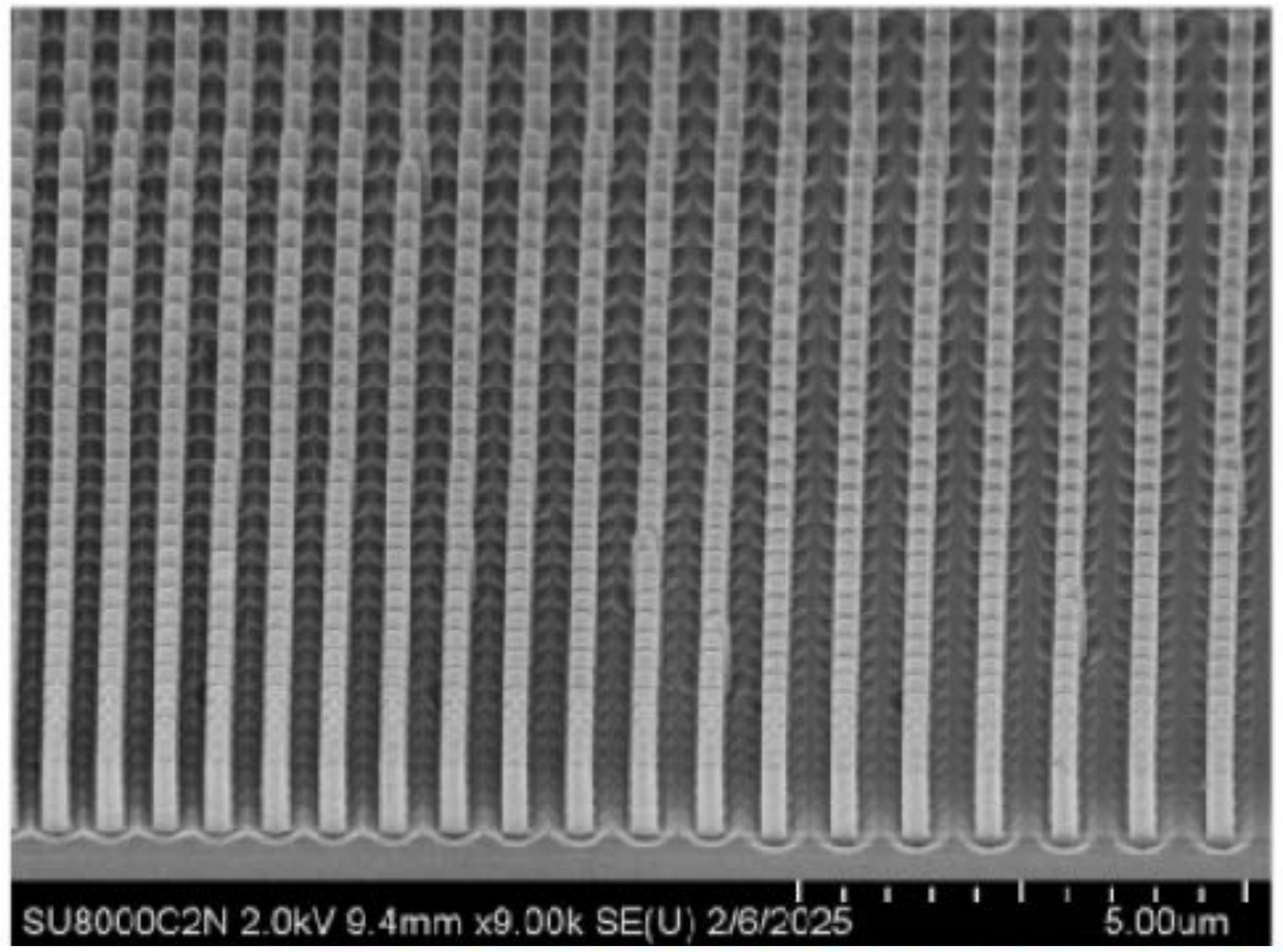

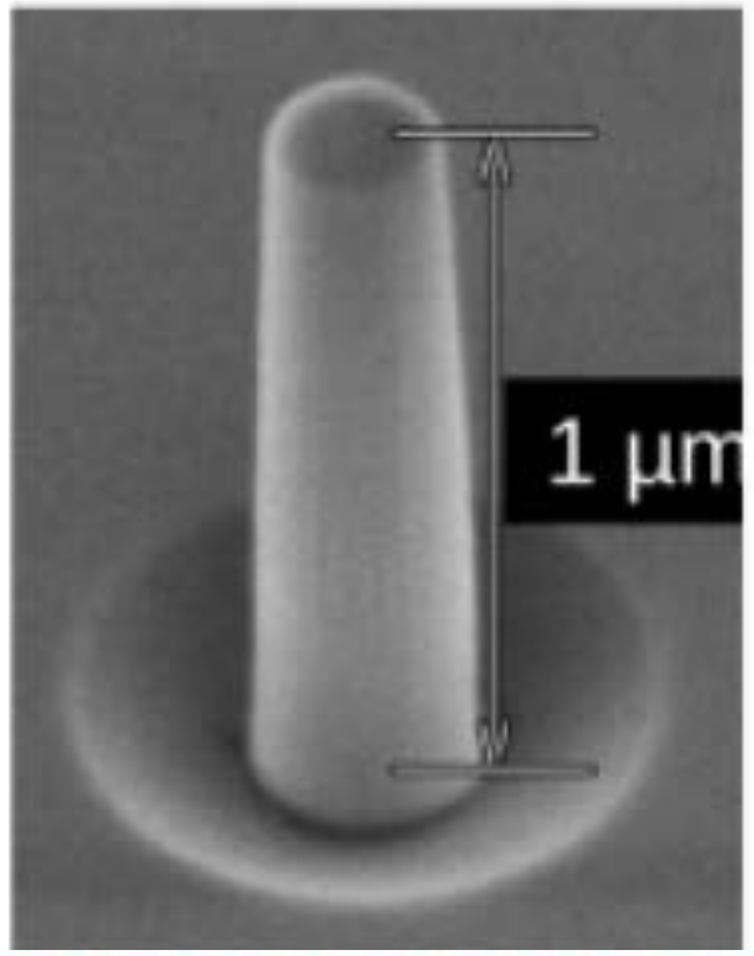

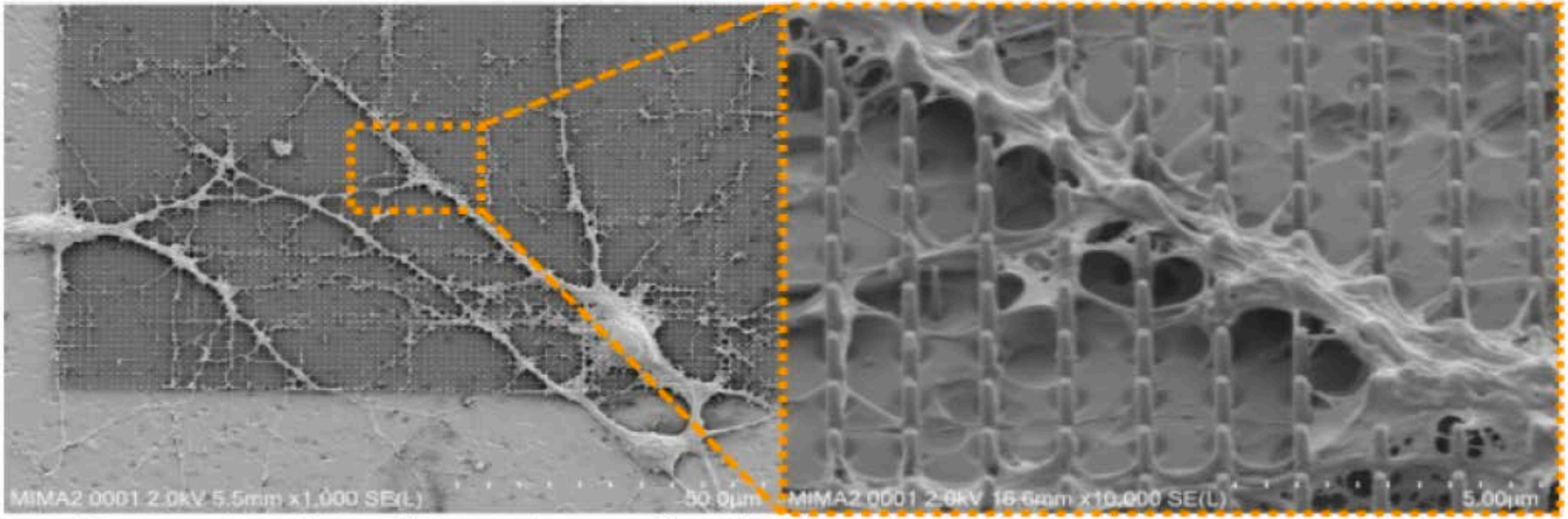

Neuron growth on diamond nanopillars fabricated at C2N. (Collab. F. Treussart LUMIN)

The real NV center: $NV^- \leftrightarrows NV^0 (+N)$

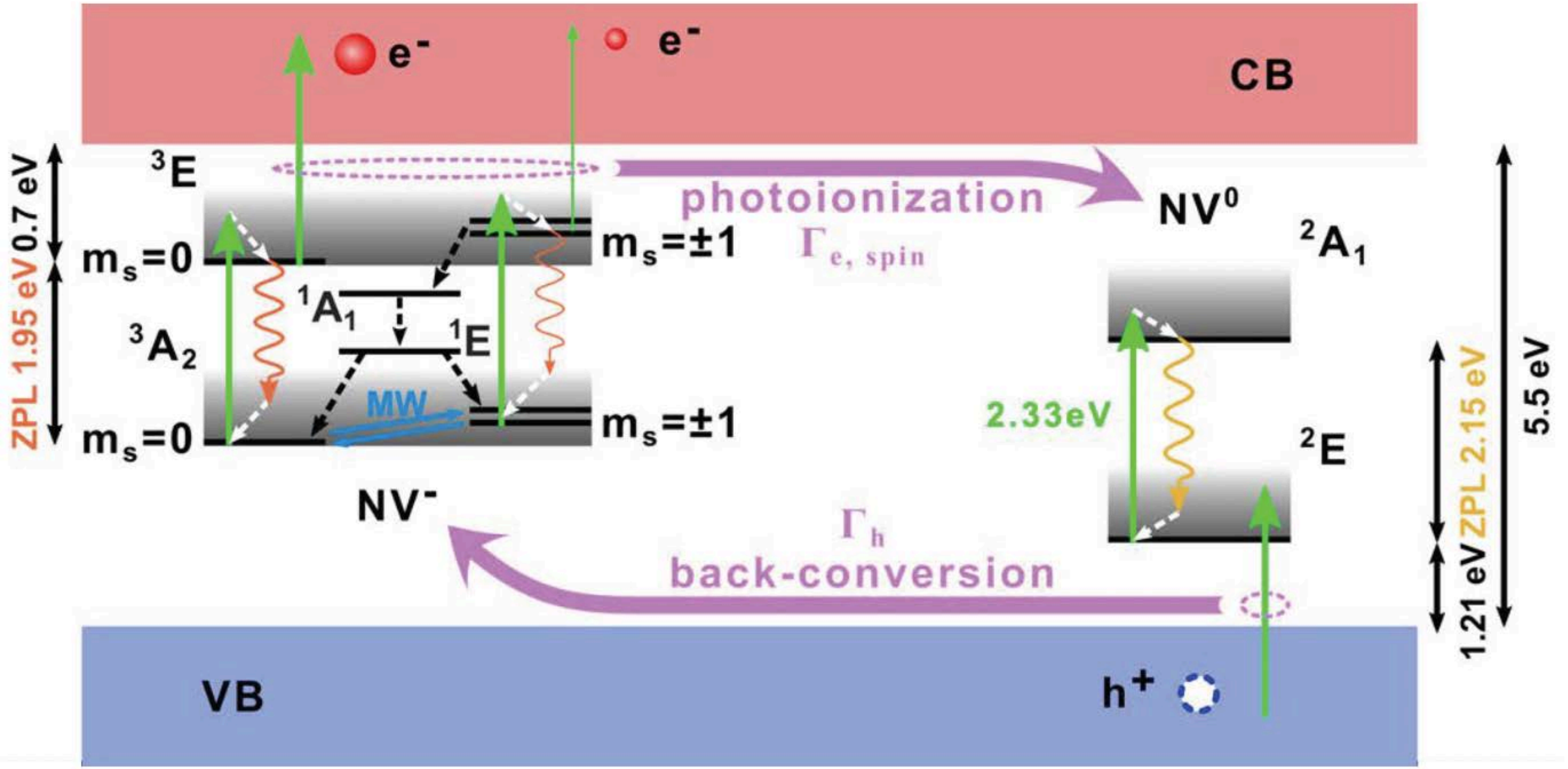

The photoinduced conversion rate $NV^- \rightarrow NV^0$ is spin dependent.
Provides the basis for the **electrical detection** of the spin resonance.

Photoconductive detection of the NV spin resonance

Electric contacts have to implemented in order to collect the charges induced by $NV^- \rightarrow NV^0$

- carbide bonding between diamond and metallic electrodes followed by annealing
  Scalable, low resistance
  Ohmic contact not ensured, adhesion and mechanical issues
- diamond graphitization by irradiation or laser illumination
  Simple, ohmic contact, good adhesion
  Parasitic resistivity of the electrodes

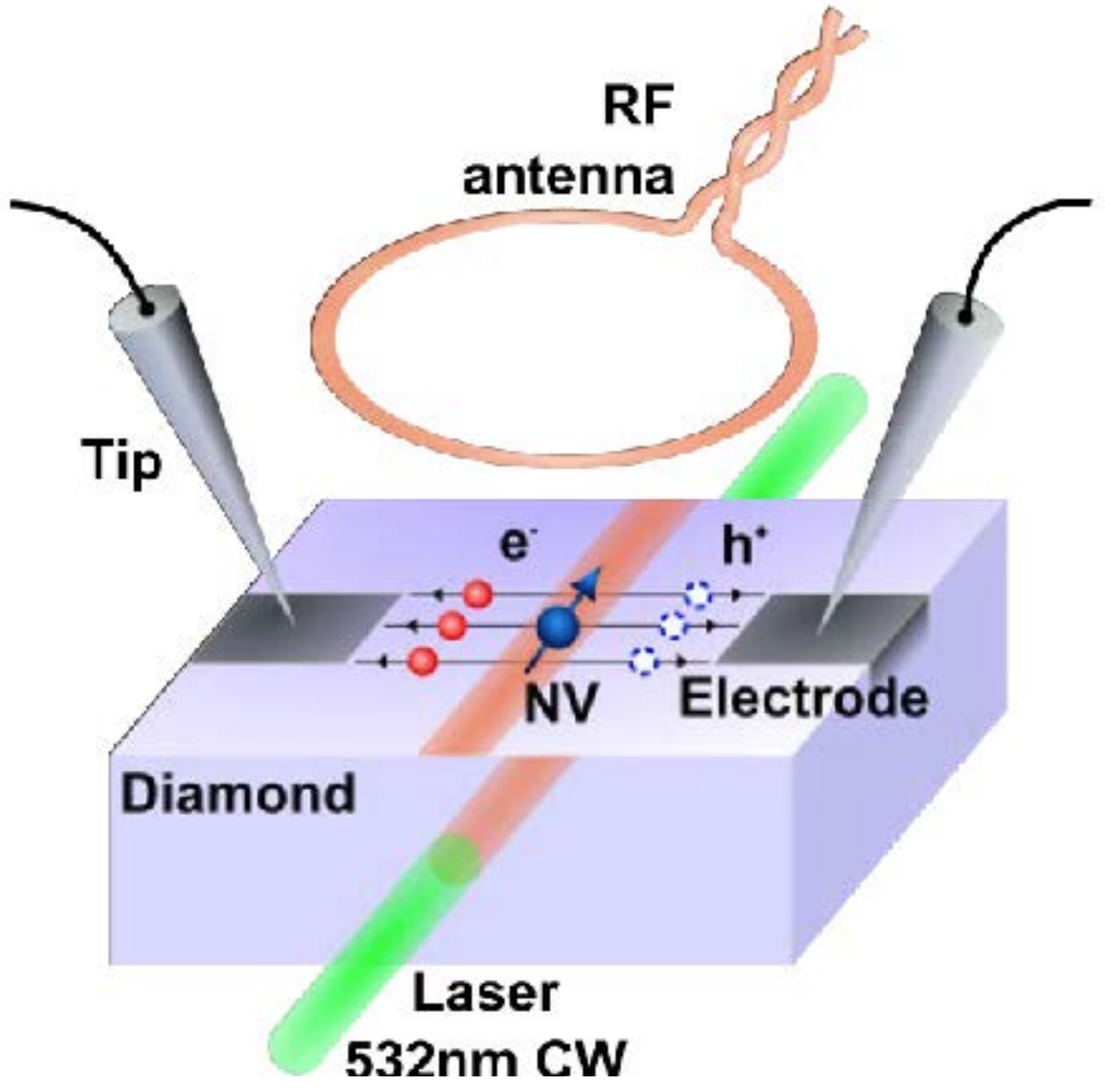

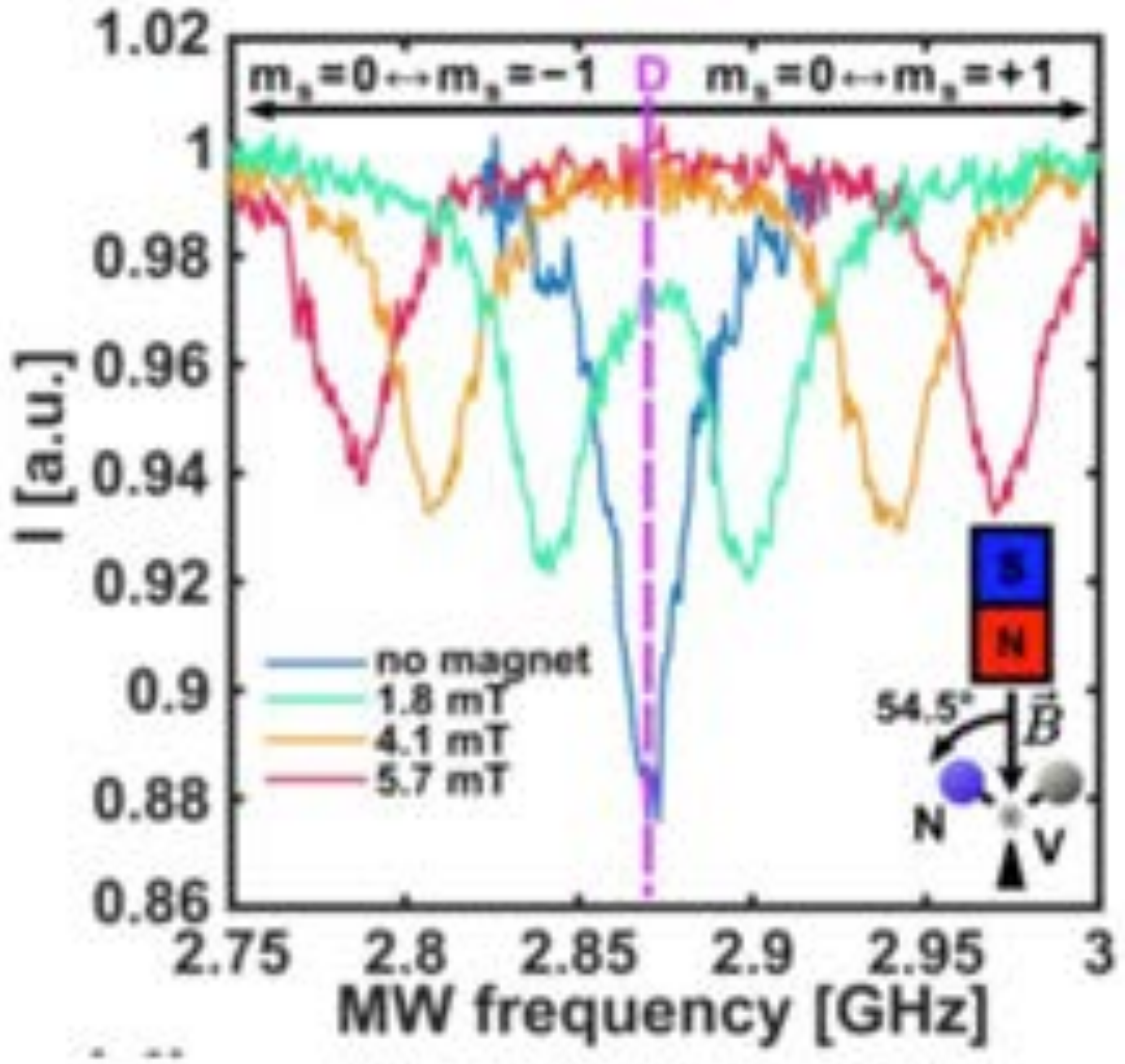

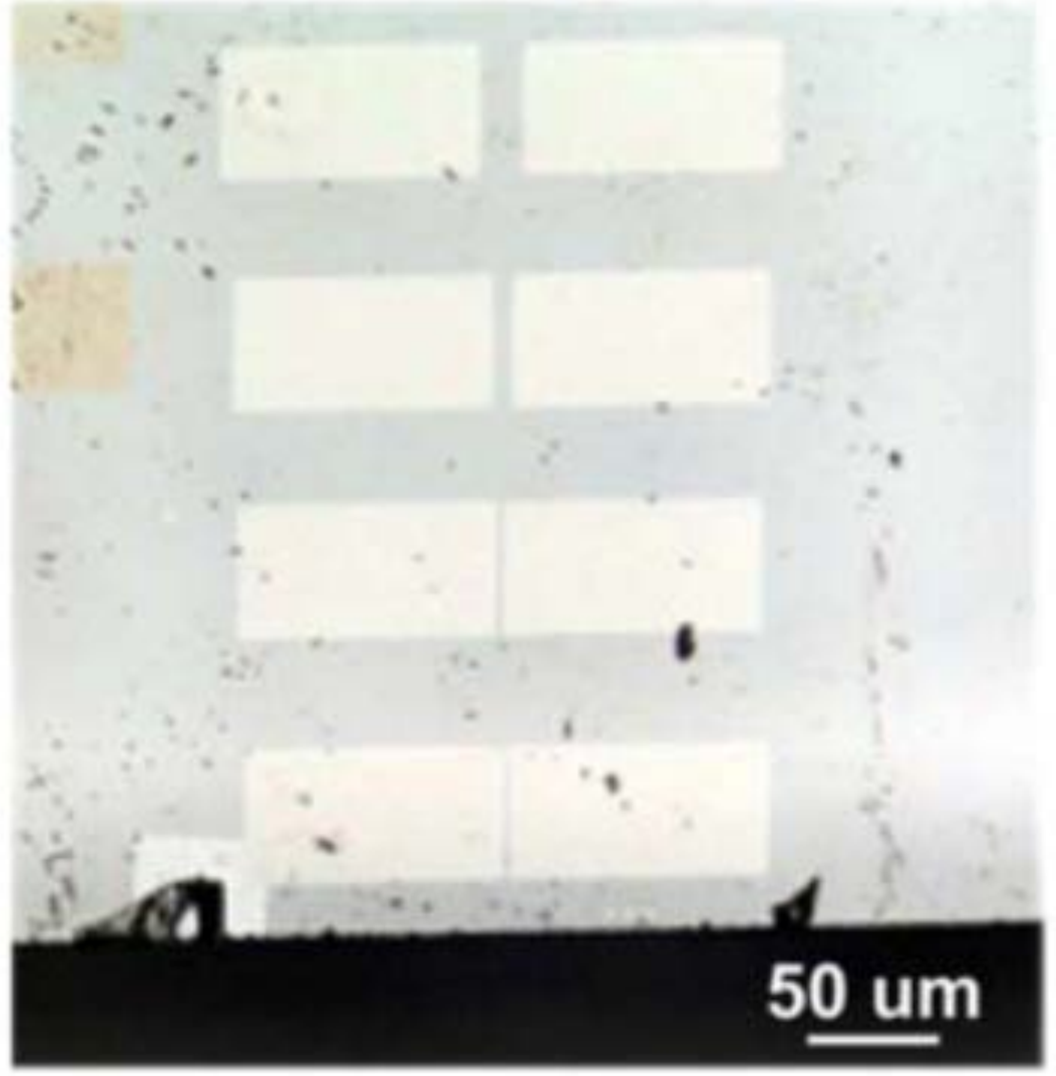

G. Villaret et al., *Appl. Phys. Lett.* 122, 194001 (2023)

Superconductivity at high pressure

year

2025: systematic computational study of binary super-hydrides
Evidence for SC ≈ 10 compounds

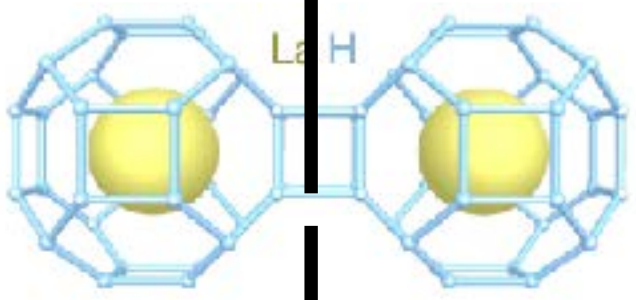

2019: lanthanum hydride
LaH_{10}
$T_C = 260\,K$ at $200\,GPa$

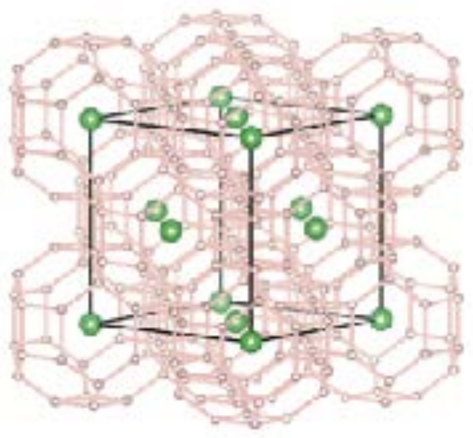

2015: sulfur hydride
SH_3
predicted and observed
$T_C = 200\,K$ at $150\,GPa$

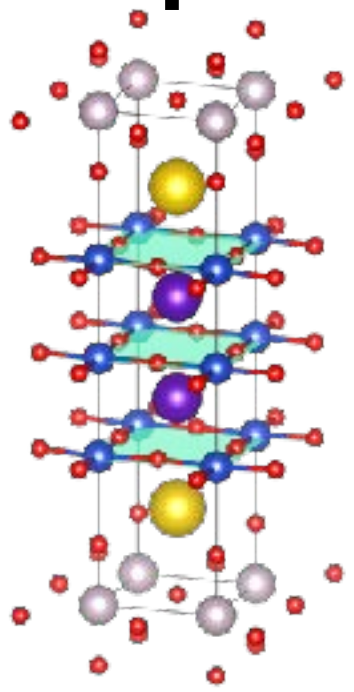

1996: record of critical temperature $T_C = 165\,K$
for cuprate Hg-1223
at pressure 30 GPa

diamond anvil cell (DAC)

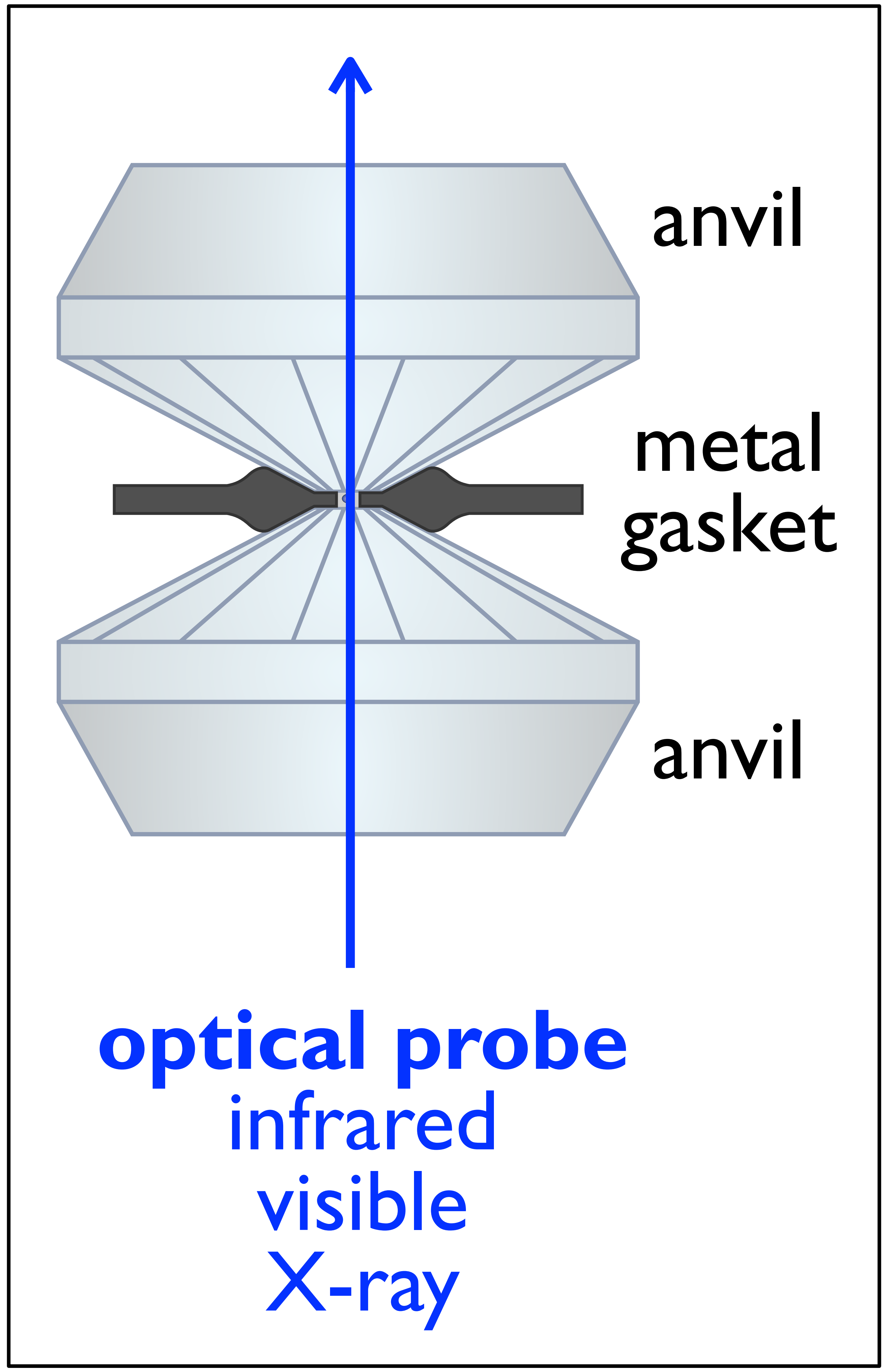

Super-hydrides:
Synthesis at high pressure using laser heating of
NH_3BH_3 + metal (uranium)

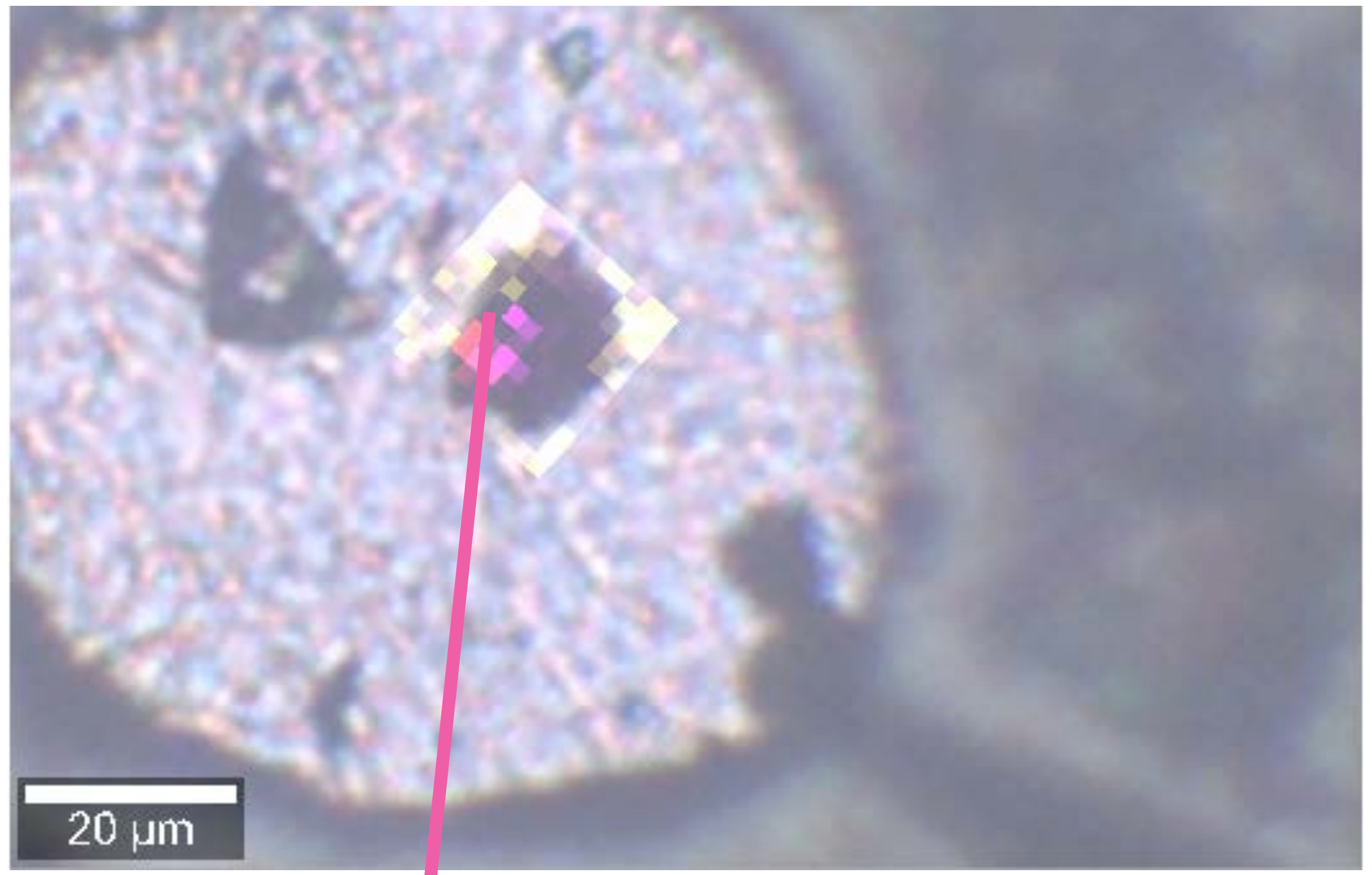

synchrotron
X-ray diffraction

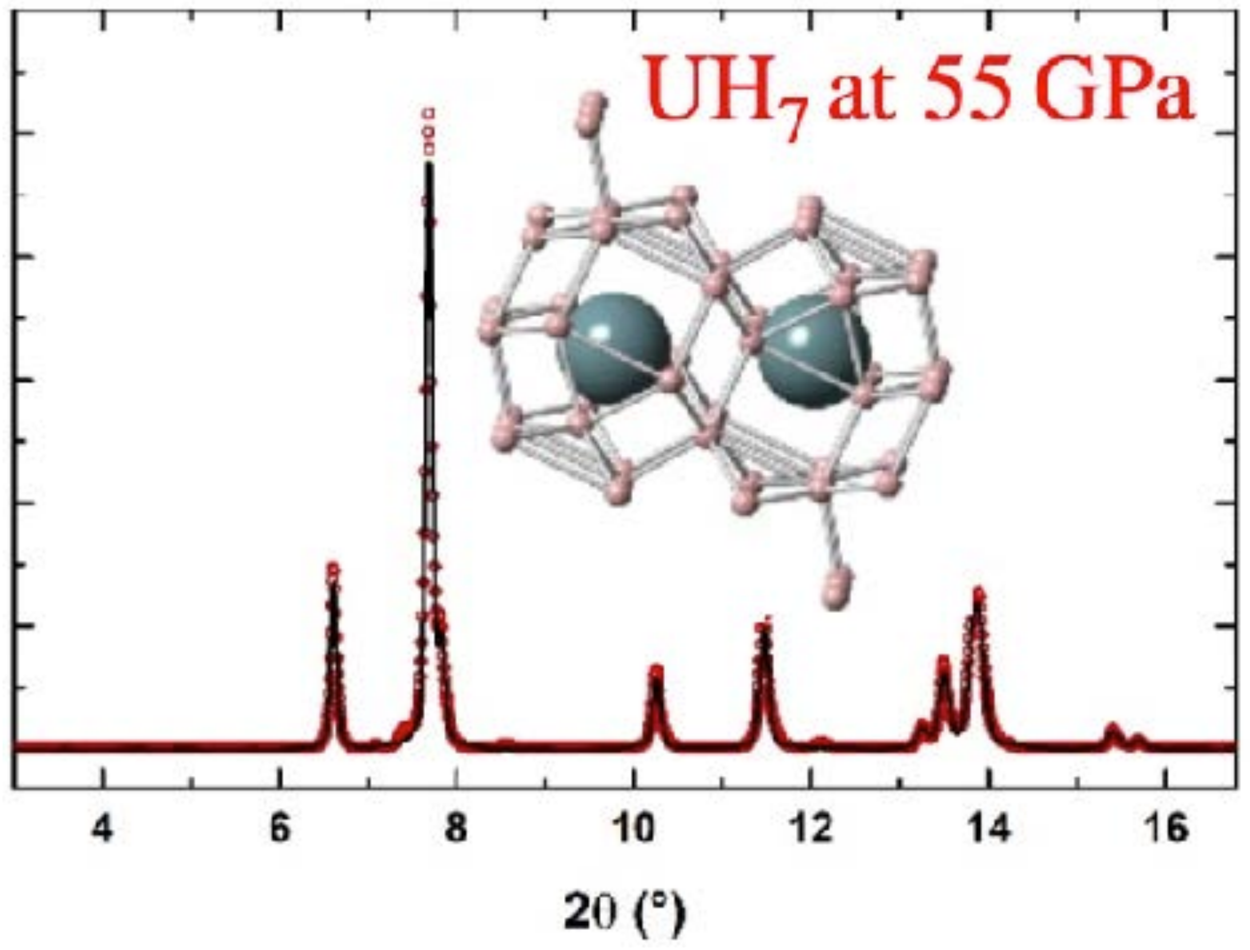

In-situ optical detection of the Meissner effect using NV-enabled anvils

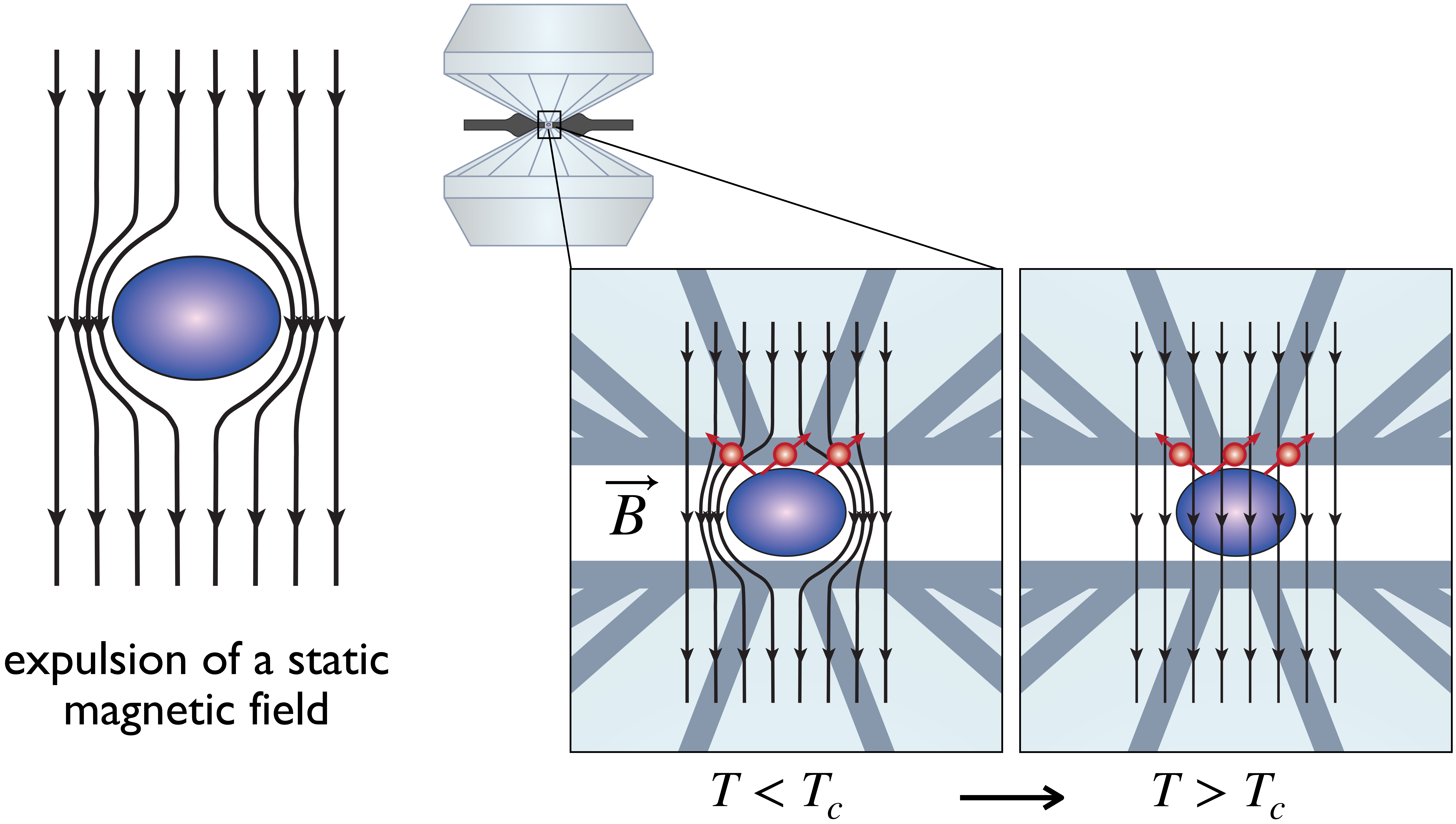

Design of NV centers in ultra-pure diamond anvils using FIB nitrogen implantation

Martin Schmidt

Nitrogen

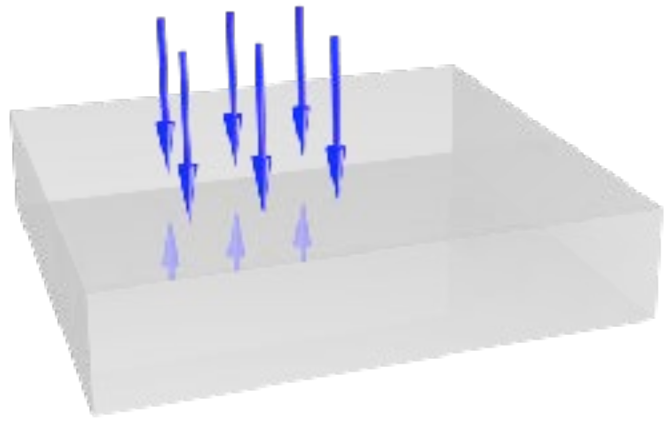

ultrapure single-crystal diamond layer

Implantation of nitrogen atoms + creation of vacancies

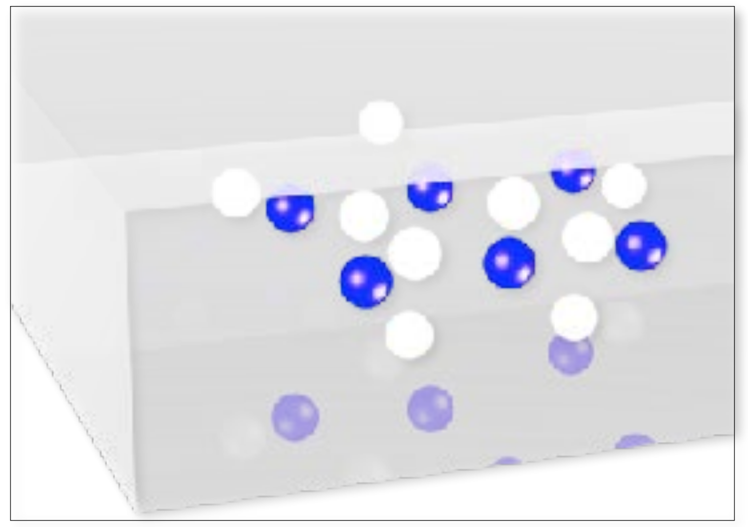

Annealing 800°C – 2h leads to creation of NV centers

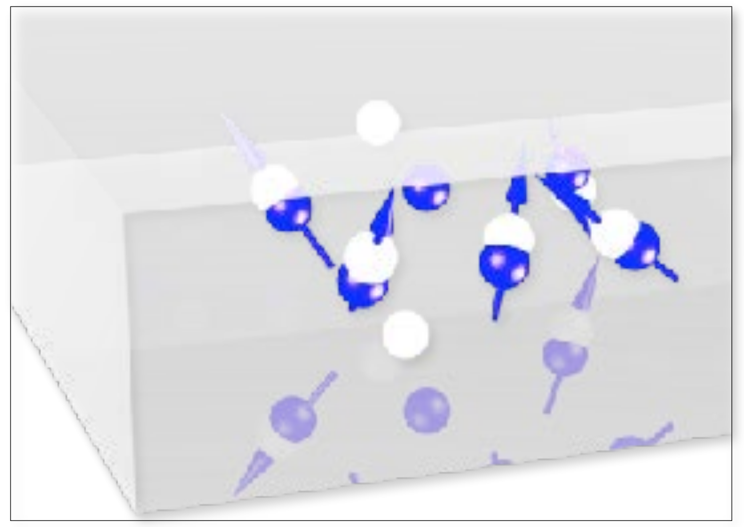

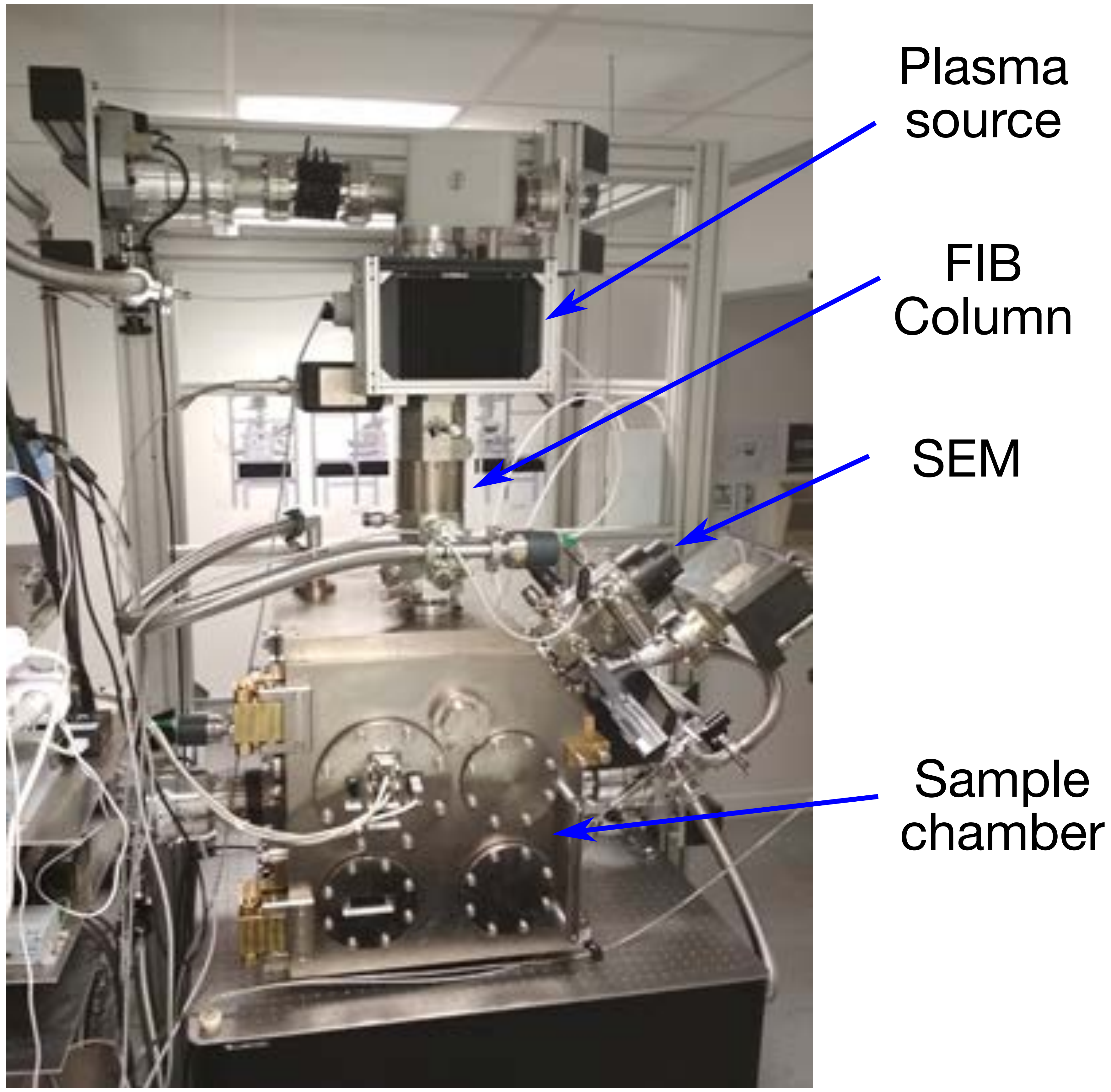

Lesik *et al.*, Physica Status Solidi A (2013)

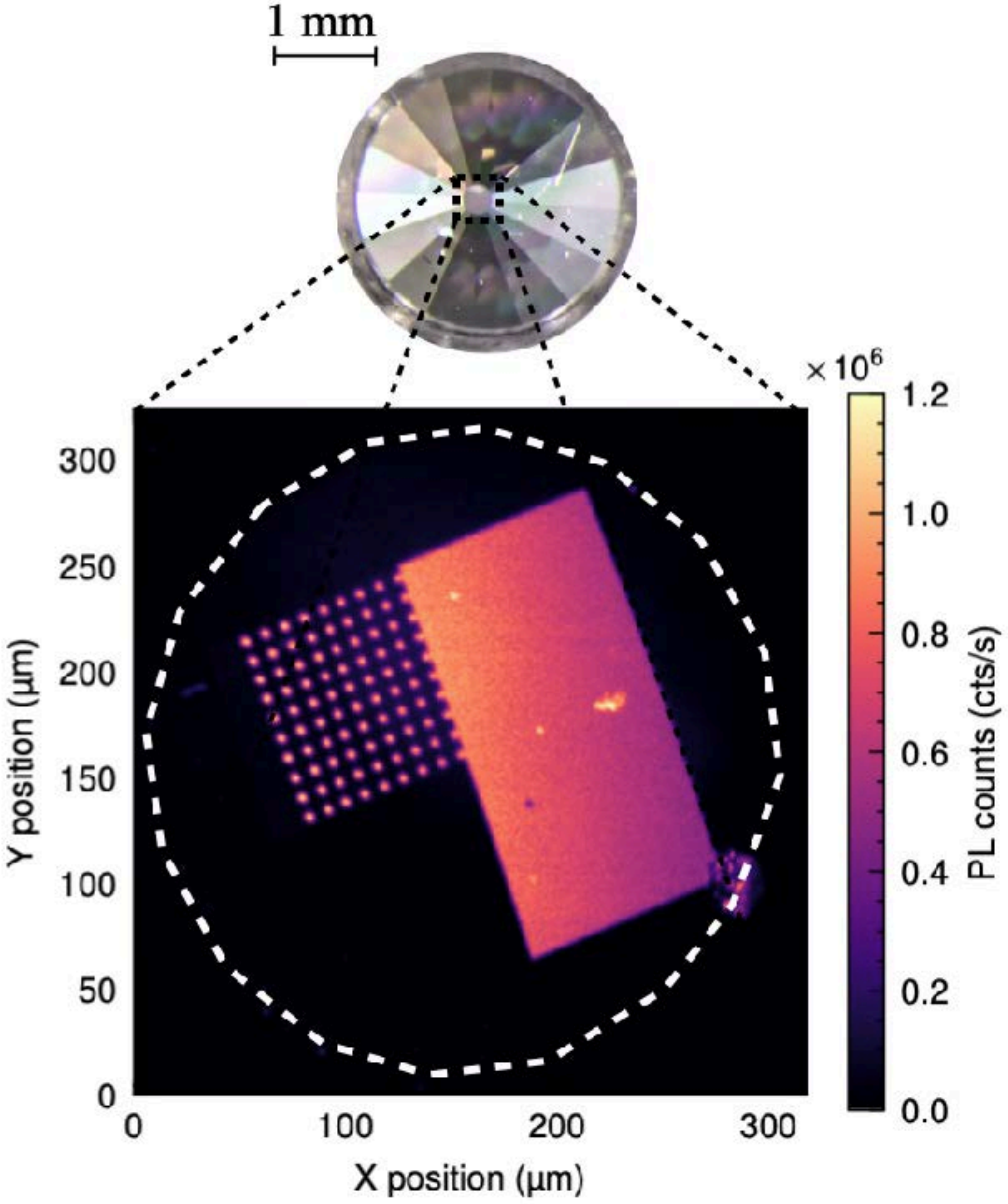

System developed in collaboration with TESCAN ORSAY which is now a commercial product

Proof-of-concept experiments (2019)

Hsieh *et al.*, Science **366**, 1349 (2019)
Norman Yao (Berkeley → Harvard)
Raymond Jeanloz (Berkeley)

Lesik *et al.*, Science **366**, 1359 (2019)
Our team (ENS Paris-Saclay & Thales)
Paul Loubeyre's team (CEA-DAM)

Yip *et al.*, Science **366**, 1355 (2019)
Sen Yang (CUHK → HKUST)
Swee Goh (CUHK)

Magnetism (up to 30 GPa)

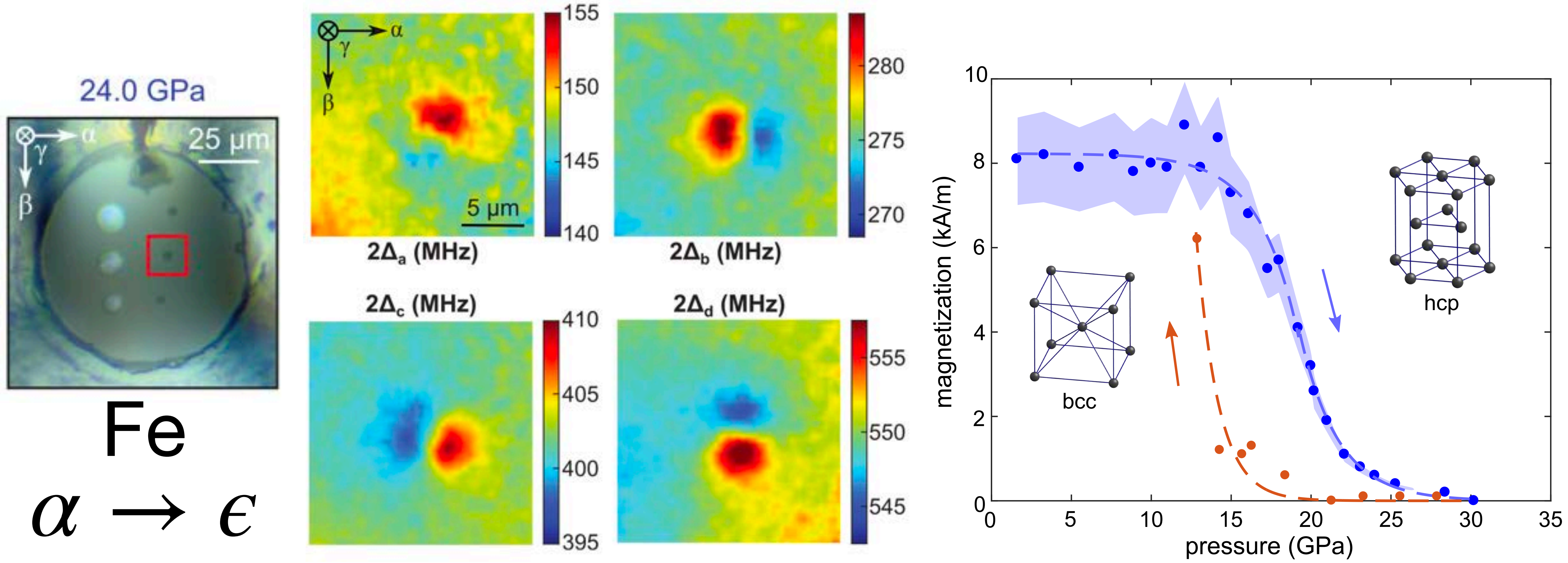

Fe
$\alpha \rightarrow \epsilon$

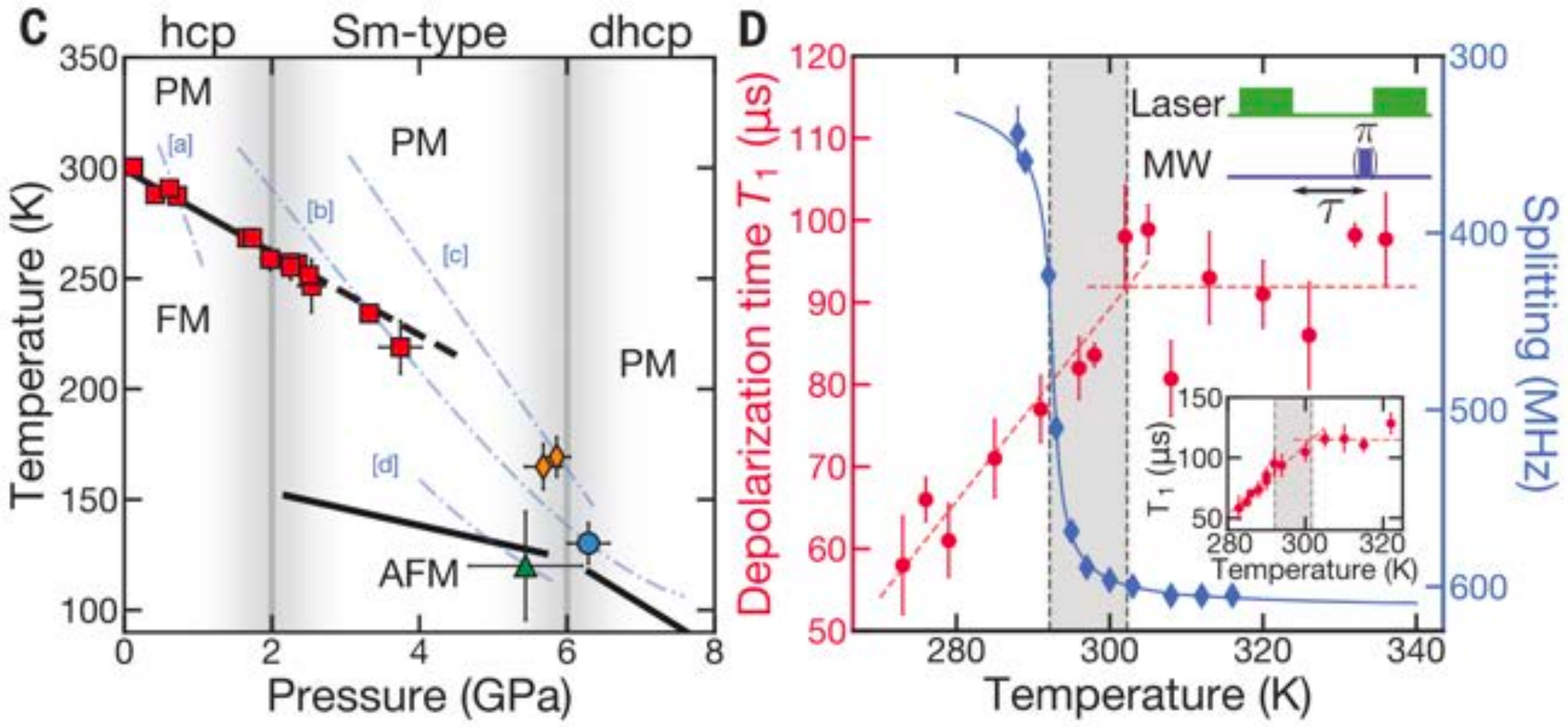

Gd

Superconductivity (up to 7 GPa)

$BaFe_2(As_{0.59}P_{0.41})_2$

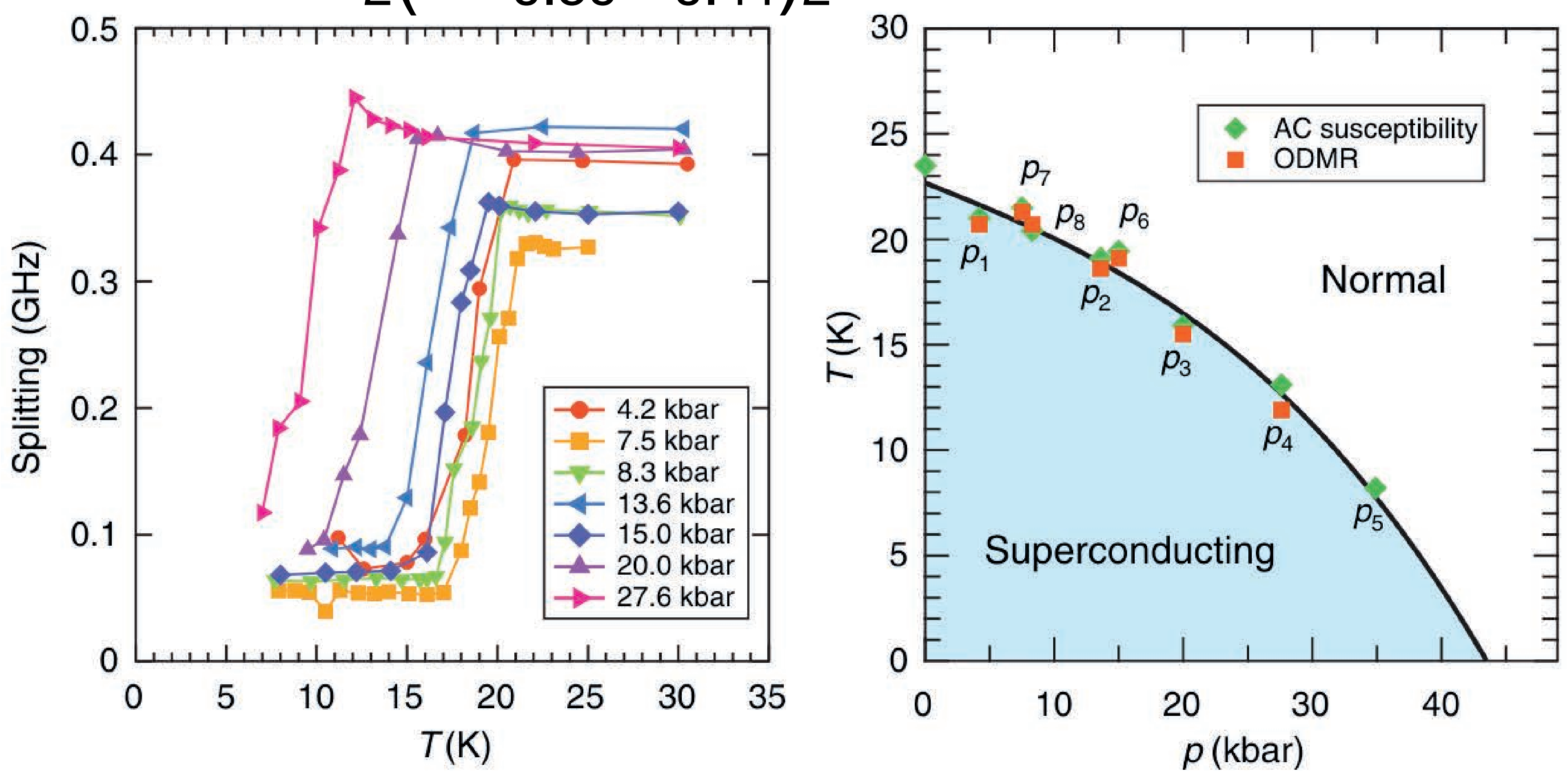

MgB_2

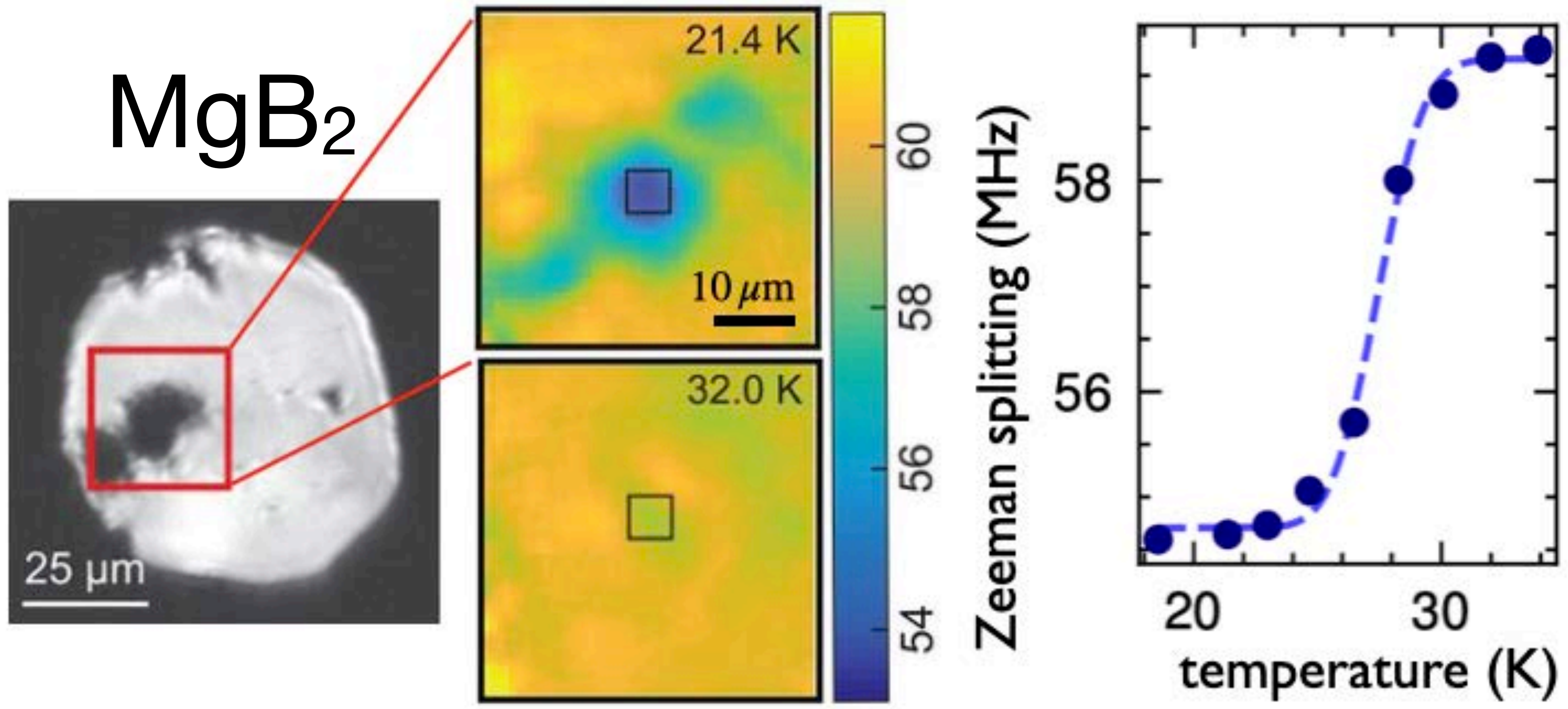

Is there a pressure limit for NV magnetic sensing?

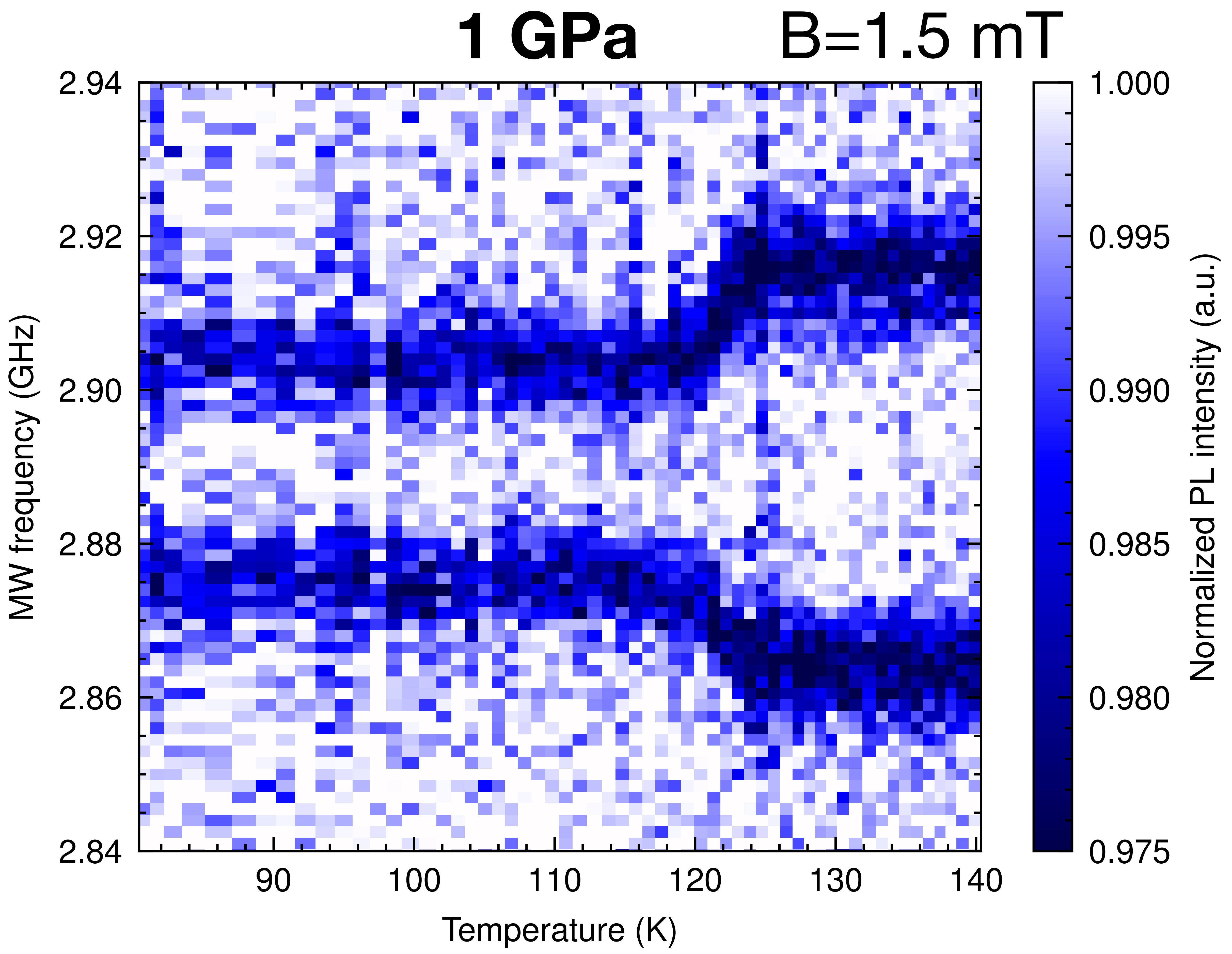

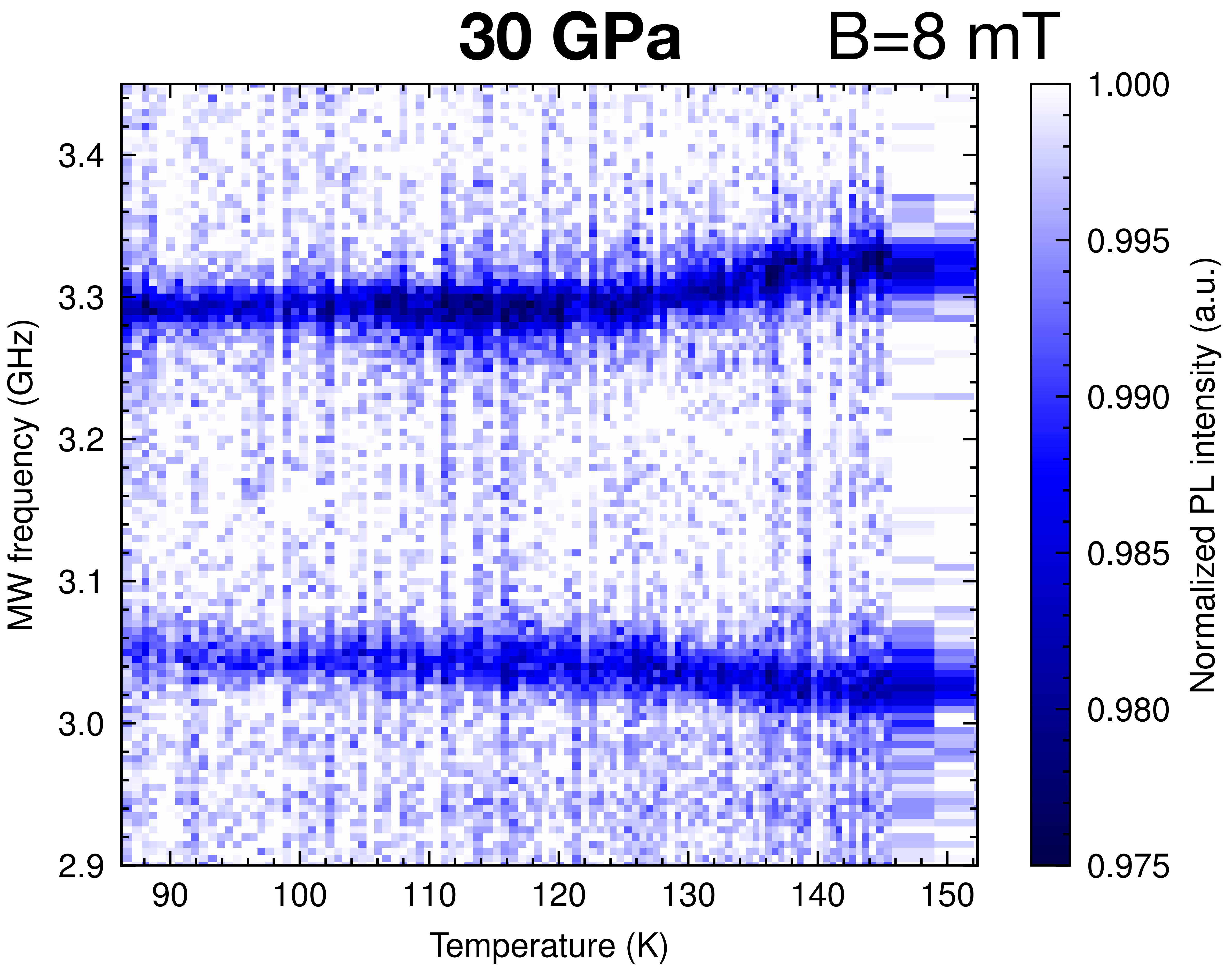

What causes the deterioration of the 'NV Meissner signal' at high pressures?

Is it possible to maintain the NV signal at pressures above 40-50 GPa?

The anvil tip is in a stressed environment

Before load

High pressure

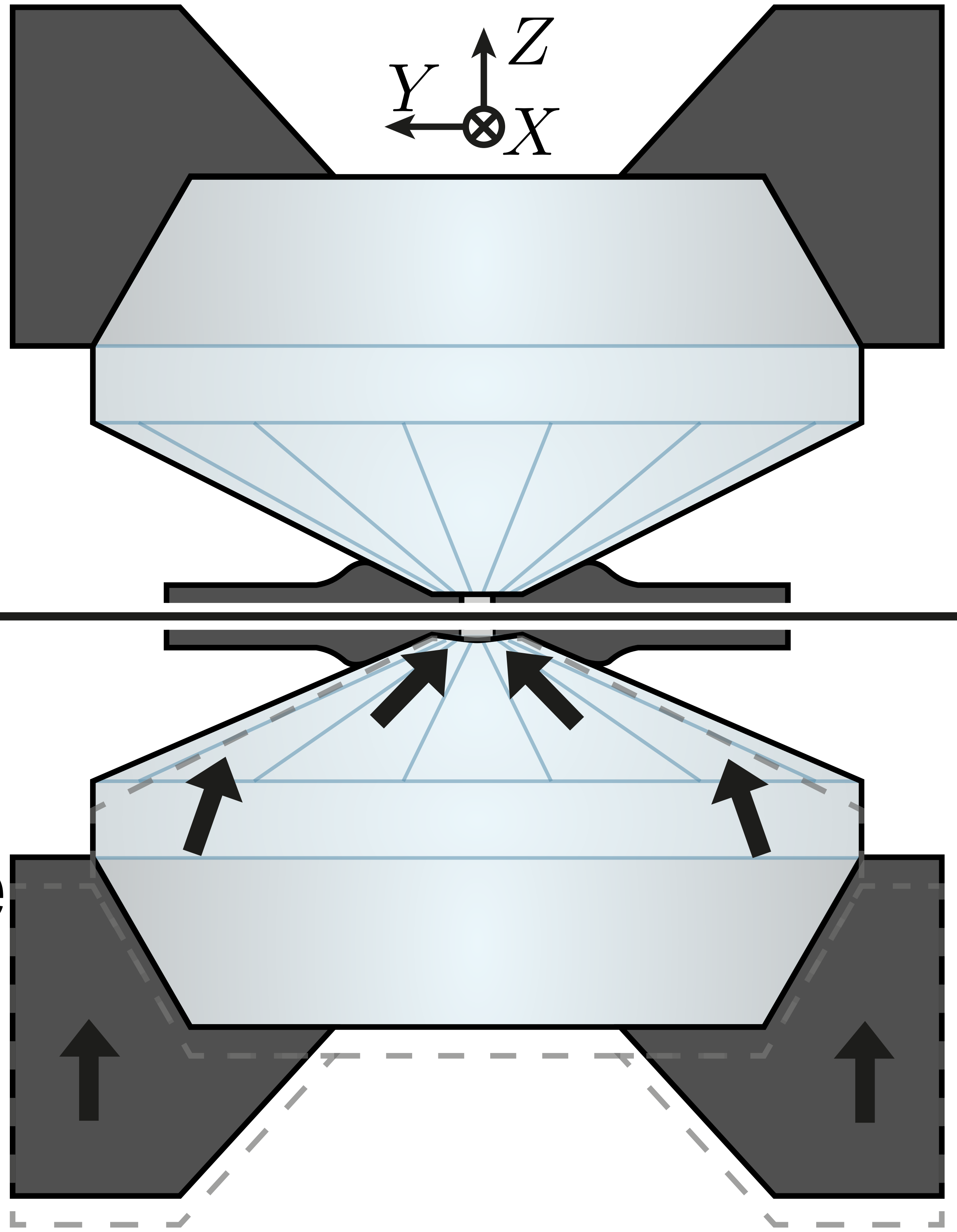

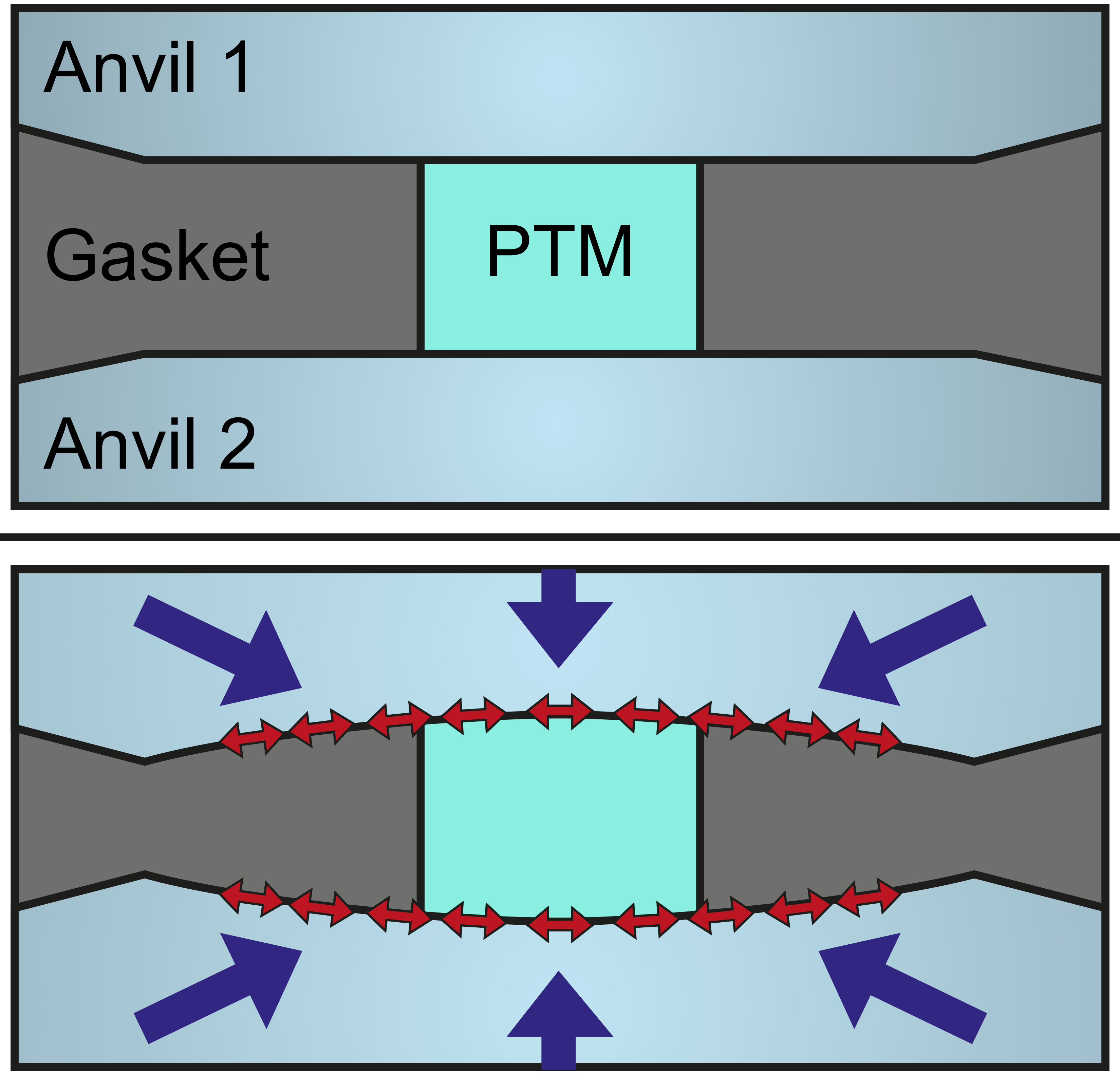

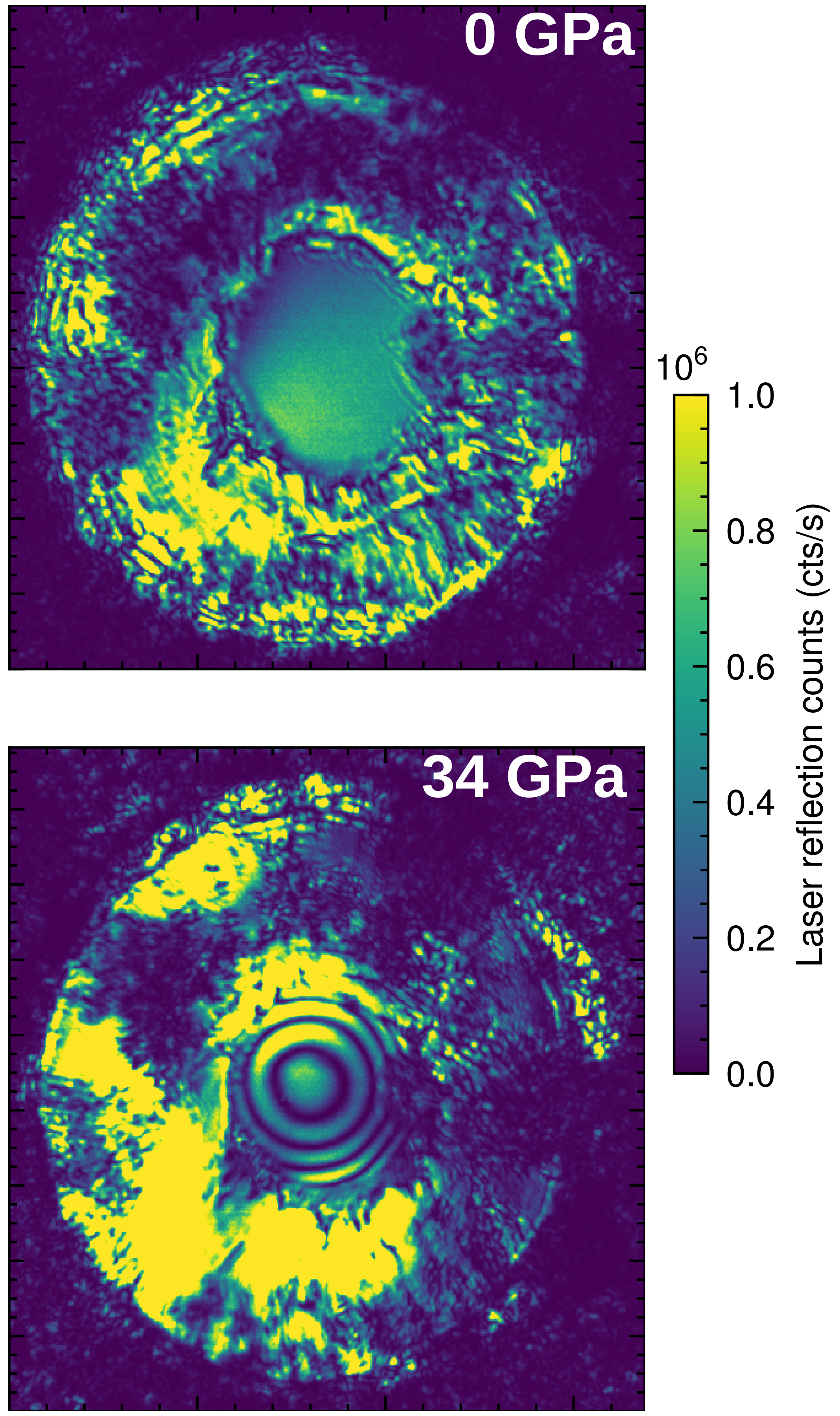

Competition between **compression** and **surface tension** at the anvil tip

➡ At high pressure, the stress in the anvil tip is compressive, but anisotropic due to anvil cupping

Stress environment in the anvil tip: Model

- The NV centers are *not* in the sample space, Rather they are located $\approx 20\,\mathrm{nm}$ beneath the anvil surface

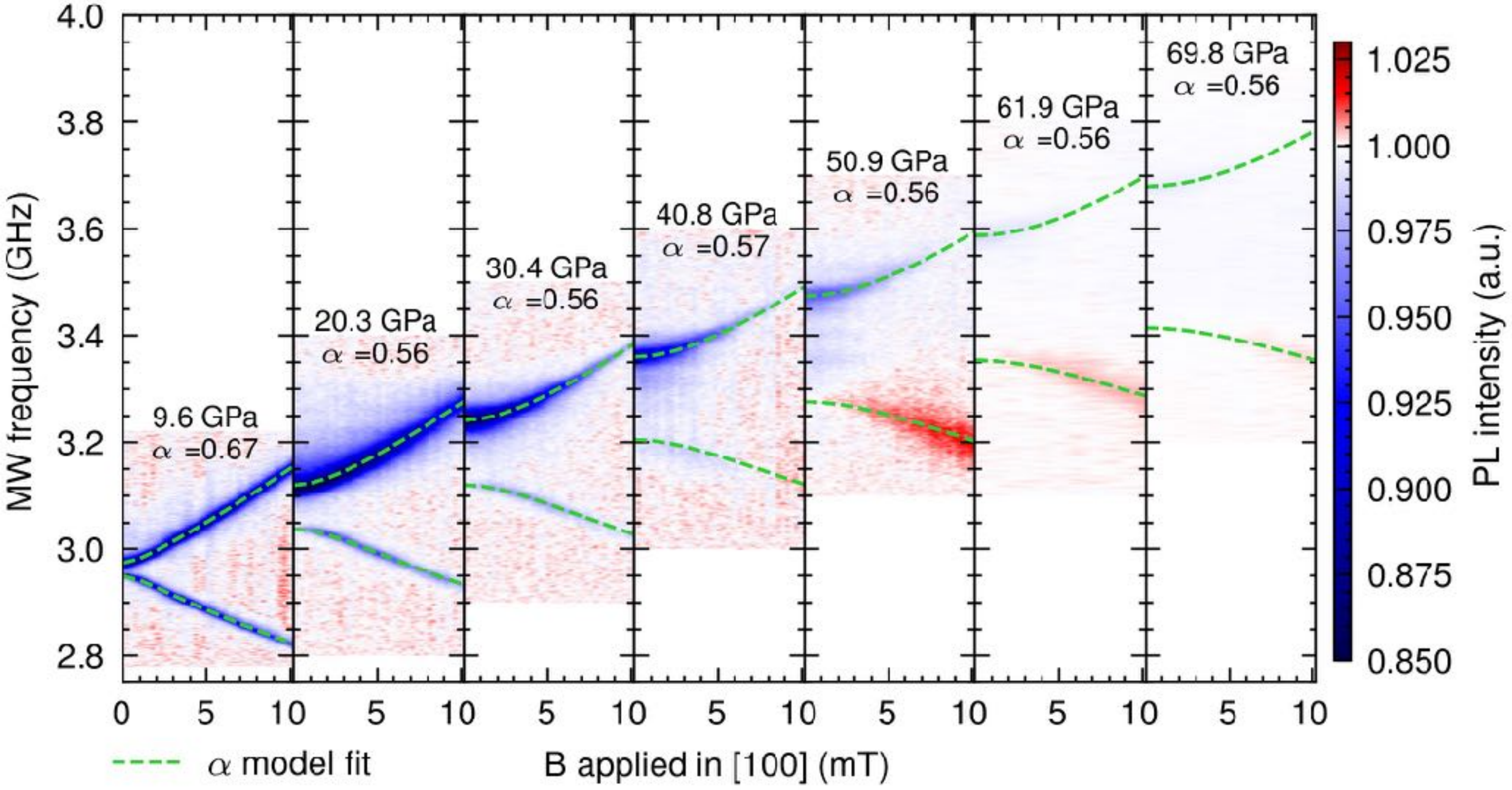

- Model of the stress tensor at the anvil tip:

$$\overleftrightarrow{\sigma} = \begin{pmatrix} \alpha P & 0 & 0 \\ 0 & \alpha P & 0 \\ 0 & 0 & P \end{pmatrix} \qquad \alpha < 1$$

Related work: K. O. Ho et al, Phys. Rev. Appl. 19, 044091 (2023)

$$\hat{H}_{NV} = D\hat{S}_Z^{\,2} + \gamma_{NV}\overrightarrow{B}\cdot\vec{S} + \hat{H}(\overleftrightarrow{\sigma})$$

➡ Perfect fit with $\alpha \simeq 0.56$

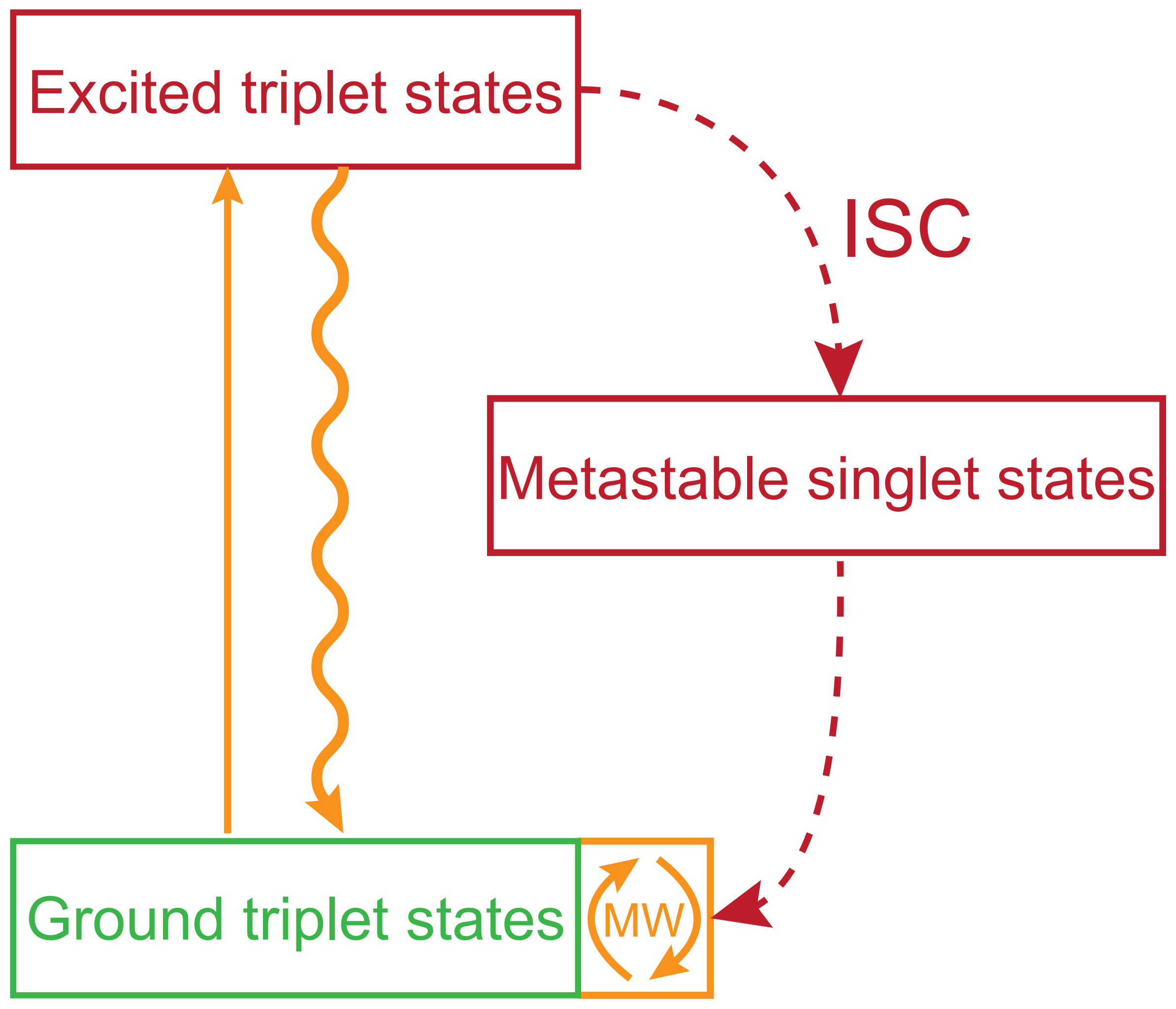

➡ Is there a way to mitigate the non-hydrostatic stress ?

Control of the stress environment by microstructuration

Non-hydrostatic stress occurs due to the competition between compression and surface tension

Idea : isolate part of the anvil surface, and immerse it into the PTM

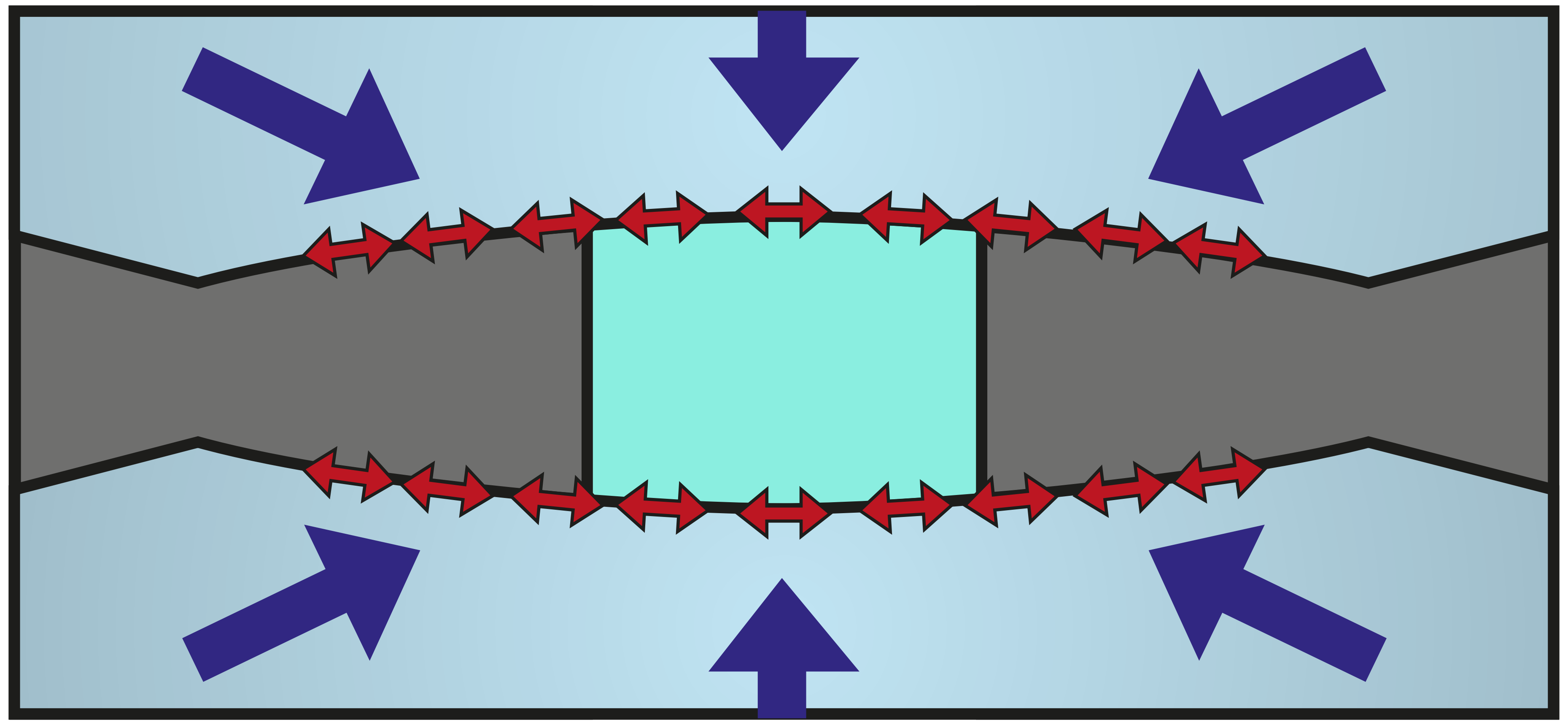

milling with FIB (or fs-laser)

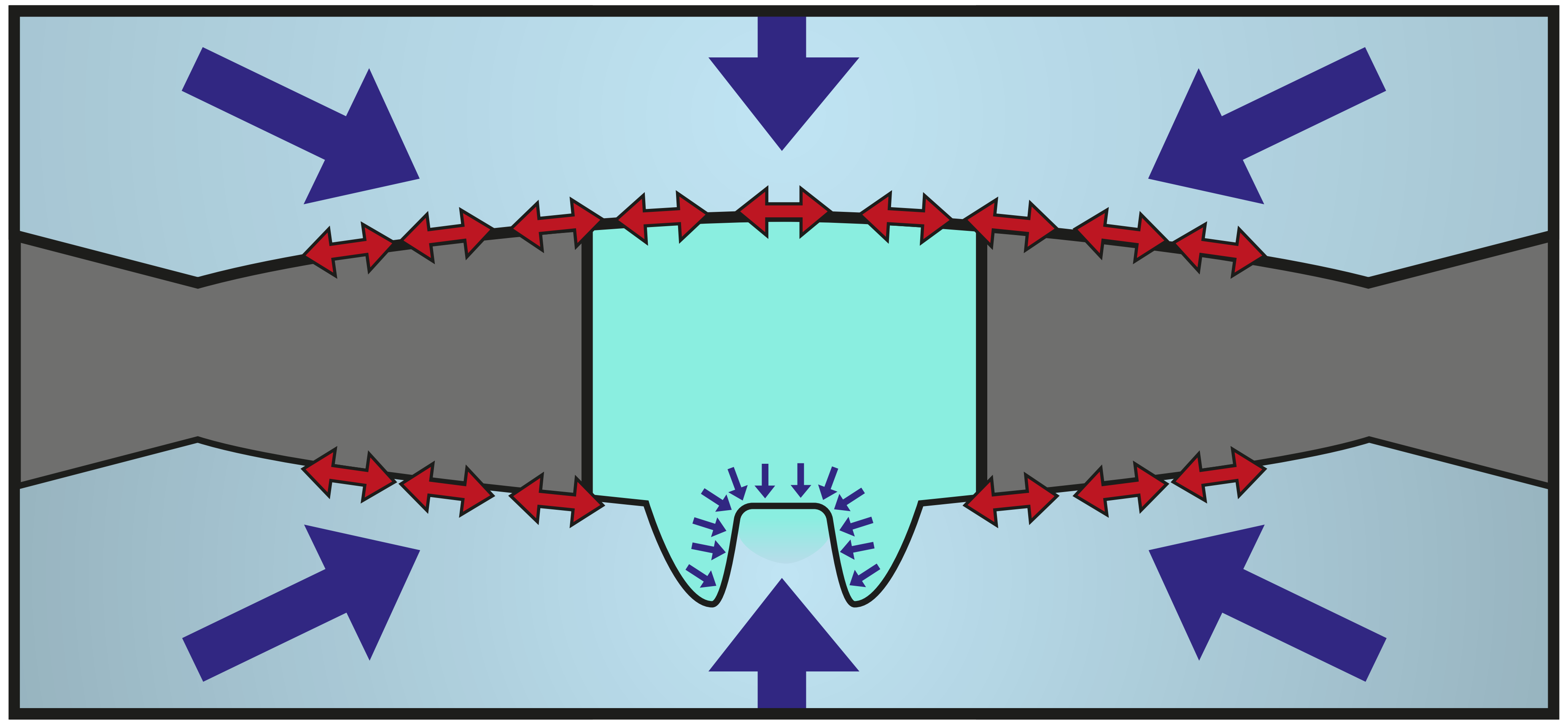

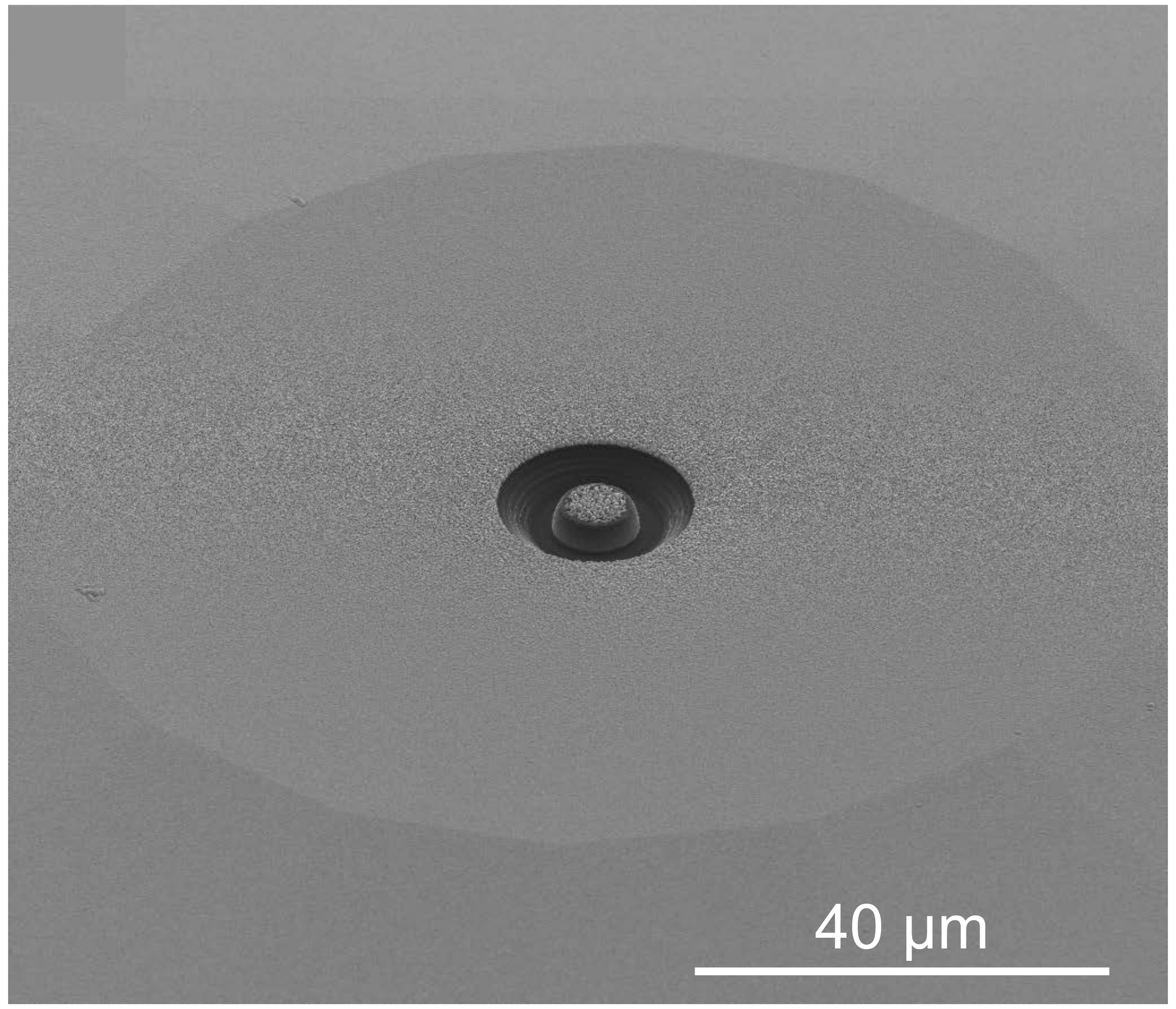

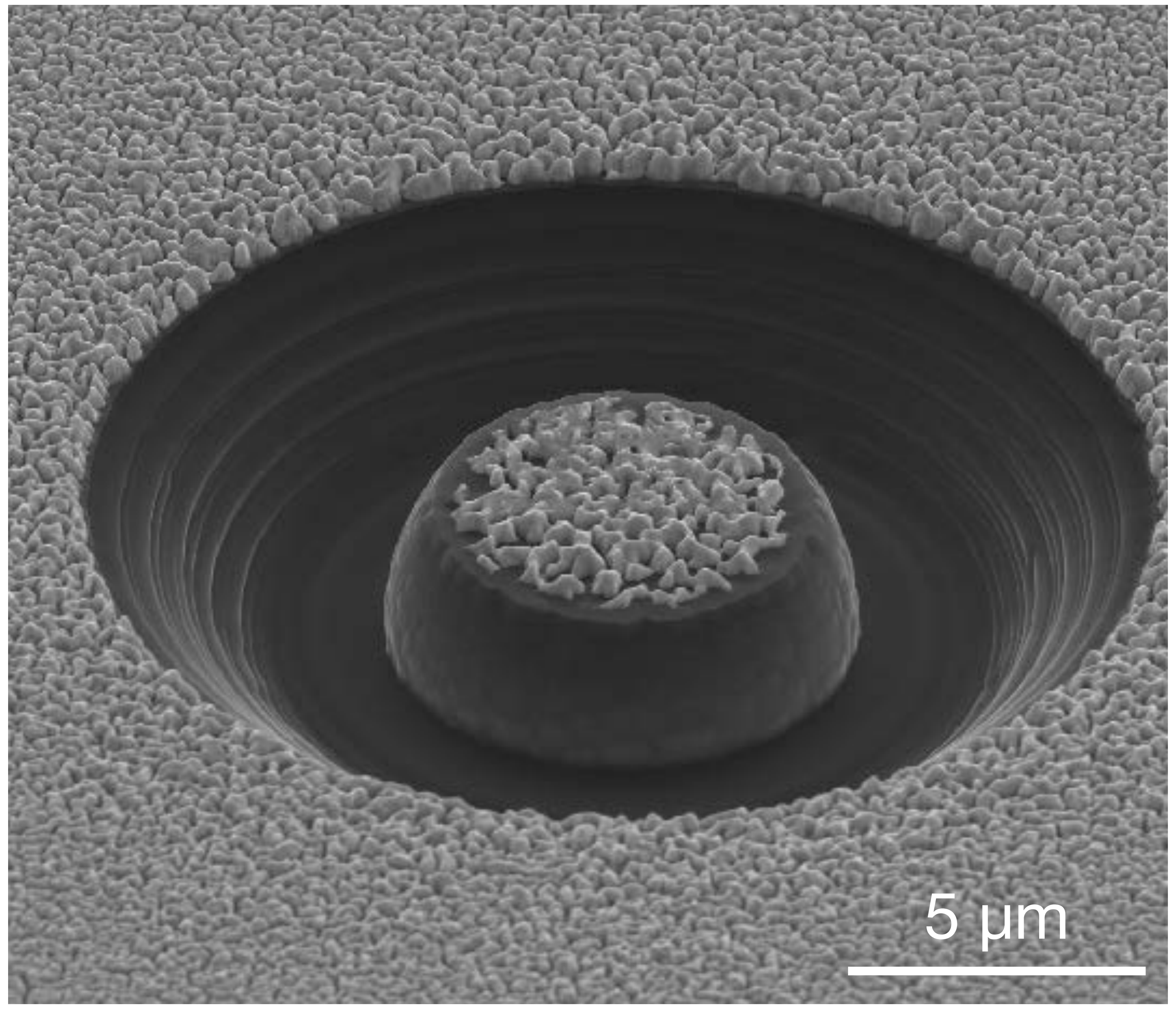

NV magnetic sensing under hydrostatic environment

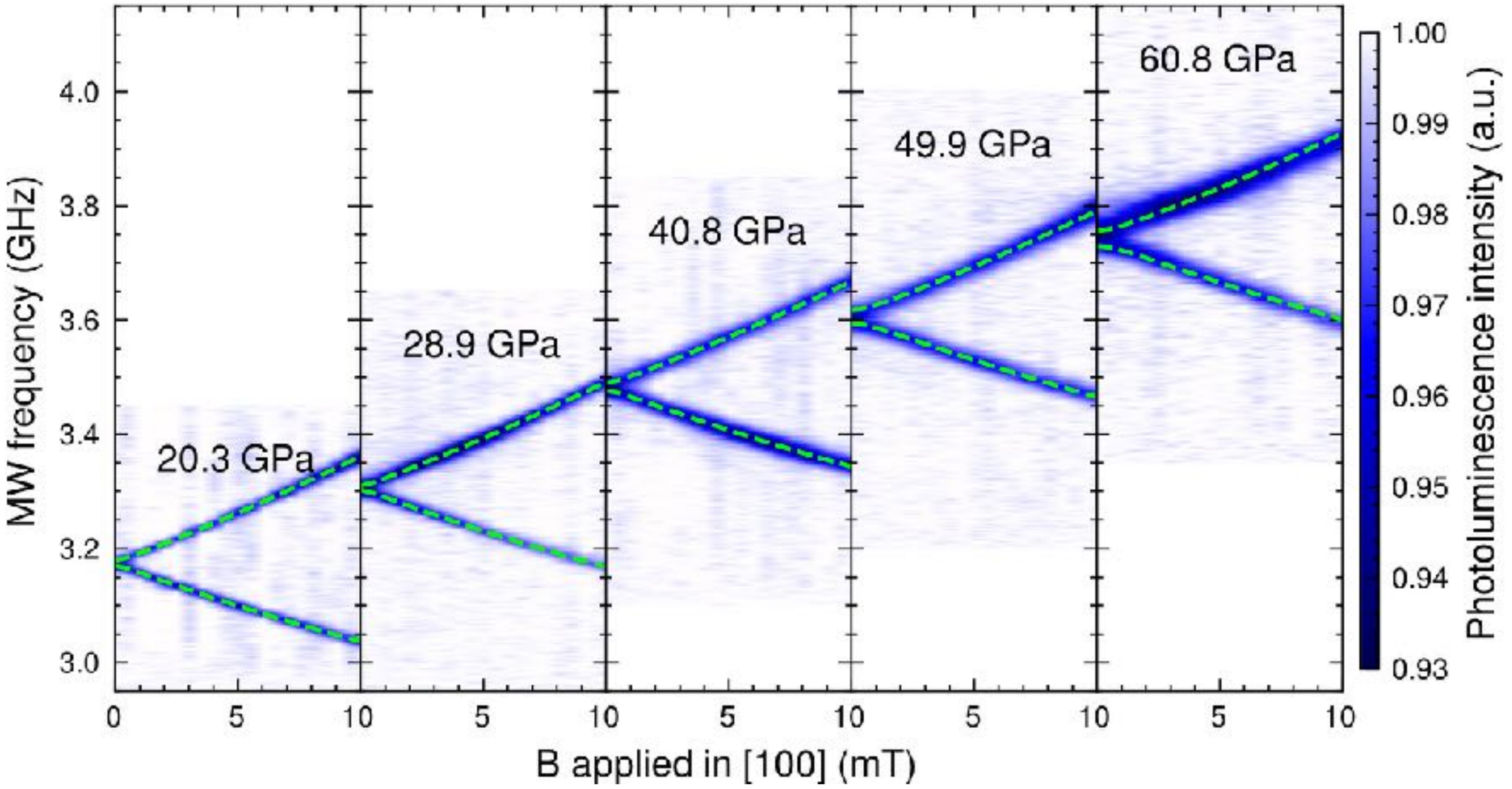

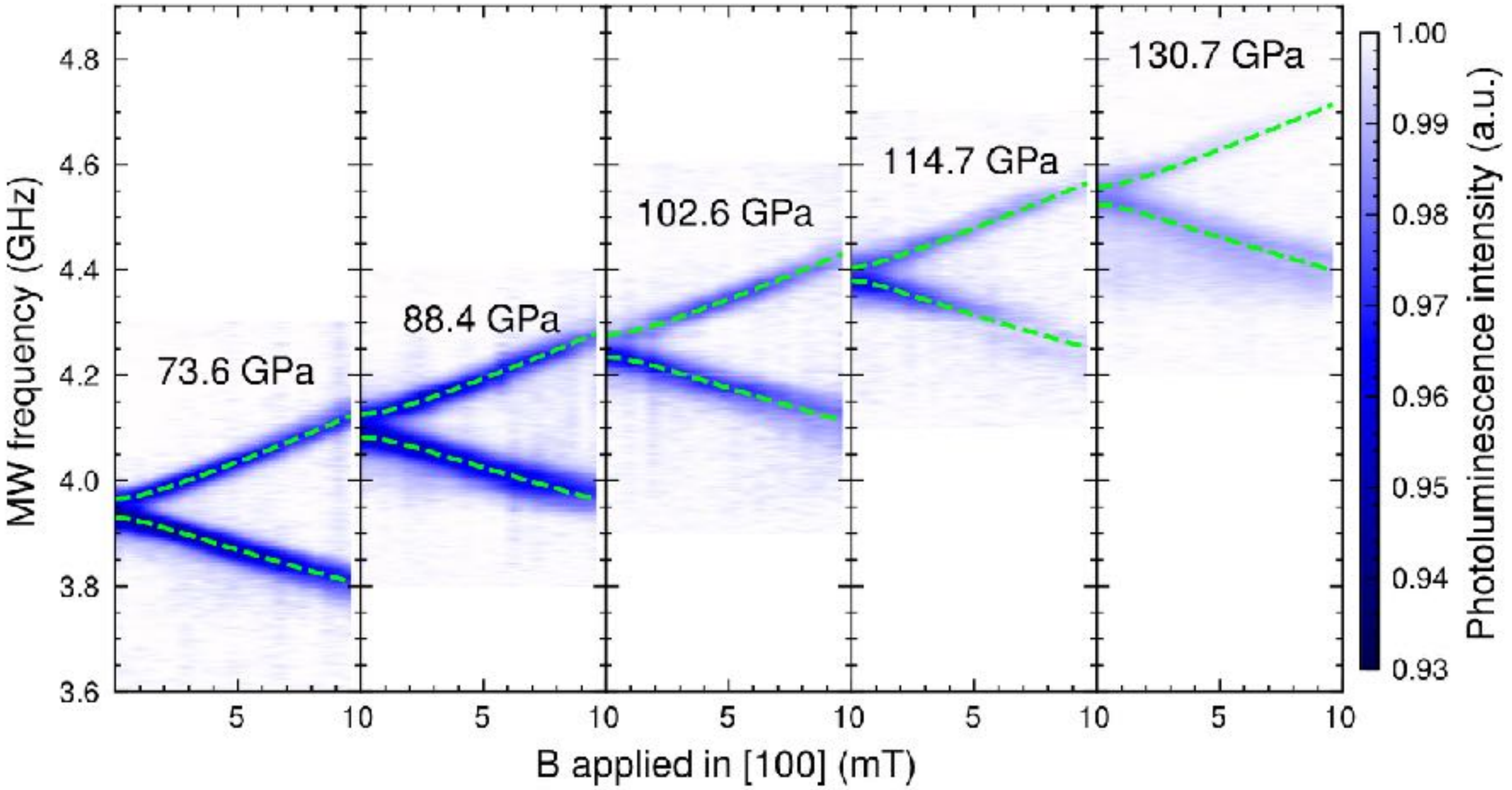

A. Hilberer et al., Phys. Rev. B **107**, L222102 (2023)

- Fit yields reduced anisotropic stress, $\alpha \simeq 0.96$
- Magnetic sensing behavior remains unchanged to 130 GPa, there is **no longer a pressure limit**
  - Confirmed in microdiamonds by Dai *et al.*, Chinese Physics Letter (2022)

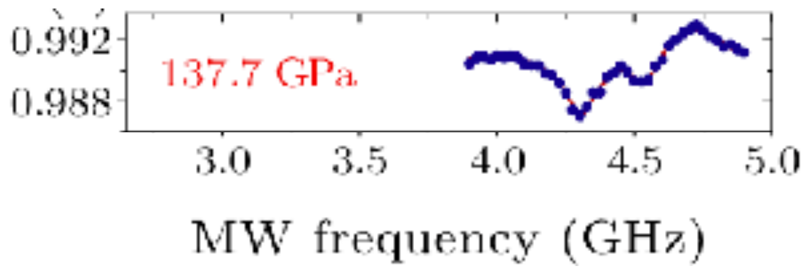

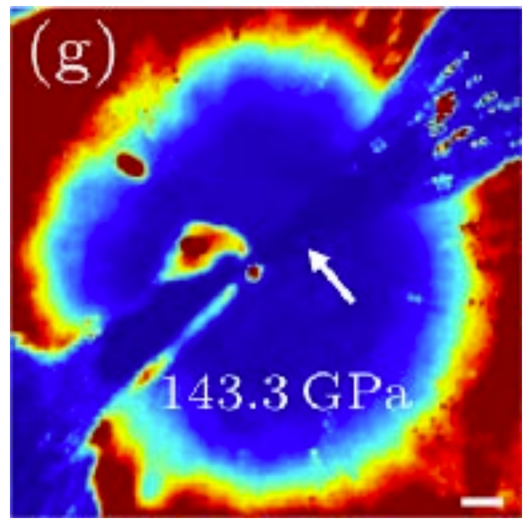

- Complementary approach : $[111]$-oriented anvil under uniaxial strain

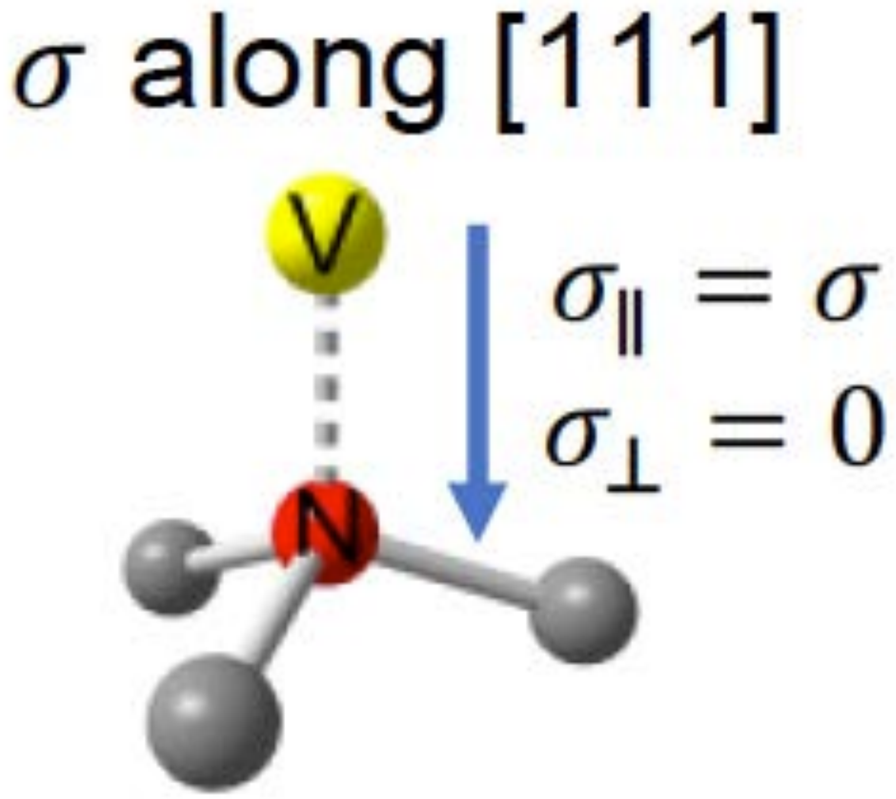

Norman Yao et al. (Harvard)
arXiv:2306.03122 (05 June 2023)
Nature **627**, 73-79 (2024)

Jiangfeng Du et al. (CAS, Hefei)
arXiv:2306.07840 (13 June 2023)
Nat. Commun. **15**, 8843 (2024)

Probes of high-pressure superconductivity

expulsion of a static magnetic field for $T < T_C$
$\rightarrow \chi_m < 0$

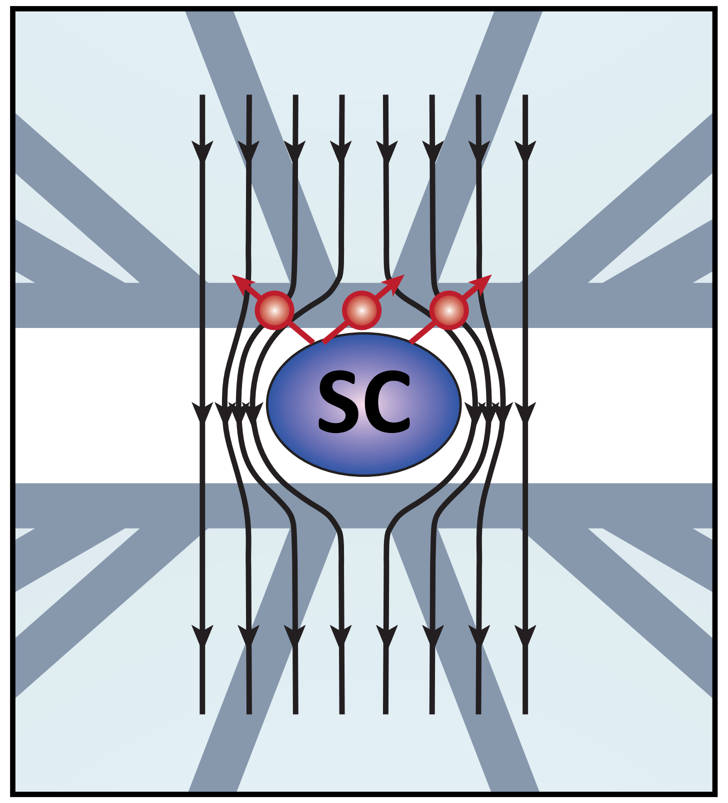

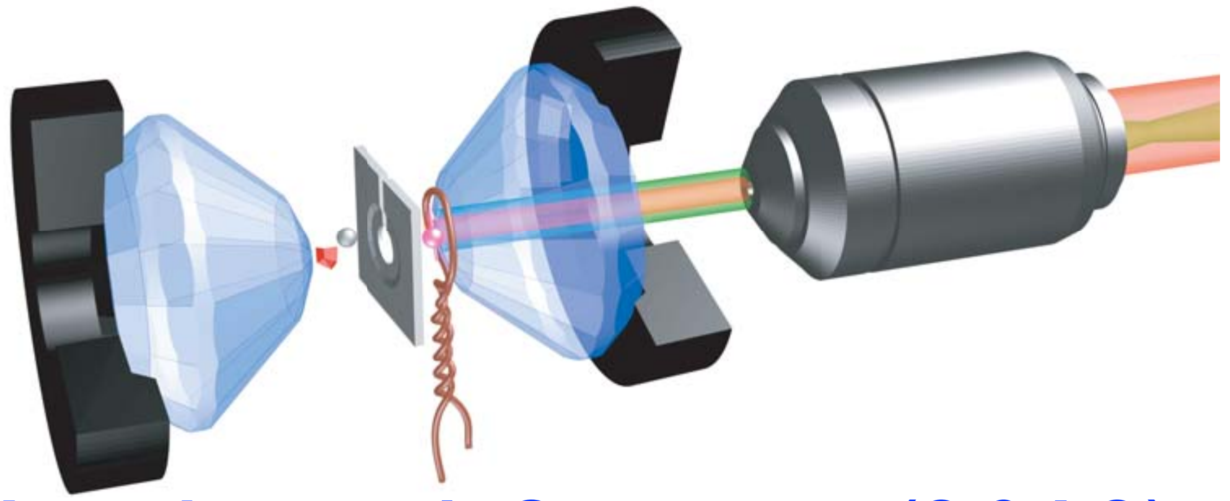

Lesik et al, Science (2019)

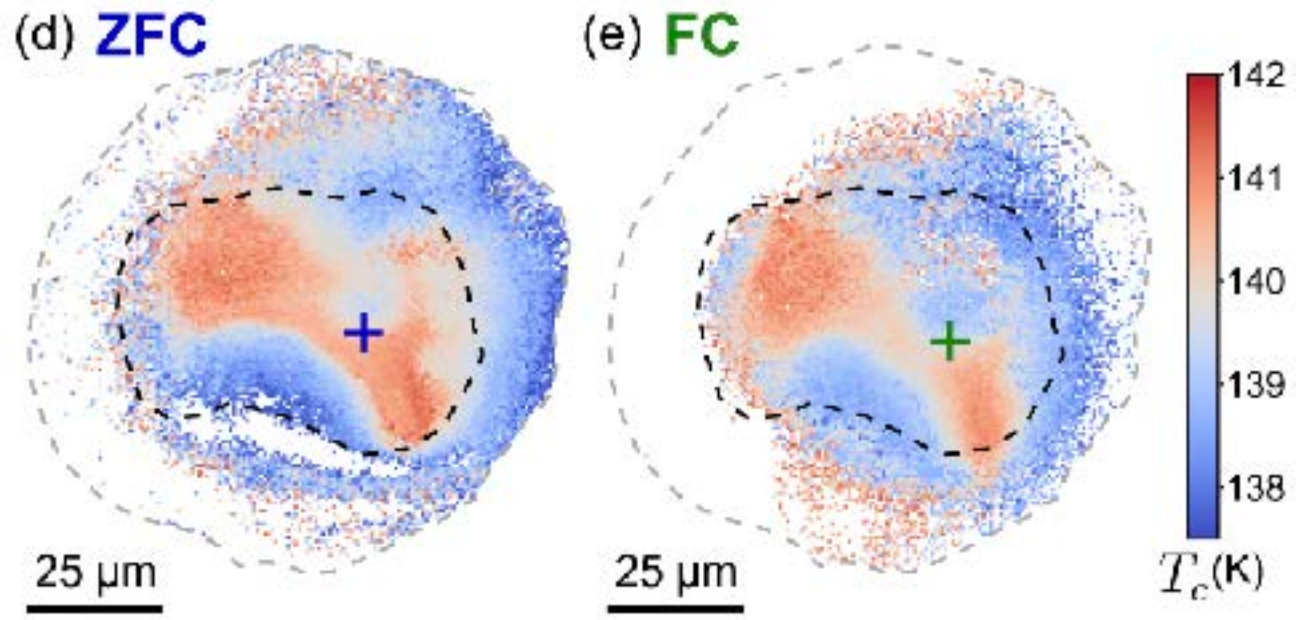

Dailledouze et al, Phys Rev Mat (2025)

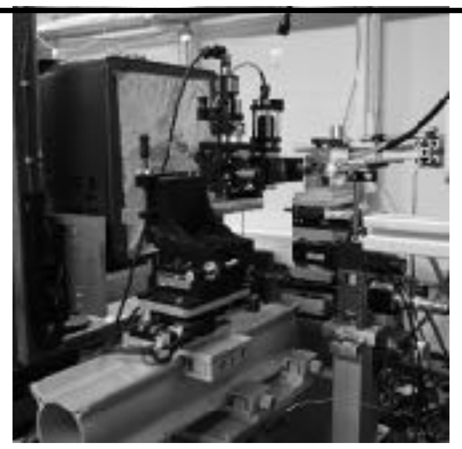

	NV centers	SQUID
DAC	standard	specific miniaturization
detected signal sensitivity	stray magnetic field produced by magnetization $< 10^{-10}$ emu	magnetization $\approx 10^{-8}$ emu
Background	negligible	$\approx 10^4$ $\times$ SC signal
Spatial resolution	$\approx \mu m$	no
Pressure range	≈ 150 GPa in hydrostatic stress Hilberer et al, Phys Rev B (2023) current record 240 GPa (with [111] anvil)	> 200 GPa
Compatibility with X-ray analysis	portable system on a synchrotron beamline Toraille, et al, New J Phys (2020)	no

Maturation des capteurs quantiques à centres NV

arxiv:2511.11791 (15 November 2025)

2025 Quantum Diamond Workshop

Findings Report

Danielle A. Braje[1,*], Matthew L. Markham[2,†], Jennifer M. Schloss[1,‡], Michael A. Slocum[3,§], Ronald L. Walsworth[4,‖]

Défis / barrières identifiès	Recommandations / Actions proposées
Chaine d'approvisionnement du diamant fragmentée ; diversite des sources, mangule de standardisation des qualites →	Dèvelopper la coordination entre foumisseurs, ingenieurs d'appareils et utillsateurs finaux', encourager la standärdisation et la transparence sur les spécifications des matériaux
Propriètes des matériaux limitées (cohérence de spin, pureté, contreie des défauts, dopage, reproductibilité) →	Soutenir la R& D en croissance de diamant, controle des defauts (p. ex, NV, SIV, autres centres), en exploitant des matériaux optimisés pour des applications ciblées
Marique de plateformes intégrées et d'appareils prèts a l'emploi →	Investir dans le developpement de prototypes integies avec conditionnement, commande electronique. compatiibilité optique, interfaces utillsateur simplifiées
Ecosystemé logiciel ét d'anaiyse fragménté chaque groupe developpe ses outils →	Encourager la creation d un ecosystéme logiciel commn, avec des outils standards (acquisition, commande, analyse de signal qua-
Difficuité à identifier les «applications gagnahtes' a court terme →	Orienter la communauté vers des demoństrations a court terme capteurs robustes, métrologie magnètique, inertielle, imagerié, thermométrie NV, etc
Manque de communication entre acteurs (matèriaux, apparells, ufilisateurs) →	Engager des projets pilotes, finances publiquement, réunissant recherche, industrie et utilisateurs finaux autour dè cas d'usage
Berrières reglementaires et absènce dé normes pour les capteurs et appareils quantiques →	Développer des normes de qualification, procédures de tèst, critères de performance repronuc dictribles
Financement disperse et peu structuré →	Aligner les financeurs publics/privés autour d'une stratégie nationale cohérente en technologies quantiques du diamant
Transition difficile du laboratoire a l'industrie (mise a l'echelle, conditionnement, couts) →	Soutenir la transition technologigue, renfércer l'ingénierie, la fabrication, l'automatisation et les chaines pre-industrielles

APPLIED PHYSICS LETTERS 107, 233502 (2015)

Wide bandwidth instantaneous radio frequency spectrum analyzer based on nitrogen vacancy centers in diamond

M. Chipaux,[1,a)] L. Toraille,[1,b)] C. Larat,[1] L. Morvan,[1] S. Pezzagna,[2] J. Meijer,[2] and T. Debuisschert[1]
[1]Thales Research & Technology, 1 Av. Augustin Fresnel, 91767 Palaiseau Cedex, France
[2]Department of Nuclear Solid State Physics, Institute for Experimental Physics II, Universität Leipzig, Linnéstr. 5, D-04103 Leipzig, Germany

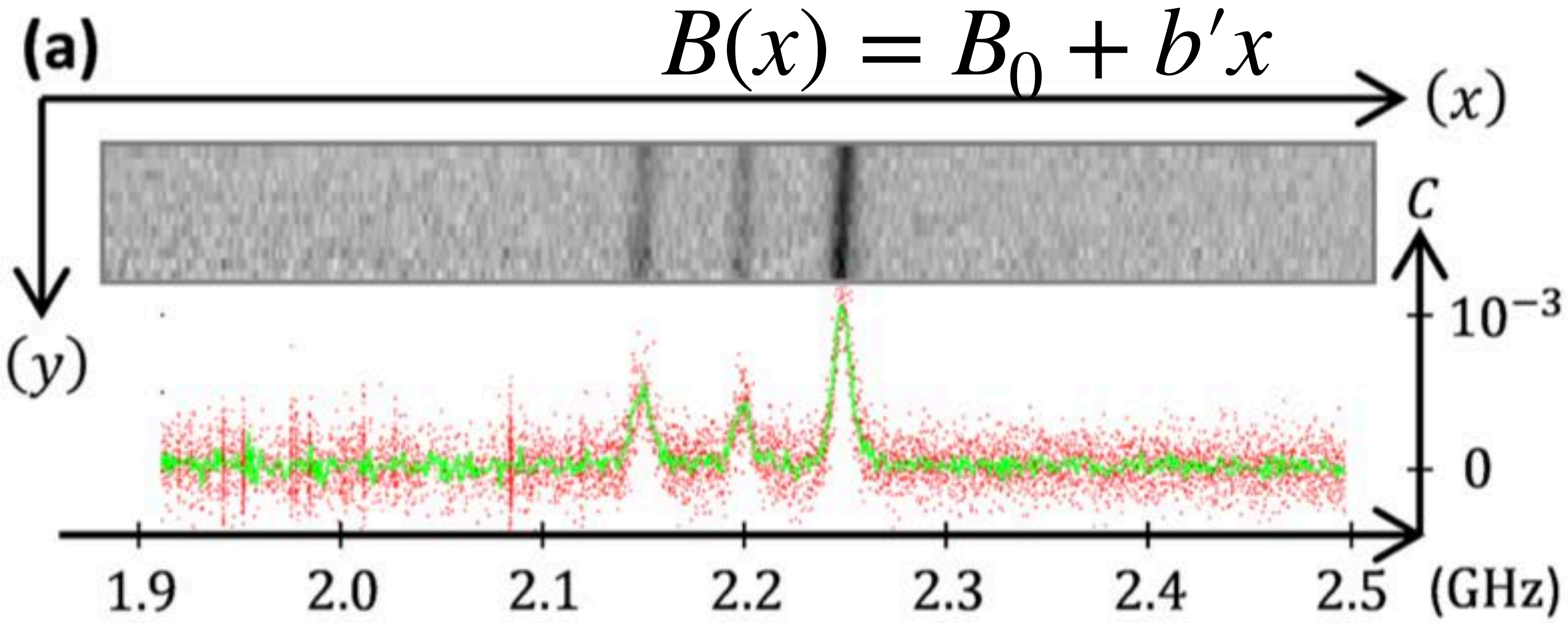

bande d'analyse de 5 GHz accordable de 10 MHz à 25 GHz

Remerciements

école normale supérieure paris-saclay

Martin Schmidt

Marie-Pierre Adam

PhD students

Cassandra Dailledouze
Léonie Evanno
Pierre Grégoire
Grégoire Le Caruyer de Beauvais
Claire Roussy
Mélissa Techer

Kin On Ho (postdoc)
Boris Yavkin (postdoc)

THALES

Ludovic Mayer

Simone Magaletti

Thierry Debuisschert

cea

Paul Loubeyre

Loïc Toraille

Antoine Hilberer

institut universitaire de France

QUANTUM FRANCE 2030

FRANCE 2030

anr

QuanTiP

Région îledeFrance

erc